TECHNISCHE UNIVERSITÄT MÜNCHEN
Wissenschaftszentrum Weihenstephan für Ernährung, Landnutzung und Umwelt
Lehrstuhl für biochemische Pflanzenpathologie

From model to crop plants: induced resistance in barley

Miriam Lenk

Vollständiger Abdruck der von der Fakultät Wissenschaftszentrum Weihenstephan für Ernährung, Landnutzung und Umwelt der Technischen Universität München zur Erlangung des akademischen Grades eines

Doktors der Naturwissenschaften

genehmigten Dissertation.

Vorsitzender: apl. Prof. Dr. Ramon Angel Torres Ruiz

Prüfender der Dissertation:

1. Prof. Dr. Jörg Durner
2. Prof. Dr. Ralph Hückelhoven

Die Dissertation wurde am 25.10.2018 bei der Technischen Universität München eingereicht und durch die Fakultät Wissenschaftszentrum Weihenstephan für Ernährung, Landnutzung und Umwelt am 05.02.2019 angenommen.

Publications related to this thesis:

Lenk, M., Wenig, M., Mengel, F., Häußler, F., and Vlot, A. C. 2018. *Arabidopsis thaliana* Immunity-Related Compounds Modulate Disease Susceptibility in Barley. Agronomy. 8:142

Lenk, M., Wenig, M., Bauer, K., Hug, F., Knappe, C., Lange, B., Häußler, F., Mengel, F., Dey, S., Vlot, A. C. 2018. Pipecolic acid is associated with innate immune responses in barley. (in preparation)

Table of contents

Summary

Plants are constantly challenged by numerous pathogens and fend off many of these with different phytohormone signalling pathways. Much is known about defence signalling in the dicotyledonous model plant *Arabidopsis thaliana*, but it is unclear to which extent knowledge from model systems can be transferred to monocotyledonous plants, including cereal crops. Here, the defence-inducing potential of *Arabidopsis* resistance-inducing compounds in the cereal crop barley was investigated.

Salicylic acid (SA) and the SA-related compounds folic acid (Fol) and azelaic acid (AzA) all induced systemic resistance against *Blumeria graminis* f. sp. *hordei* (*Bgh*). In addition, Fol induced systemic susceptibility against *Xanthomonas translucens* pv. *cerealis* (*Xtc*). In contrast, the SAR compound pipecolic acid (Pip) induced resistance against both *Xtc* and *Bgh*. None of the compounds had an effect on growth of the necrotrophic fungus *Pyrenophora teres*. Therefore, barley induced resistance seems to share at least some signalling compounds with the model plant *Arabidopsis*, especially in defence against *Bgh*, while resistance against *Xtc* seems to be controlled by different pathways. In addition, protection against *Bgh* induced with SA, Fol, AzA, or Pip might not leave the plant vulnerable to necrotrophic pathogens, at least not to *P. teres*. Nitric oxide levels increased in leaves of Pip-treated barley plants, which had been reported before for *Arabidopsis*. Therefore, Pip might induce resistance at least in part via similar molecular mechanisms in barley and *Arabidopsis*. Interestingly, the genes upregulated during bacteria-induced resistance of barley, 4 *WRKY* and *Ethylene Response Factors,* were not induced by Pip. Since these genes had previously been associated with bacteria-induced systemic immunity in barley, this project aimed to confirm their physiological relevance in induced resistance. CRISPR/Cas was established in barley and employed to knock out 2 of the transcription factors. Using a fluorescence reporter system, it was shown that CRISPR/Cas constructs are functional in barley protoplasts, also revealing different mutation efficiencies for different gRNAs. The CRISPR/Cas constructs were functional in stably transformed barley plants, creating (homozygous) mutants of the target genes. Several *wrky38/1* lines produced in the course of this work are currently used in phytopathological experiments to examine the role of *WRKY38/1* in induced resistance of barley.

Zusammenfassung

Pflanzen werden ständig von zahlreichen Krankheitserregern bedroht und verteidigen sich gegen viele von ihnen mit Hilfe von unterschiedlichen Phytohormon-Signalkaskaden. Über die Abwehrsignale in der zweikeimblättrigen Modellpflanze *Arabidopsis thaliana* ist viel bekannt. Jedoch ist unklar, inwieweit Erkenntnisse aus diesem Modellsystem auf einkeimblättrige Pflanzen übertragen werden können, insbesondere auf Getreidepflanzen. In dieser Arbeit sollte das abwehrverstärkende Potenzial von resistenzinduzierenden Verbindungen aus *Arabidopsis* in der einkeimblättrigen Kulturpflanze Gerste untersucht werden.

Bei diesen Untersuchungen zeigte sich, dass Salicylsäure (SA) und die mit ihr in Verbindung stehenden Substanzen Folsäure (Fol) und Azelainsäure (AzA) eine systemische Resistenz gegen *Blumeria graminis* f. sp. *hordei* (*Bgh*) induzierten. Darüber hinaus bewirkte Fol eine systemische Empfindlichkeit gegen *Xanthomonas translucens* pv. *cerealis* (*Xtc*). Im Gegensatz dazu induzierte Pipecolinsäure (Pip) eine Resistenz gegen *Xtc* und *Bgh*. Keine der Verbindungen hatte einen Einfluss auf das Wachstum des nekrotrophen Pilzes *Pyrenophora teres*. Daher scheint die induzierte Resistenz in Gerste zumindest einige Signalverbindungen mit der Modellpflanze *Arabidopsis* zu teilen, insbesondere bei der Verteidigung gegen *Bgh*, während die Abwehr gegen *Xtc* auf unterschiedliche Weise gesteuert wird. Darüber hinaus scheint der mit SA, Fol, AzA oder Pip induzierte Schutz gegen *Bgh* die Pflanze nicht gegen nekrotrophe Pathogene anfällig zu machen, hier speziell gezeigt für *P. teres*. In Blättern von Pip-behandelten Gerstenpflanzen wurde ein Anstieg des NO-Spiegels beobachtet, wie er zuvor für *Arabidopsis* berichtet worden war. Daher könnte Pip zumindest teilweise über ähnliche molekulare Mechanismen bei Gerste und *Arabidopsis* Resistenz induzieren. Die vier *WRKY* und *Ethylene Response Factors*, die während der durch Bakterien ausgelösten Resistenz von Gerste transkriptionell induziert werden, gehören jedoch nicht zum molekularen Mechanismus von Pip. Da diese Gene zuvor mit bakteriell induzierter systemischer Abwehr in Gerste assoziiert worden waren, sollte in diesem Projekt ihre physiologische Relevanz für die induzierte Resistenz bestätigt werden. Die CRISPR/Cas-Technik wurde in Gerste etabliert und es war möglich, zwei der Transkriptionsfaktoren gezielt auszuschalten. Mittels eines Fluoreszenz-Reportersystems konnte gezeigt werden, dass die verwendeten CRISPR/Cas-Konstrukte in Gersteprotoplasten funktional sind. Es wurden

unterschiedliche Mutationseffizienzen für verschiedene gRNAs gezeigt. Die CRISPR/Cas-Konstrukte waren in stabil transformierten Gerstenpflanzen funktionstüchtig und erzeugten (homozygote) Mutanten der Zielgene. Mehrere im Rahmen dieser Arbeit erzeugten *wrky38/1* Linien werden derzeit in phytopathologischen Experimenten verwendet, um die Rolle von *WRKY38/1* bei der induzierten Resistenz von Gerste zu untersuchen.

Abbreviations

In addition to SI units, metric prefixes, element symbols, chemical formulas, and the abbreviations for nucleotides, the following abbreviations were used:

°C	degree Celsius
ABA	abscisic acid
AzA	azelaic acid
Bgh	*Blumeria graminis* f. sp. *hordei*
bp	base pair(s)
BTH	benzothiadiazole
cfu	colony forming units
crRNA	CRISPR RNA
CRISPR/Cas	clustered regularly interspaced short palindromic repeats/CRISPR-associated
CTAB	cetyltrimethylammoniumbromid
DA	dehydroabietinal
DMSO	dimethyl sulfoxide
DNA	desoxyribonucleic acid
dpi	days post inoculation
EDTA	ethylenediaminetetraacetate
ERF	*Ethylene Response Factor*
ET	ethylene
ETI	effector-triggered immunity
Fol	folic acid
G3P	glycerol-3-phosphate
gRNA	guide RNA
h	hour(s)
ISR	induced systemic resistance
M	mock
MeJA	methyl jasmonate
MES	2-(N-morpholino)ethanesulfonic acid
min	minute(s)
NHP	N-hydroxy-pipecolic acid
JA	jasmonic acid
PAM	protospacer-adjacent motif

PAMP	pathogen-associated molecular pattern
(RT-q)PCR	(reverse transcription quantitative) polymerase chain reaction
PEX	petiole exudate
Pip	pipecolic acid
Psj	*Pseudomonas syringae* pv. *japonica*
PTI	PAMP-triggered immunity
R	*Resistance*
RNA	ribonucleic acid
ROS	reactive oxygen species
rpm	revolutions per minute
SA	salicylic acid
SAR	systemic acquired resistance
SDS	sodium dodecyl sulfate
sec	second(s)
sgRNA	single guide RNA
T7EI	T7 endonuclease I
T_m	melting temperature
TALEN	transcription-activator-like effector nuclease
tracrRNA	transactivating CRISPR RNA
Xtc	*Xanthomonas translucens* pv. *cerealis*
ZNFs	zinc-finger nuclease

List of Figures and Tables

Figures

Tables

1 Introduction

1.1 Plant defence

Plants are constantly challenged with a plethora of pathogens, including herbivorous insects, fungi, oomycetes, bacteria and viruses (Panstruga et al. 2009; Spoel and Dong 2012). To cope with these attacks, plants have evolved an effective immune system of pre-formed and inducible defence mechanisms. The former include morphological barriers, for instance the plant cell wall, cuticle, phytoanticipins, and antimicrobial proteins. Inducible defence mechanisms include processes like cell wall reinforcement by lignin and callose or the synthesis of phytoalexins and defence-related proteins or enzymes (Glazebrook 2005; Jones and Dangl 2006; Panstruga et al. 2009; Spoel and Dong 2012).

After the first contact between plant and pathogen, conserved structures such as bacterial flagellin or fungal chitin, so-called pathogen-associated molecular patterns (PAMPs), encounter pattern recognition receptors on the cell surface. This triggers a first immune response termed PAMP-triggered immunity (PTI) (Jones and Dangl 2006; Spoel and Dong 2012; Zipfel and Felix 2005). During long-term evolution of plant-pathogen-interactions, some pathogens developed effector proteins to suppress PTI. In response to this development, plants evolved resistance (*R*) genes, which encode proteins that directly or indirectly recognise effectors, and on recognition elicit so-termed effector-triggered immunity (ETI) (Glazebrook 2005; Henry et al. 2013; Jones and Dangl 2006; Spoel and Dong 2012).

Both PTI and ETI are associated with the induction of various cellular responses. These include the synthesis of antimicrobial compounds, the generation of reactive oxygen species (ROS), the activation of mitogen-activated protein kinases, transcriptional reprogramming, and the accumulation of phytohormones such as salicylic acid (SA) (Glazebrook 2005; Jones and Dangl 2006; Klessig et al. 2018; Spoel and Dong 2012; Vlot et al. 2009). SA is known to affect the redox status of plants, thereby leading to transcriptional reprogramming and enhanced transcription of *PATHOGENESIS-RELATED (PR)* genes, which are thought to promote resistance (Fu and Dong 2013; Klessig et al. 2018; Pajerowska-Mukhtar et al. 2013; van Loon et al. 2006; Vlot et al. 2009). Furthermore, SA not only helps the plant to defend itself

against a present infection, it is also involved in the induction of a process protecting the plant in case of future pathogen challenge (Klessig et al. 2018). This response is termed systemic acquired resistance (SAR). When bacteria (or other pathogens) infect a plant, they induce ETI in the locally infected leaves, resulting (among other processes) in rising SA levels also in the systemic leaves, which protect the plant from subsequent pathogen attacks (Jones and Dangl 2006; Klessig et al. 2018; Vlot et al. 2009).

1.1.1 The role of salicylic acid in resistance

SA is a phytohormone and involved in many different plant processes, including seed germination, vegetative growth, root initiation and growth, flowering, fruit yield, senescence, photosynthesis, stomatal closure, thermogenesis, responses to different abiotic stressors, and plant disease resistance (Klessig et al. 2018; Vlot et al. 2009; and references therein). Exogenous application of SA can induce defence gene expression and resistance in several plant species, both monocots and dicots (Klessig et al. 2018).

SA biosynthesis in *Arabidopsis thaliana* is induced by pathogen attack and catalysed by ICS1 (ISOCHORISMATE SYNTHASE1; Seyfferth and Tsuda 2014; Vlot et al. 2009 and references therein). SA accumulates during defence responses such as PTI and ETI (Malamy et al. 1990; reviewed in Klessig et al. 2018; Vlot et al. 2009). In addition, SA leads to the accumulation of NO and ROS and thereby can induce programmed cell death resulting in a hypersensitive response that is thought to limit pathogen spread (Chen et al. 1993; Durner et al. 1997; Jones and Dangl 2006; Klessig et al. 2000). In addition, SA leads to extensive transcriptional reprogramming and induced expression of defence-related genes (Gruner et al. 2013; Seyfferth and Tsuda 2014).

A very important factor in downstream signalling of SA is NPR1 (NONEXPRESSOR OF PR GENES 1), a transcriptional co-activator of defence gene expression termed the master regulator of SA responses (Fu and Dong 2013; Klessig et al. 2018; Pajerowska-Mukhtar et al. 2013). SA accumulation leads to activation of thioredoxins and changes in the cellular redox status, creating more reducing conditions. This affects NPR1, which in the non-induced state is present in the cytosol as an oligomer formed by intermolecular disulphide bonds. Accumulation of SA leads to reductional monomerisation of NPR1, which re-localises from the cytosol to the nucleus (Mou et

al. 2003; Tada et al. 2008). In the nucleus, NPR1 interacts with TGA and additional transcription factors to activate gene expression of *PR* and other defence-related genes (Kesarwani et al. 2007; Kinkema et al. 2000). NPR1 and its paralogues NPR3 and NPR4 can bind SA and might function as SA receptors, although their exact mode of interaction is controversial (Ding et al. 2018; Fu et al. 2012; Wu et al. 2012).

1.1.2 Hormone cross-talk in plant immunity

Several phytohormones are involved in plant defence responses against pathogens. The traditional three main players are SA, jasmonic acid (JA), and ethylene (ET), but recent evidence hints at the additional contribution of other hormones (Figure 1 and Pieterse et al. 2012; Robert-Seilaniantz et al. 2011; Shigenaga and Argueso 2016). SA is required for PTI and ETI (Shigenaga and Argueso 2016; Vlot et al. 2009), inducing expression of defence-related transcription factors and a large set of resistance-related genes (see above and Klessig et al. 2018; Pieterse et al. 2012). JA is produced after necrotrophic pathogen or insect attack and induces a different set of defence genes, for example defensins with antifungal activity (Penninckx et al. 1996). ET works mostly in concert with JA, is required for certain components of PTI signalling, and can also influence gene expression (Robert-Seilaniantz et al. 2011; Shigenaga and Argueso 2016).

Pathogens of different lifestyles have different demands on their hosts and are combatted using different mechanisms; while biotrophic pathogens feed on living cells, necrotrophic pathogens acquire their nutrients from degraded and dead tissue. Biotrophs are mostly opposed using SA signalling, which induces programmed cell death and thereby can contain the biotrophic pathogen, whereas necrotrophs are combatted using JA/ET-dependent pathways (Beckers and Spoel 2006; Glazebrook 2005; Pieterse et al. 2012; Robert-Seilaniantz et al. 2011).

In plant immunity, cross talk between phytohormones is important and is believed to help achieve the best possible (defence) outcome. In phytohormone cross talk, an interaction is never defined by a single hormone, but rather by a complex network of interdependent positive and negative interactions (Pieterse et al. 2012; Robert-Seilaniantz et al. 2011; Shigenaga and Argueso 2016). The result of these interactions leads to responses in the plant, which allow it to appropriately respond to an invading pathogen.

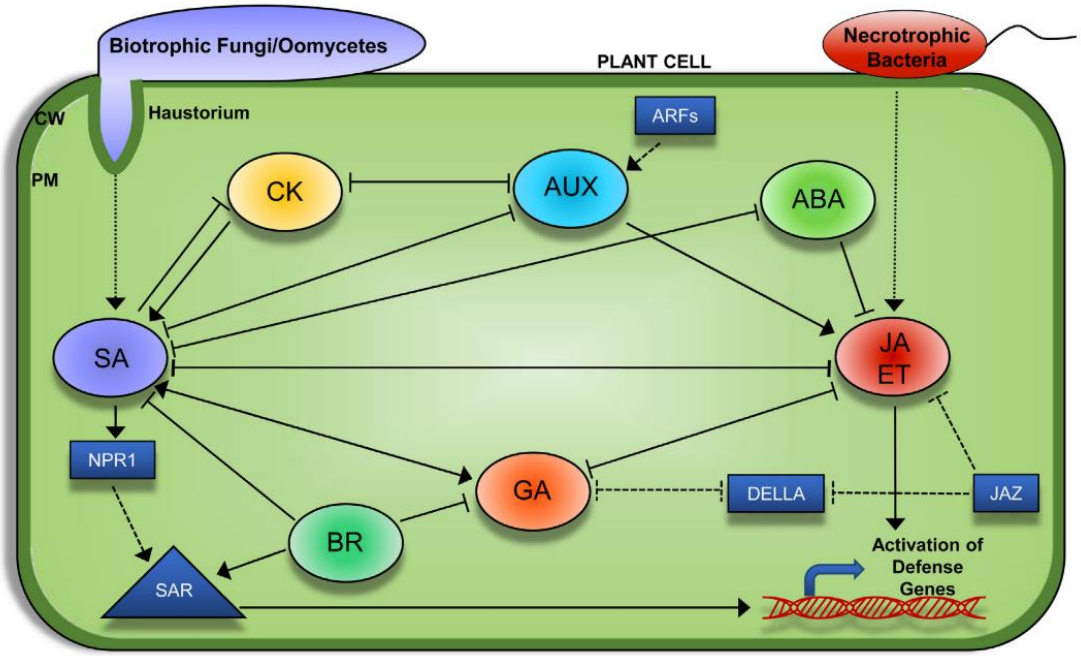

Figure 1. Hormone crosstalk in plant immunity, adapted from Shigenaga and Argueso 2016. Biotrophic pathogens are generally fended off via an up-regulation of SA-signalling, while against necrotrophic pathogens, JA/ET signalling is induced. In order to allow fine-tuning in complex environments, other hormones can influence immune responses. These hormones work either by up- or down-regulation of either SA or JA/ET signalling. Blue boxes depict transcription factors or associated proteins involved in hormone signalling. CW: cell wall; PM: plasma membrane; JA: jasmonic acid; ET: ethylene; CK: cytokinin; AUX: Auxin; GA: gibberellins; BR: brassinosteroids.

Concerning the three main players in plant defence, mostly synergistic interactions are reported between JA and ET (Glazebrook 2005; Pieterse et al. 2012; Robert-Seilaniantz et al. 2011; Zhu et al. 2011). In addition, the SA and JA signalling pathways are interdependent; there is substantial cross talk between the two, comprising synergistic as well as antagonistic interactions, depending on the defence situation (Beckers and Spoel 2006; Glazebrook 2005; Pieterse et al. 2012). SA-induced repression of JA-related expressional changes requires the presence of NPR1, but not its translocation to the nucleus (Spoel et al. 2003). Because SA-JA cross talk is often antagonistic, SA-induced resistance against biotrophic pathogens can enhance susceptibility against necrotrophic pathogens and vice versa (Robert-Seilaniantz et al. 2011; Spoel et al. 2007). In *Arabidopsis*, for example, SA induces resistance against hemibiotrophic bacteria and at the same time enhances susceptibility to the necrotrophic fungal pathogen *Alternaria brassicicola* (Spoel et al. 2007).

1.1.3 Systemic Acquired Resistance (SAR)

SAR can be seen as long-distance PTI/ETI and a sort of immune memory in plants (Gourbal et al. 2018; Hilker et al. 2016; Mauch-Mani et al. 2017), in which an infection primes non-infected, distant tissues for more effective defence responses. During SAR, SA levels in the infected and systemic tissues rise, NPR1 translocates to the nucleus, and transcripts of *PR* as well as other defence-related genes accumulate. This establishes a status of heightened alert; the plant is “primed” to respond more quickly to a secondary infection (Conrath et al. 2006; Gourbal et al. 2018). SAR is most effective against pathogens fended off via SA-dependent responses (Glazebrook 2005; Spoel and Dong 2012; Vlot et al. 2009). It is usually triggered by a local, foliar infection and elicits long-lasting, broad-spectrum resistance in systemic plant tissues (reviewed in Fu and Dong 2013; Henry et al. 2013; Klessig et al. 2018; Shah et al. 2014; Vlot et al. 2009). Many signals and genes involved in SAR have been discovered in *Arabidopsis*.

During SAR, long distance signals are generated in the infected leaves and travel to the systemic leaves, presumably via the phloem (Figure 2 and Shah et al. 2014). Recent evidence suggests that signal transmission also occurs via volatile compounds, in particular monoterpenes, which appear to be transmitted via the air (Riedlmeier et al. 2017). Phloem-mobile candidate long-distance SAR signals include methyl salicylate (Park et al. 2007), glycerol-3-phosphate (G3P) (Chanda et al. 2011; Wang et al. 2018), the C_9 dicarboxylic acid azelaic acid (AzA) (Jung et al. 2009), the diterpene dehydroabietinal (Chaturvedi et al. 2012), pipecolic acid (Pip) as well as N-hydroxy-pipecolic acid (NHP) (Chen et al. 2018; Hartmann et al. 2018; Návarová et al. 2012), and the lipid-transfer proteins DIR1 (DEFECTIVE IN INDUCED RESISTANCE 1) and DIR1-like (Champigny et al. 2013; Maldonado et al. 2002) (reviewed in Gao et al. 2015; Shah et al. 2014; Vlot et al. 2017).

As part of the systemic response, SA levels increase in systemic leaves, but less pronouncedly than in the local infected leaves (Chanda et al. 2011; Gao et al. 2014). Many of the effects caused by SA during SAR are dependent on NPR1 (Fu and Dong 2013) and *npr1* mutants display enhanced susceptibility and impaired SAR (Klessig et al. 2018). NPR1 induces transcription of defence-related genes, including *PR* genes with antimicrobial activities, which prepares the plant for a subsequent infection

(Kinkema et al. 2000; Klessig et al. 2018; Pajerowska-Mukhtar et al. 2013; Shigenaga and Argueso 2016).

There seems to be a second, parallel SAR signalling pathway that functions interdependently with SA signalling (see Figure 2). It depends on the SAR compounds Pip, ROS, NO, AzA, and G3P (Gao et al. 2015; Wang et al. 2018; Wendehenne et al. 2014). Besides SA accumulation, pathogens trigger an increase of Pip levels in infected leaves (Návarová et al. 2012). Pip in turn induces accumulation of NO and ROS, which function in a positive feedback loop with each other (Wang et al. 2014, 2018). In addition, NO and ROS increase chemical hydrolysis of C_{18} unsaturated fatty acids, producing AzA (Wang et al. 2014; Wittek et al. 2014). AzA accumulation in turn stimulates G3P biosynthesis (Yu et al. 2013). DIR1, AzA, G3P, and possibly Pip can be transported to systemic tissues via the phloem (Champigny et al. 2013; Lim et al. 2016; Návarová et al. 2012; Wang et al. 2018). The lipid transfer proteins AZI1 (AZELAIC ACID INDUCED1) and/or DIR1 might contribute to the mobility of some compounds (Cecchini et al. 2015; Champigny et al. 2013; Jung et al. 2009; Maldonado et al. 2002).

In summary, there are two parallel SAR pathways. One is mediated by SA, the other by Pip, NO, ROS, AzA and G3P (see Figure 2; Wang et al. 2018; Wendehenne et al. 2014).

Additional SAR-related compounds do not fit straight into these two pathways or their exact role in them has not been elucidated yet. The diterpene dehydroabietinal (DA) is a putative mobile signal and is translocated to distal leaves (Chaturvedi et al. 2012). Exogenous application of very low amounts of DA induces systemic immunity in *Arabidopsis* by enhancing SA accumulation and *PR1* expression throughout the plant. In addition, DA requires NPR1 as well as DIR1 and acts synergistically with AzA and possibly MeSA (Chaturvedi et al. 2012; Fu and Dong 2013; Vlot et al. 2017). Another component of SAR is LEGUME LECTIN-LIKE PROTEIN 1 (LLP1). A local infection induces *LLP1* expression both at the infection site and in the systemic tissue (Armijo et al. 2013; Breitenbach et al. 2014). LLP1 is required for systemic rather than local defence responses and possibly acts in parallel with SA (Breitenbach et al. 2014).

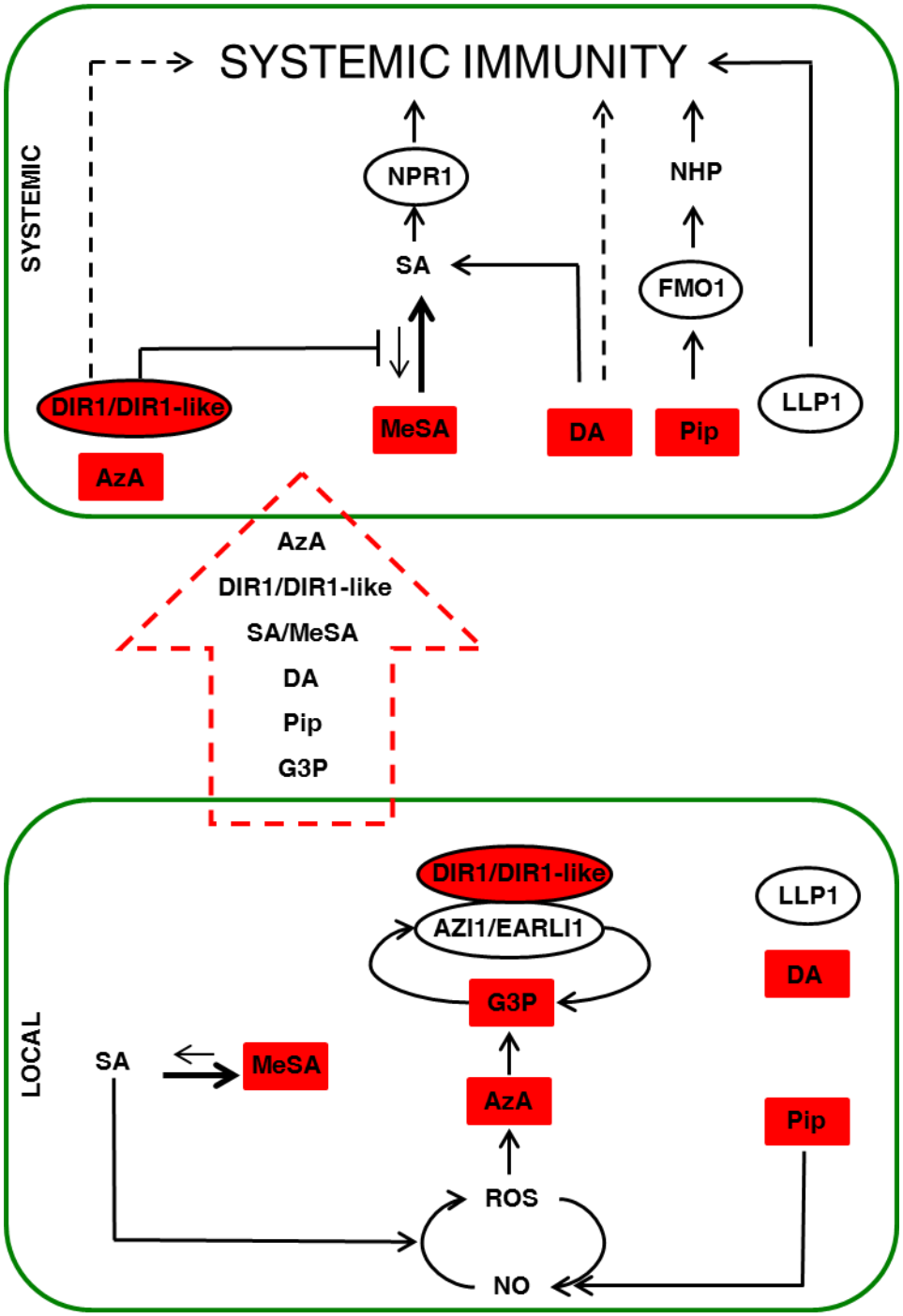

Figure 2. Signalling during systemic acquired resistance, adapted from Vlot et al. 2017. Solid arrows represent established and broken arrows represent hypothetical interactions. Proteins are shown as circles, metabolites as squares or without frame. Proteins and metabolites in red are putative phloem-mobile signals (phloem transport is implied by the broken red arrow). AzA: azelaic acid, AZI1: AZELAIC ACID INDUCED 1, DA: dehydroabietinal, DIR1: DEFECTIVE IN INDUCED RESISTANCE 1, EARLI1: EARLY ARABIDOPSIS ALUMINUM INDUCED 1, FMO1: FLAVIN-DEPENDENT MONOXYGENASE 1, G3P: glycerol-3-phosphate, LLP1: LEGUME LECTIN-LIKE PROTEIN 1, MeSA: methyl salicylate, NHP: N-hydroxypipecolic acid, NO: nitric oxide, NPR1: NONEXPRESSOR OF PATHOGENESIS-RELATED GENES 1, Pip: pipecolic acid, ROS: reactive oxygen species, SA: salicylic acid.

Some of the compounds involved in SAR accumulate in the phloem after pathogen attack, among them SA, AzA, G3P, and Pip (Jung et al. 2009; Lim et al. 2016; Métraux et al. 1990; Návarová et al. 2012). AzA and G3P were proposed to be symplastically loaded onto the phloem via plasmodesmata while SA appeared to be transported via an apoplastic route (Lim et al. 2016). Only small proportions of SA and AzA are transported to the systemic tissue, and the majority of accumulation in systemic leaves appears to come from *de novo* synthesis (Cecchini et al. 2015; Meuwly et al. 1995; Yu et al. 2013). Importantly, *de novo* biosynthesis of the SAR-related compounds SA and Pip/NHP in systemic leaves is crucial for SAR establishment; therefore, transport of these (and possibly other) molecules from the local to the systemic leaves might not be as important as previously thought (Ding et al. 2016; Vernooij et al. 1994; Wang et al. 2018).

1.1.4 Folates in induced resistance

Folate precursors accumulate in *Arabidopsis* after infection with avirulent *Pseudomonas syringae* pv. *tomato* DC3000 (Wittek et al. 2015). Furthermore, application of folic acid (Fol) to *Arabidopsis* induces resistance against virulent *Pseudomonas syringae* pv. *tomato* DC3000 and enhances transcription of the SA marker gene *PR1*, both locally and systemically (Wittek et al. 2015). This suggests that Fol is involved in SA-mediated immunity in *Arabidopsis.* In line with this hypothesis, Fol-induced resistance is dependent on SA biosynthesis and signalling (Wittek et al. 2015). Analogous to SA, Fol induces local susceptibility to the necrotrophic fungus *A. brassicicola* (Wittek et al. 2015).

In addition to *Arabidopsis*, pepper (*Capsicum annuum*) responds to the folate precursor para-aminobenzoic acid with induced resistance against *Cucumber mosaic virus* and *Xanthomonas axonopodis.* This resistance response is associated with enhanced expression of SA-dependent *PR* genes (Song et al. 2013). Whereas BTH application to pepper results in yield loss (along with enhanced resistance to *Cucumber mosaic virus* and *Xanthomonas axonopodis)*, application of the folate precursor did not cause loss of yield. In contrast, the yield of plants treated with the folate precursor was even higher than that of control plants (Song et al. 2013).

Together, this suggests that Fol and folate precursors can induce resistance against several phytopathogens in different plant species, at least in dicots, in the absence of adverse effects on yield.

1.1.5 Azelaic acid in systemic resistance

The C_9 dicarboxylic acid AzA is generated from precursor C_{18} unsaturated fatty acids and accumulates in petiole exudates of infected leaves (Jung et al. 2009; Wittek et al. 2014; Zoeller et al. 2012). Notably, AzA is systemically mobile and is symplastically loaded onto the phloem via plasmodesmata (Cecchini et al. 2015; Lim et al. 2016; Yu et al. 2013). Its transport is promoted by the lipid transfer protein AZI1, which is thought to mobilise AzA from its site of biosynthesis, the chloroplast, and to support its movement to plasmodesmata (Cecchini et al. 2015). Although it is mobile in the plant, only small proportions of AzA are transported to the systemic tissue (Yu et al. 2013).

Local application of AzA induces a SAR-like state in the treated plants, priming and thereby protecting the systemic tissue against a subsequent infection with the hemibiotrophic bacteria *Pseudomonas syringae* pv. *maculicola* or *tomato* (Cecchini et al. 2015; Jung et al. 2009; Yu et al. 2013). This induced resistance requires functional SA synthesis and signalling. In fact, AzA primes *Arabidopsis* to accumulate higher SA levels more quickly after a subsequent infection (Jung et al. 2009). In addition to SA, AzA function requires G3P, inducing its accumulation (Yu et al. 2013). Finally, AzA- as well as G3P-induced resistance are dependent on DIR1 and AZI1 (Yu et al. 2013).

Although SA is an important component of SAR and required for many processes therein, it does not seem to be the one common downstream signal that all other signals converge upon (see above text and Wendehenne et al. 2014). First, application of AzA or G3P does not induce SA accumulation (in the absence of pathogen infection) and second, SA cannot rescue SAR in mutants defective in NO, ROS, or G3P biosynthesis (Chanda et al. 2011; Jung et al. 2009; Wang et al. 2014). Vice versa, NO and ROS cannot restore SAR in SA biosynthesis mutants (Wang et al. 2014; Wendehenne et al. 2014). This implies that in *Arabidopsis*, two parallel signalling pathways that are interdependent regulate SAR. As noted above, one of these pathways depends on SA, the other on AzA, G3P, ROS, NO, and Pip (Gao et al. 2015; Wang et al. 2018; Wendehenne et al. 2014).

1.1.6 Pipecolic acid in systemic resistance

Pip is another well-researched SAR-associated signal that induces resistance upon application (Návarová et al. 2012). This is likely not due to direct defence induction by Pip, but rather by Pip priming defence against these pathogens, inducing a state of heightened alert that allows quicker and stronger defence responses (Bernsdorff et al. 2016; Návarová et al. 2012). Genes in the Pip biosynthetic pathway, *AGD2-like defence response protein 1* (*ALD1*) and *SAR-deficient4* (*SARD4*), are required for functional SAR (Ding et al. 2016; Mishina and Zeier 2006; Návarová et al. 2012; Song et al. 2004). Root application of Pip can complement the defect of *ald1* in induced resistance (Návarová et al. 2012). Pip biosynthesis via SARD4 seems to be limited to the systemic tissue and is necessary for SAR establishment, while a local accumulation of Pip does not necessarily lead to acquired resistance, strengthening the importance of *de novo* synthesis of signalling molecules in SAR (Ding et al. 2016).

Another gene involved in and required for Pip signalling is *FLAVIN-DEPENDENT MONOXYGENASE 1* (*FMO1*), which is induced systemically and essential for the establishment of SAR in systemic tissues of locally infected plants (Mishina and Zeier 2006). Pip application does not induce resistance in the *fmo1* mutant, indicating that FMO1 functions downstream of Pip in resistance induction (Bernsdorff et al. 2016; Návarová et al. 2012). Recently, FMO1 has been reported to catalyse the conversion of Pip to its bioactive form NHP (Chen et al. 2018; Hartmann et al. 2018). Analogous to Pip, NHP accumulates in infected *Arabidopsis* plants and this accumulation is crucial for SAR (Chen et al. 2018; Hartmann et al. 2018). Exogenous application of NHP to *Arabidopsis* induces resistance to *Pseudomonas syringae* pv. *maculicola* and *Hyaloperonospora arabidopsidis*, providing the same or a higher level of protection as Pip (Chen et al. 2018; Hartmann et al. 2018).

Although Pip and NHP appear to be systemically mobile (Chen et al. 2018; Návarová et al. 2012; Wang et al. 2018), experiments using petiole exudates showed that ALD1 and thus *de novo* biosynthesis of Pip and probably its bioactive derivative NHP are necessary in the systemic tissue for SAR signal recognition or propagation (Wang et al. 2018).

Recently, a molecular mechanism for Pip-mediated signalling and resistance induction has been proposed (Figure 3). Pip (and probably NHP) seems to work upstream and induce accumulation of NO and ROS, which in turn leads to accumulation of AzA, and

this induces G3P biosynthesis (Wang et al. 2018). Therefore, Pip and NHP can be placed in the NO, ROS, AzA, and G3P branch of SAR that functions parallel to SA (Wendehenne et al. 2014), although SA also amplifies systemic Pip-induced responses (Bernsdorff et al. 2016).

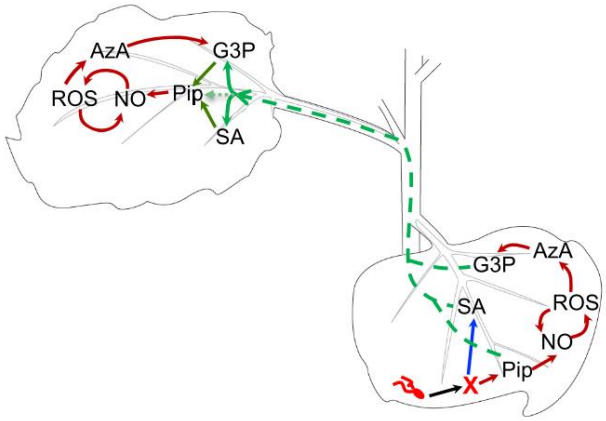

Figure 3. Molecular mechanisms in systemic acquired resistance with a focus on pipecolic acid (Pip), adapted from Wang et al. 2018. Pathogen inoculation triggers salicylic acid (SA) and Pip accumulation in infected leaves. Pip in turn induces accumulation of nitric oxide (NO) and reactive oxygen species (ROS), which function in a positive feedback loop with each other. This leads to oxidation, as a result of which azelaic acid (AzA) levels rise, which in turn stimulates glycerol-3-phosphate (G3P) biosynthesis. SA, G3P, SA, and possibly Pip can be transported via phloem. In systemic leaves, SA, G3P and Pip, which is synthesised de novo, accumulate, which again stimulates accumulation of NO, ROS and AzA, leading to systemic resistance.

Pip is produced in several plant species, both monocots and dicots, among them important crop species such as potato (*Solanum tuberosum*; Pálfi and Dézsi 1968, Zacharius et al. 1954), maize (*Zea mays*; Kiyota et al. 2015), rice (*Oryza sativa*; Pálfi and Dézsi 1968), wheat (*Triticum aestivum*; Garcia-Seco et al. 2017), and barley (*Hordeum vulgare*; Møller 1974). Whether Pip has a function in defence in these economically relevant species remains to be investigated, which is further complicated by the limited use of monocotyledonous and crop plants in SAR research.

1.1.7 Induced resistance in monocots

In monocotyledonous plants, little is known about SAR and the signalling mechanisms involved. Key players in SA signalling, including NPR1, the master regulator of SA signalling (Fu and Dong 2013; Klessig et al. 2018; Pajerowska-Mukhtar et al. 2013), several *PR* genes and SA-associated transcription factors are conserved between dicots and monocots, (reviewed in Balmer et al. 2013b; Sharma et al. 2013). Most studies in the field of monocot induced resistance focus on agronomically important

plant species such as banana (*Musa acuminata*; Wu et al. 2013), maize (*Zea mays*; Balmer et al. 2013a; Morris et al. 1998), rice (*Oryza sativa*; Sharma et al. 2013), and wheat (*Triticum aestivum*; Ahmed et al. 2017; Wang et al. 2017; Yang et al. 2013). Although monocotyledonous plants produce SA and perform SA signalling, the role of SA during their defence responses is less clear and seems to vary between different species (Klessig et al. 2018). In banana, SA is involved in resistance against *Fusarium oxysporum* f. sp*. cubense* (Wu et al. 2013). The SA analogue benzothiadiazole (BTH) induces defence in maize against downy mildew (*Peronosclerospora sorghi*) and this resistance is associated with enhanced expression of *PR1* and *PR5* (Morris et al. 1998). In rice, resistance against *Xanthomonas oryzae* pv. *oryzae* and *Magnaporthe oryzae* is dependent on SA (Sharma et al. 2013). In wheat, SA accumulates after infection with and contributes to resistance against *F. graminearum*, and this is correlated with induction of *PR1* (Makandar et al. 2012). SAR in wheat against *Puccinia striiformis* f. sp. *tritici* might be associated with G3P (Yang et al. 2013), but local resistance to the same pathogen was negatively associated with *Ta*DIR1-2, an ortholog of *At*DIR1 (Ahmed et al. 2017). Treatments with BTH induce resistance in maize (Morris et al. 1998), wheat (Görlach et al. 1996), and barley (Beßer et al. 2000; Dey et al. 2014; Jansen et al. 2005a).

SA-associated immune responses in barley (*Hordeum vulgare*) often are studied in interaction with *Blumeria graminis* f. sp. *hordei* (*Bgh*), commonly named powdery mildew, an obligate biotrophic fungal pathogen that thrives on living host cells (Thordal-Christensen et al. 2000). Since it causes reduced yield and serves as a model to study other mildews and obligate biotrophic pathogens (Hückelhoven and Panstruga 2011), *Bgh* appeared on the list of the top 10 fungal pathogens by Dean et al. 2012. In contrast to biotrophic pathogens of rice, *Bgh* inoculation does not result in SA accumulation in infected barley leaves (Hückelhoven et al. 1999; Jain et al. 2004; Vallelian-Bindschedler et al. 1998). Nevertheless, SA soil drench treatment of barley seedlings had a weak effect on *Bgh* infectivity (Beßer et al. 2000; Kogel et al. 1995), whereas soil drench treatment with BTH strongly enhanced barley resistance to *Bgh* (Beßer et al. 2000).

Notably, antagonistic cross talk between plant responses to biotrophic and necrotrophic pathogens also occurs in barley. Barley plants resistant to the biotrophic fungus *Bgh* due to a mutation at the *Mlo* locus (*Mildew Locus O*) are more sensitive to

the necrotrophic fungus *Bipolaris sorokiniana* (Kumar et al. 2001). Another barley pathogen from the necrotrophic side of the spectrum is the fungus *Pyrenophora teres*. *P. teres* is the causal agent of net and spot form net blotch, a major disease in many barley-growing areas, which can lead to severe yield loss, underlining the fungus' economic importance (Liu et al. 2011). In this work, *P. teres* is used to investigate barley responses to necrotrophic pathogens.

Recently, Dey et al. showed that in barley systemic resistance to the hemibiotrophic bacterium *Xanthomonas translucens* pv. *cerealis* (*Xtc*) can be triggered by prior infiltration of a single barley leaf with the hemibiotrophic bacterium *Pseudomonas syringae* pv. *japonica* (*Psj*) (Dey et al. 2014). Unlike SAR in *Arabidopsis*, systemic immunity in barley was neither associated with SA nor with NPR1. In addition, local infiltration of SA or its functional analogue BTH did not induce systemic resistance to *Xtc*. Rather, local methyl jasmonate (MeJA) and abscisic acid (ABA) treatments, which in *Arabidopsis* induce systemic susceptibility to *P. syringae* (Cui et al. 2005) or antagonise SAR (Yasuda et al. 2008), respectively, triggered systemic resistance in barley to *Xtc* (Dey et al. 2014). Interestingly, Illumina-based RNA sequencing revealed a link of bacteria-induced resistance in barley with transcripts of *Ethylene Response Factors* (*ERF*s) and *WRKY* transcription factors (Dey et al. 2014).

Three *ERF* and three *WRKY* transcripts were found to accumulate in the systemic leaves of locally infected barley plants: *HvERF-like*, *HvERF4*, *HvERF44411*, *HvWRKY22*, *HvWRKY28*, and *HvWRKY38*/1 (Dey et al. 2014). Subsequent qPCR analysis confirmed local as well as systemic inductions of the transcript accumulation of *HvERF-like*, *HvERF44411*, *HvWRKY22*, and *HvWRKY38*/1 at 1 or 2 days after infection with *Psj* (Dey et al. 2014). In addition, application of resistance-inducing ABA or MeJA activated local and systemic expression of *HvERF-like*, *HvERF44411*, *HvWRKY22*, and *HvWRKY38*/1 at 5 days after infiltration, except for *HvERF-like*, which was not locally induced after MeJA application (Dey et al. 2014). Therefore, it is conceivable that these ERF and WRKY transcription factors play a role in the establishment of systemic immunity in barley (Dey et al. 2014).

Induced resistance of barley will be further investigated to corroborate the biological relevance of the findings described above by mutagenizing the *ERF* and *WRKY* genes found in the RNA sequencing approach.

1.2 The CRISPR/Cas system

1.2.1 CRISPR/Cas – origins and genome editing tool

In order to investigate the role of the candidate ERF and WRKY transcription factors potentially involved in barley systemic resistance, knockout mutants need to be generated. The necessary targeted mutations can be introduced using genome editing methods like ZNFs (zinc-finger nucleases), TALENs (transcription-activator-like effector nucleases) or CRISPR/Cas (clustered regularly interspaced short palindromic repeats/CRISPR-associated). Among these techniques, CRISPR/Cas is the most simple and versatile tool.

CRISPR/Cas was originally found as part of the adaptive immune system of prokaryotes, protecting them against bacteriophage species already encountered (Barrangou et al. 2007). After the first contact, short fragments of the invader's DNA (spacers) are integrated into the prokaryote genome between two adjacent repeats at a CRISPR locus (Barrangou et al. 2007). During subsequent infections, the CRISPR locus is transcribed and processed into small interfering CRISPR RNAs (crRNAs) which assemble with the transactivating CRISPR RNA (tracrRNA) and the Cas9 protein (see Figure 4a). This complex scans the DNA for a protospacer-adjacent motif (PAM, 5'-NGG-3' for Cas9 of *Streptococcus pyogenes*), where it induces DNA-RNA hybridisation of the crRNA and the viral DNA 5' to the PAM. This destabilises the target DNA and allows Cas9 to introduce a double-strand break, thereby destroying the viral DNA and establishing immunity (Jinek et al. 2012).

Thus, CRISPR/Cas allows RNA-guided sequence-specific cleavage of DNA, making it a good candidate for inducing targeted DNA changes at almost any loci with known sequences. The only restriction is the presence of a GG sequence in proximity to the desired cut site (Jinek et al. 2012). In addition, since it relies on base-pairing for specificity, CRISPR/Cas is easier to use than previously known programmable endonucleases (TALENs and ZFNs), which use amino acid sequences to confer specific DNA binding (Komor et al. 2017). For use in the lab, the CRISPR/Cas system was simplified by uniting the crucial parts of crRNA and tracrRNA in one molecule, thereby creating the (single) guide RNA (Jinek et al. 2012). This sgRNA or gRNA possesses a variable part, into which a target sequence of 20 bp, the guide, can be inserted to "guide" the Cas9 protein to the sequence-identical site of interest and

induce a double-strand break (see Figure 4b). Most often, Cas9 from *S. pyogenes* is used. However, Cas9 proteins from several other organisms have come into use recently because they recognise other PAM sequences, e.g., for *Staphylococcus aureus* Cas9 5'-NNGRRT-3' (Komor et al. 2017). This further increases the number of DNA sequences that can be targeted during Cas9-induced mutagenesis, because the Cas9 can be choosen according to the sequence that is present at the site of interest instead of having to choose the target site according to the required PAM sequence.

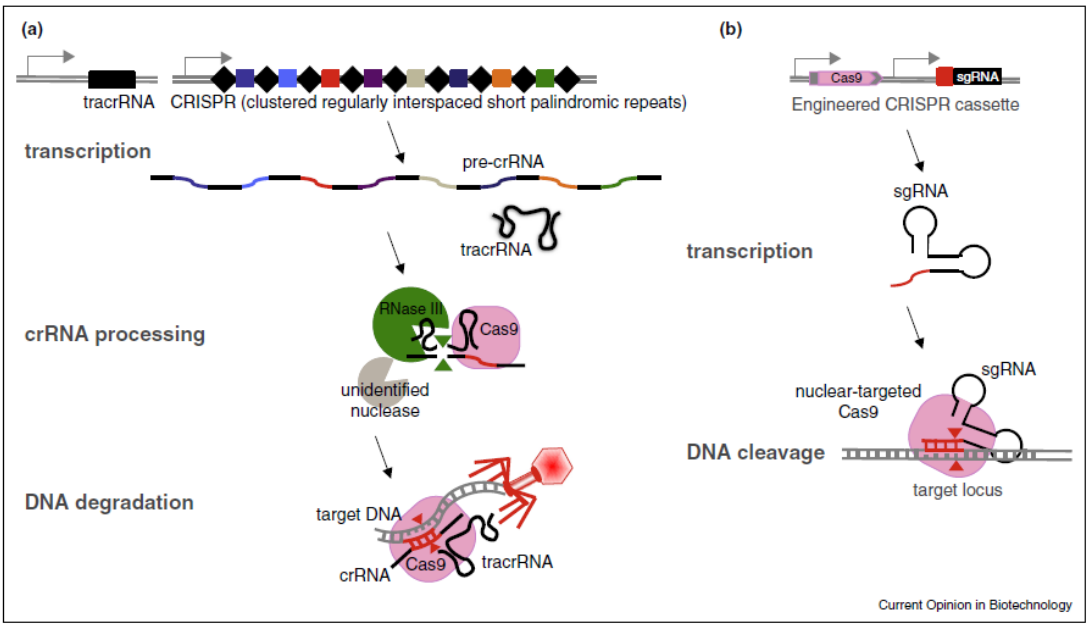

Figure 4. The CRISPR/Cas system in nature (a) and laboratory (b), adapted from Belhaj et al. 2015. (a) Short fragments of viral DNA are integrated into the host genome between two repeats of a CRISPR locus. The CRISPR region is transcribed and processed into small interfering CRISPR RNAs (crRNAs), assembling with the transactivating CRISPR RNA (tracrRNA) and the Cas9 protein. This complex induces DNA-RNA hybridisation of the crRNA and the viral DNA, thereby destabilising the target DNA and allowing Cas9 to introduce a double-strand break, destroying the viral DNA, and establishing immunity. **(b)** Elements of CRISPR/Cas needed for generation of mutations in lab. The Cas9 protein and the single guide RNA (sgRNA), which unites the crucial parts of crRNA and tracrRNA, are expressed from a transgene. Cas9 and sgRNA form a complex that screens DNA for the target locus where a double-strand break is formed and a mutation can arise.

In most cases, the double-strand break is repaired by non-homologous end joining (Bortesi and Fischer 2015). This often results in a random insertion or deletion, which can produce a frameshift mutation and thus a gene knockout.

Since there are almost no limitations for the target and it is easy to adjust the system for different targets of Cas9, the use of the CRISPR/Cas system has rapidly increased. The system has been modified multiple times, starting with the simplification of the Cas9-associated RNAs (Jinek et al. 2012) and the use of Cas9 derived from different

organisms as mentioned above. Usually, the sequences for *Cas9* and the gRNA are introduced by transforming the plant, which then possesses a transgene from which Cas9 and the gRNA are expressed. A recent development is the application of ribonucleoprotein complexes consisting of purified Cas9 and associated gRNA. These complexes can be introduced into cells of plant embryos by particle bombardment. Plants grown from these embryos will have mutations without having possessed a transgene (Liang et al. 2017).

In this work, the classical transgene method for CRISPR/Cas gene editing will be used. Immature barley embryos will be transformed with *Agrobacterium tumefaciens* carrying a vector that allows for integration of a *Cas9*- and gRNA-containing transgene into the barley genome. This transgene will be expressed and Cas9 as well as gRNAs will lead to the mutagenesis of the target genes.

Several species have been modified using the CRISPR/Cas method. These include different animals but also plant species (reviewed in Belhaj et al. 2015; Bortesi and Fischer 2015) such as *Arabidopsis thaliana*, *Nicotiana benthamiana* (Li et al. 2013), rice, wheat (Shan et al. 2013), and barley (Kapusi et al. 2017; Kumar et al. 2018; Lawrenson et al. 2015).

1.2.2 CRISPR/Cas in barley

Recently, CRISPR/Cas has been successfully used to generate mutations in barley (Kapusi et al. 2017; Kumar et al. 2018; Lawrenson et al. 2015). The reported mutation rates varied remarkably, lying between 10 and 78% in the transformed T_0 lines, which can be explained by the use of different vector sets encoding different promoters to drive expression of CRISPR/Cas components. Mutations were reported to be heritable to T_1 and T_2 generations, by which the transgene encoding the Cas9 protein can be allowed to segregate out and transgene-free, homozygous mutants are produced. Two studies reported the generation of transgene-free, homozygous mutant plants already in the T_1 generation (Kapusi et al. 2017; Kumar et al. 2018). It should be noted that the mutation rates reported in these studies (about 78%) were remarkably higher than the mutation rates reported in the third paper (10-23%, Lawrenson et al. 2015). Therefore, it seems that the mutation rates are the main determinants as to how fast homozygous plants can be generated. In summary, CRISPR/Cas has been shown to work effectively in barley and can be used for efficient generation of knockout mutants.

One of the studies on CRISPR/Cas in barley reported a resistance phenotype of Cas9-edited plants (Kumar et al. 2018). CRISPR/Cas was used to knockout *MORC1* (*Microrchidia1*). *MORC1* loss of function lead to increased resistance of barley plants to *Bgh* and *F. graminearum*. This was associated with an increased expression of defence-related genes (*HvPR1b*, *HvPR2*, and *HvPR5*) in *morc1* plants that became more pronounced after infection with *Bgh*.

Here, CRISPR/Cas will be used for mutagenesis of *ERF* and *WRKY* transcription factors associated with bacteria-induced resistance in barley in order to study possible immunity-related phenotypes in the mutant plants. This will clarify whether the *ERF*s and *WRKY*s play a role in (induced) defence responses of barley.

1.3 Project objective

The main aim of this study was to investigate induced resistance in barley in more detail. First, the effect of *Arabidopsis* SAR-related molecules on barley immune responses against different pathogens was tested. The compounds that were investigated for their role in defence are SA, Fol, AzA, and Pip, which all induce resistance in *Arabidopsis* against the bacterium *P. syringae* (Breitenbach et al. 2014; Jung et al. 2009; Návarová et al. 2012; Wittek et al. 2015). Their effects were tested on defence of barley against the hemibiotrophic bacterium *Xtc*, the biotrophic fungus *Bgh*, and the necrotrophic fungus *P. teres*. With these barley pathogens, different pathogenic lifestyles (biotrophic, hemibiotrophic, and necrotrophic) and bacteria as well as fungi are covered, providing insights into different defence mechanisms used by barley plants.

Second, chemically induced defence responses of barley were compared to those of *Arabidopsis* to uncover signalling routes used in barley, in which little is known about induced resistance processes in comparison to the model plant *Arabidopsis*. Similarities and differences in the molecular mechanisms associated with these processes in the two plant species were examined, which can help in the transfer of knowledge between model and crop plants. In addition, chemically and bacteria-induced resistance of barley were compared to examine if these defence responses share signalling components.

Third, site-directed mutagenesis was used in order to create mutants of the transcription factors whose transcript accumulation was found to be associated with bacteria-induced systemic resistance in barley (Dey et al. 2014). Knockout mutants of candidate *ERF* and *WRKY* genes were generated using the genome-editing tool CRISPR/Cas for mutagenesis of barley. Since the CRISPR/Cas vectors used in this work (provided by Johannes Stuttmann, Universität Halle) had not been used in barley before, a transient system for quick validation of their functionality for Cas9-induced generation of mutations in barley was established. Stable transgenic plants expressing Cas9 and a gRNA targeted at the gene(s) of interest were generated with the help of collaborators in Gießen (Karl-Heinz Kogel and Jafargholi Imani). Cas9-induced mutagenesis lead to plants with loss of function mutations in the candidate genes. These mutant plants can be used in experiments to investigate the physiological relevance of the *ERF*s and *WRKY*s in defence responses of barley; in these experiments, it can be examined whether the gene knockout leads to changes in induced resistance.

2 Results

2.1 Salicylic acid-related compounds in induced resistance of barley

2.1.1 Folic acid and azelaic acid enhance the susceptibility of barley to *Xanthomonas translucens* pv. *cerealis*

Exogenous SA or BTH application enhances the resistance of barley to the biotrophic fungus *Bgh* (Beßer et al. 2000), but not to the hemibiotrophic bacterium *Xtc* (Dey et al. 2014). Here, the barley response to *Xtc* was examined after application of Fol and AzA, which each trigger SA-mediated resistance and/or SAR against the hemibiotrophic bacterium *P. syringae* pv. *tomato* in *Arabidopsis* (Jung et al. 2009; Wittek et al. 2015). In 3-week-old barley plants, the first true leaves were syringe-infiltrated with 50 or 500 µM Fol, 1 mM AzA, or the corresponding 0.025% MeOH mock control. Five days later, the second true leaves of the treated plants were syringe-infiltrated with *Xtc* and the resulting *in planta Xtc* titres determined at 4 days post-inoculation (dpi). Similar to SA, Fol and AzA did not enhance the systemic immunity of barley to *Xtc* (Figure 5). Whereas AzA application did not influence *Xtc* growth in the systemic tissue (Figure 5B), growth of the systemic *Xtc* inoculum was enhanced by a local Fol application (Figure 5A), suggesting the induction of enhanced susceptibility in barley against *Xtc* by Fol.

Fol enhances *Arabidopsis* resistance to *P. syringae* when applied at concentrations of 50 to 100 µM (Wittek et al. 2015). If 50 µM Fol was applied to the first leaves of 3-week-old barley plants, the growth of subsequently applied *Xtc* bacteria in the systemic leaves was enhanced in three out of ten experiments and a strong tendency in the same direction was observed in further two experiments. Analysing all experiments together, the data suggest that application of 50 µM Fol can, similarly to 500 µM Fol, enhance barley systemic susceptibility to *Xtc* (Figure 5C), albeit perhaps less robustly.

Next, local barley responses to the compounds used above were tested. To this end, 1 mM SA, 500 µM Fol, 1 mM AzA, or the appropriate mock control were applied onto the leaves of 4-week-old barley plants by spray treatment. One day later, treated leaves were syringe-infiltrated with *Xtc* and the resulting in planta *Xtc* titres determined at 4 dpi (all experiments were performed by Marion Wenig). SA and Fol appeared to

moderately elevate local *Xtc* titres, with a significant trend observed only after Fol treatment. AzA application caused an increase of the *Xtc* titre (Figure 6). Thus, in addition to systemic susceptibility, Fol might also moderately enhance the local susceptibility of barley to the hemibiotrophic bacterium *Xtc.* The effect appeared more robust in the systemic compared to local treated tissues (Figure 5A/C, Figure 6). AzA enhanced local, but not systemic susceptibility to *Xtc*.

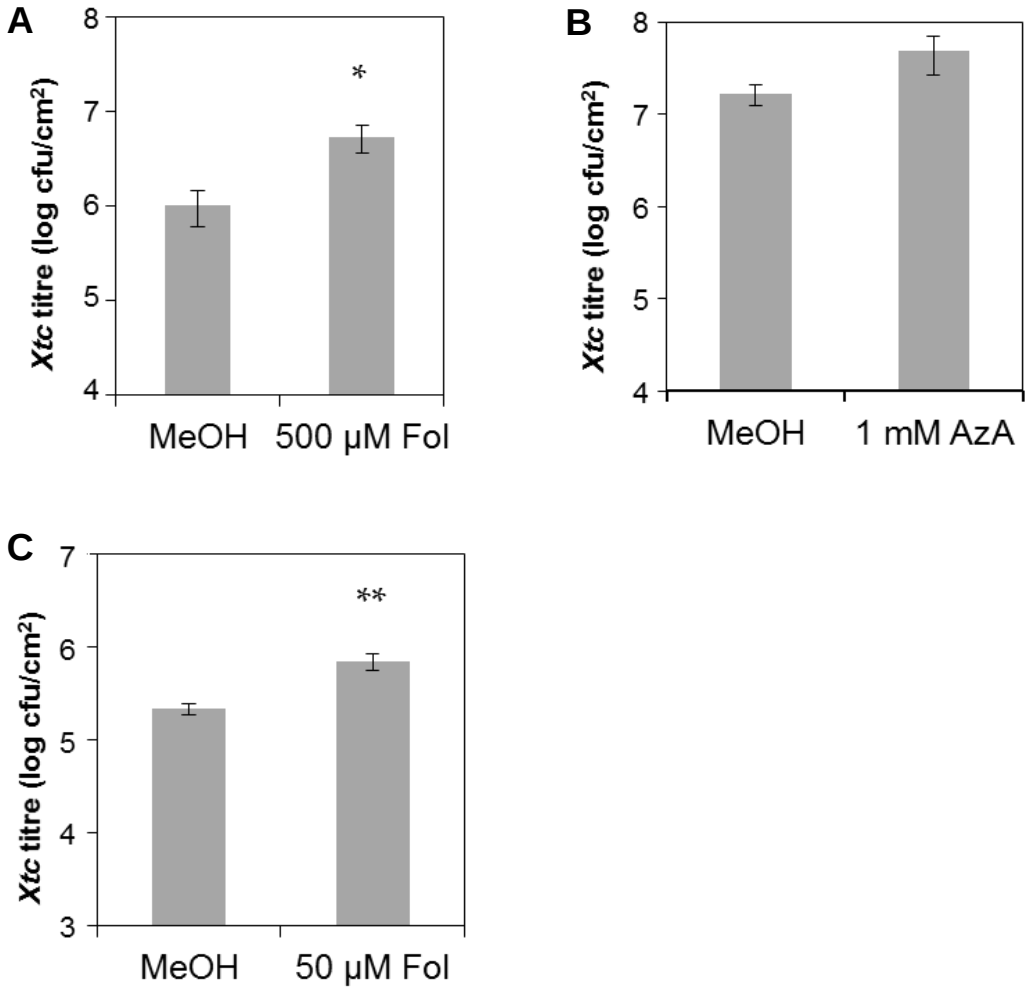

Figure 5. *Xanthomonas translucens pv. cerealis* (*Xtc*) titres in the systemic leaves of barley after local application of folic acid (Fol) or azelaic acid (AzA). Barley cultivar Golden Promise (GP) plants were infiltrated in the first true leaf with 0.025% methanol (MeOH) as control, 500 µM Fol **(A)**, 1 mM AzA **(B)**, or 50 µM Fol **(C)** in 10 mM $MgCl_2$ as indicated below the panels. Five days later, the second true leaves of the plants were inoculated with *Xtc* by syringe infiltration. The resulting *Xtc* titres in leaf 2 at 4 dpi are shown. Bars represent the average of 18-36 replicates from 5 (A: 4x greenhouse, 1x growth chamber; B: 3x greenhouse, 2x growth chamber) to 9 (C: 8x greenhouse, 1x growth chamber) biologically independent experiments +/- standard error; replicates were as follows: **(A)** MeOH: 19 (4+4+3+4+4), Fol: 18 (4+4+3+4+3), **(B)** MeOH: 19 (4+3+3+4+5), AzA: 20 (4+4+4+4+4), **(C)** MeOH: 34 (4+3+4+4+3+4+4+4+4+4), Fol: 36 (4+4+4+4+4+4+4+4+4+4). Asterisks above bars indicate statistically significant differences from the control treatments (*t*-test; * P<0.05, ** P<0.005).

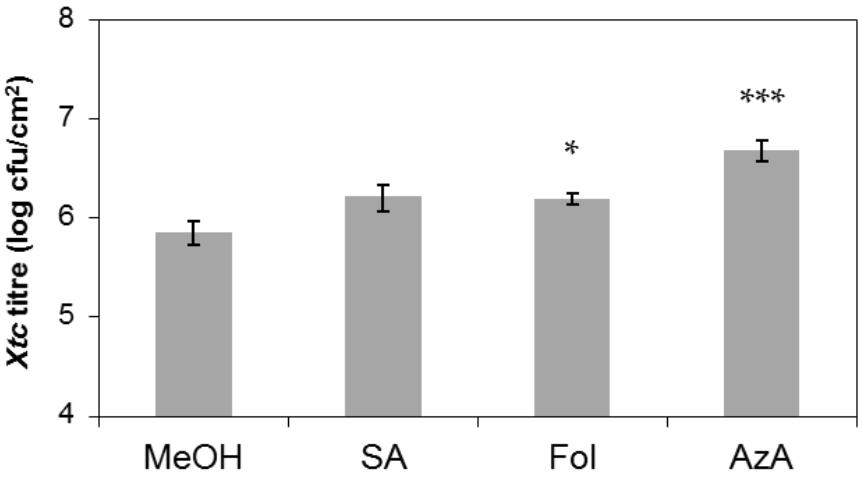

Figure 6. *Xtc* titres in salicylic acid (SA)-, Fol- and AzA-treated barley plants. Barley cultivar GP plants were sprayed with 0.05% MeOH as control, 1 mM SA, 500 µM Fol, or 1 mM AzA in 0.01% Tween-20 as indicated below the panel. One day later, the second true leaves of the plants were inoculated with *Xtc* by syringe infiltration. The resulting *Xtc* titres in leaf 2 at 4 dpi are shown. Bars represent the average of 8-9 replicates from 3 biologically independent greenhouse experiments +/- standard error, replicates were as follows: MeOH: 9 (3+3+3), SA: 9 (3+3+3), Fol: 8 (3+3+2), AzA: 8 (3+3+2); asterisks above bars indicate statistically significant differences from the mock control treatment (one-way ANOVA and post-hoc Dunnett's test, * P<0.05, *** P<0.0005). The experiments were performed by Marion Wenig.

2.1.2 Folic acid enhances the resistance of barley to powdery mildew

In *Arabidopsis* Fol triggers SA-mediated immunity against hemibiotrophic bacteria (Wittek et al. 2015). In barley, SA and in particular its functional analogue BTH enhances immunity against the biotrophic fungus *Bgh* while Fol enhances barley susceptibility to *Xtc* (Figure 5, Figure 6; Beßer et al. 2000). Therefore, the effects of SA, Fol, and AzA on barley susceptibility to *Bgh* were compared. To this end, the first true leaves of 3-week-old barley plants were syringe-infiltrated with 1 mM SA, 500 µM Fol, 1 mM AzA, or 0.025% MeOH as control treatment. Five days later, the plants were inoculated with *Bgh*. The resulting *Bgh* infection was quantified on a fluorescence microscope 6 days later. The fungus was stained using the fluorescent dye DAF-FM DA (4-amino-5-methylamino-2',7'-difluorofluorescein diacetate), which usually is used to detect and quantify NO (Kojima et al. 1999) and, as shown in Figure 7, also has a high affinity for *Bgh*.

If leaf discs from *Bgh*-infected leaves were stained with DAF-FM DA, the resulting fluorescence intensities reflected visual differences in *Bgh* infection levels and were quantified as a measure for fungal growth (Figure 8). To this end, the stained leaf discs

were loaded onto 96-well plates and scanned by a spinning disc (confocal) microscope (Figure 7).

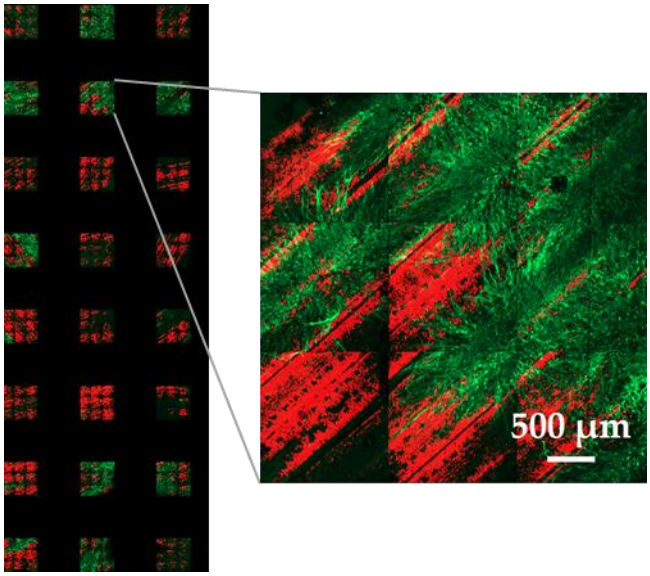

Figure 7. Merged z-stack 3x3 tiled images of 4-amino-5-methylamino-2',7'-difluoro-fluorescein diacetate (DAF-FM DA)- stained discs of *Blumeria graminis* f. sp. *hordei* (*Bgh*)-infected barley (GP) leaves in the first 3 columns of a 96-well plate. Enlarged: merged image of a single well. Chlorophyll fluorescence is shown in red, DAF-FM DA fluorescence in green.

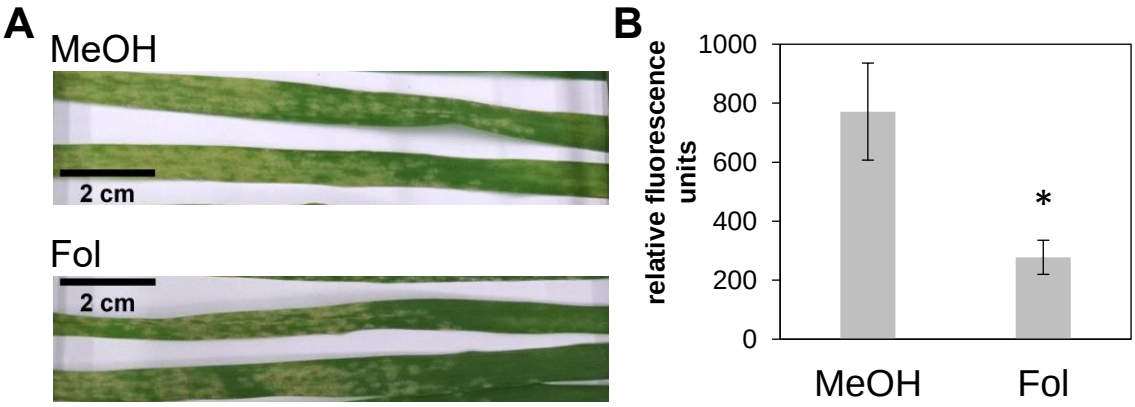

Figure 8. Fol induces resistance to *Bgh*. Barley cultivar GP plants were infiltrated in the first true leaf with 0.025% MeOH as control and 500 µM Fol in 10 mM $MgCl_2$ as indicated above the pictures **(A)** or below the panel **(B)**. Five days later, the plants were infected with *Bgh* spores. **(A)** Photographs of the second (systemic) leaves, taken on the day of the harvest, 6 days after infection. (**B**) Leaf discs were cut out of the leaves photographed in **(A)** and stained with DAF-FM DA. Fluorescence was recorded using a spinning disc (confocal) microscope. Bars represent the average of 22 (MeOH) to 23 (Fol) replicates from one experiment +/- standard error; asterisk above bar indicates statistically significant difference from the control treatment (*t*-test, $P < 0.05$).

A local infiltration of Fol in leaf 1 of barley reduced *Bgh* growth on the Fol-treated leaf (Figure 9A) as well as on systemic leaf 2 of the treated plants (Figure 9B) as evidenced by a ~50% decrease in DAF-FM DA fluorescence on the leaves of *Bgh*-infected Fol-treated compared to mock-treated plants. In contrast, SA and AzA infiltration did not induce significant changes in the DAF-FM DA fluorescence of the treated leaves and thus had no local effect on *Bgh* growth (Figure 9A). Nevertheless, SA and AzA

appeared to reduce *Bgh* propagation, although the differences to the control were not significant (P=0.0518 in the case of SA, Figure 9A). In the systemic leaves, *Bgh*-associated DAF-FM DA fluorescence was decreased by SA and AzA to a similar extent as by Fol (Figure 9B). Thus, Fol might induce local and systemic resistance to *Bgh*, while SA and AzA appear to trigger systemic resistance.

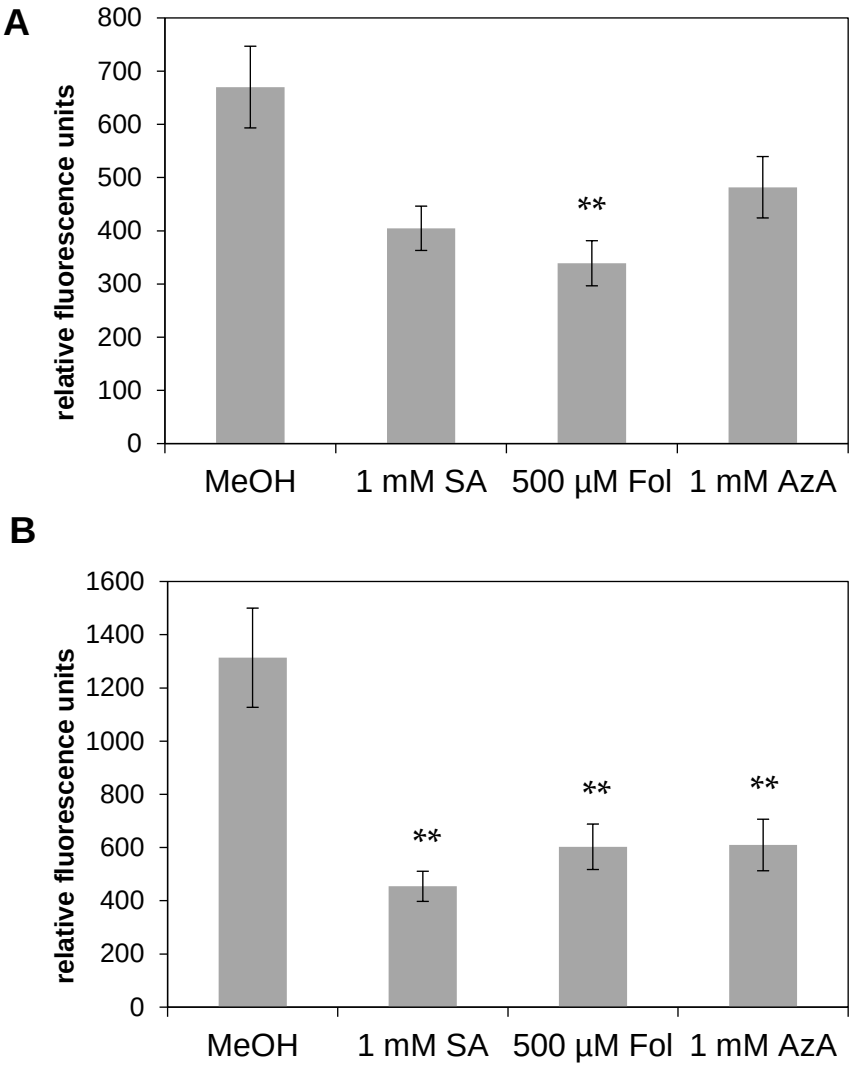

Figure 9. Relative fluorescence of DAF-FM DA staining of *Bgh* in leaves of barley plants after application of SA, Fol, or AzA to leaf 1. Barley cultivar GP plants were infiltrated in the first true leaf with 0.025% MeOH as control, 1 mM SA, 500 µM Fol, or 1 mM AzA in 10 mM $MgCl_2$ as indicated below the panel. Five days later, the plants were infected with *Bgh* spores. Leaf discs were cut out of the first (local) **(A)** and second (systemic) **(B)** true leaf and stained with DAF-FM DA. Fluorescence was recorded using a spinning disc (confocal) microscope. Bars represent the average of 37-64 replicates from 2 (SA treatment in B) to 3 (all other treatments) independent experiments +/- standard error; replicates were as follows: **(A)** MeOH: 57 (22+14+21), SA: 62 (22+16+24), Fol: 55 (19+19+17), AzA: 58 (19+18+21); **(B)** MeOH: 55 (20+22+13), SA: 37 (17+20), Fol: 64 (21+23+20), AzA: 53 (6+24+23). Asterisks above the bars indicate statistically significant differences from the mock control treatment (one-way ANOVA and poct hoc Dunnett's test, ** P<0.005).

2.1.3 Salicylic acid-related compounds do not alter barley susceptibility to *Pyrenophora teres*

In *Arabidopsis*, SA induces local, but not systemic susceptibility to the necrotrophic fungal pathogen *Alternaria brassicicola* (Spoel et al. 2007; Wittek et al. 2015). This most likely happens due to negative crosstalk between the SA and JA pathways, with SA inhibiting JA-mediated defence against *A. brassicicola*. A similar effect was observed for Fol, as its application increased the size of lesions caused by *A. brassicicola* on the treated, but not on systemic leaves (Wittek et al. 2015).

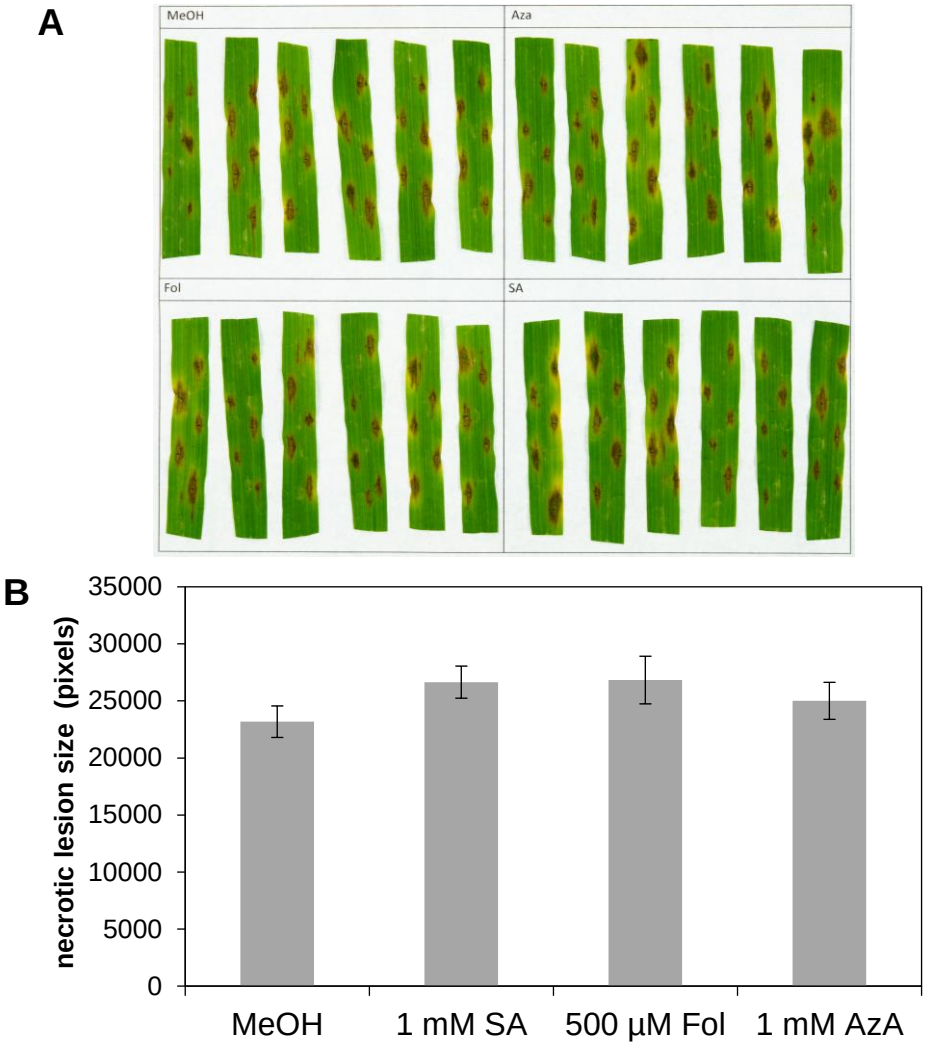

Figure 10. Lesions caused by *Pyrenophora teres* on the second leaves of barley after application of SA, Fol, or AzA on leaf 2. Barley cultivar GP plants were infiltrated in the second true leaf with 0.025% MeOH as control, 1 mM SA, 500 µM Fol, or 1 mM AzA in 10 mM $MgCl_2$ as indicated. One day later, the same leaves were inoculated with *P. teres* by pipetting droplets of a solution containing *P. teres* spores onto the leaf surface. The resulting necrotic lesions were photographed at 4 dpi **(A)** and measured using ImageJ **(B)**. Bars in **(B)** represent the average of 35 replicates from 6 (Fol) or 42 replicates from 7 (all other treatments) independent experiments (each experiment with 6 replicates per treatment, except one experiment with Fol comprising 5 replicates) +/- standard error.

Here, the effects of SA, Fol, and AzA on barley local and systemic defence responses to the necrotrophic fungus *P. teres* were examined. To this end, leaves of 3-week-old barley plants were syringe-infiltrated with 1 mM SA, 50 or 500 µM Fol, 1 mM AzA, or 0.025% MeOH as control treatment. The same or systemic leaves were inoculated with *P. teres* 1 or 5 days later, respectively, and necrotic lesions were measured at 4 dpi using the ImageJ macro PIDIQ (Laflamme et al. 2016), which was modified to recognise the brown lesions caused by *P. teres*. The outcome varied strongly between different replicate experiments. Strikingly, SA application caused increases in *P. teres* lesion sizes in 4 out of 8 experiments if leaves systemic to the site of SA treatment were inoculated. However, taking all data together SA, Fol, and AzA did not significantly influence *P. teres* lesion sizes either locally (Figure 10) or systemically (Supplemental Figure 1), suggesting that these compounds do not affect the susceptibility of barley to *P. teres*.

2.2 The role of pipecolic acid in induced resistance of barley

2.2.1 Pipecolic acid accumulates in barley after infection and induces resistance to *Xanthomonas translucens* pv. *cerealis*

The hemibiotrophic bacterium *Psj* has been shown to induce systemic immunity in barley against the hemibiotrophic bacterium *Xtc*. This form of systemic immunity phenotypically resembles *Arabidopsis* SAR (Dey et al. 2014). In order to test if this is indeed a similar process, an inter-species petiole exudate experiment was conducted. Petiole exudates (PEX) from *Psj*-infiltrated barley cv. Barke leaves were collected and infiltrated into leaves of wild type *Arabidopsis* plants of the cultivar Col-0. Two days later, leaves were harvested and analysed for transcript accumulation of the SAR marker gene *PR1*. *PR1* transcript accumulation was significantly induced in *Arabidopsis* by PEX from *Psj*-treated compared to mock-treated barley plants (Supplemental Figure 2, experiment performed by Claudia Knappe). Since barley PEX induced a marker gene of SAR in *Arabidopsis*, both plant species might share one or more SAR signals.

Because further experiments by others showed an elevated accumulation of Pip in the PEX and leaves of *Psj*-treated compared to mock-treated barley plants (Bauer, Dey, Knappe, Lange, and Vlot, unpublished), it was tested if Pip induces resistance in

barley if exogenously applied. To this end, Pip was applied to barley plants by soil drench and the plants were subsequently infected with *Xtc*. The resulting *in planta Xtc* titres at 4 dpi were significantly lower in plants pre-treated with Pip compared to those in control plants (Figure 11).

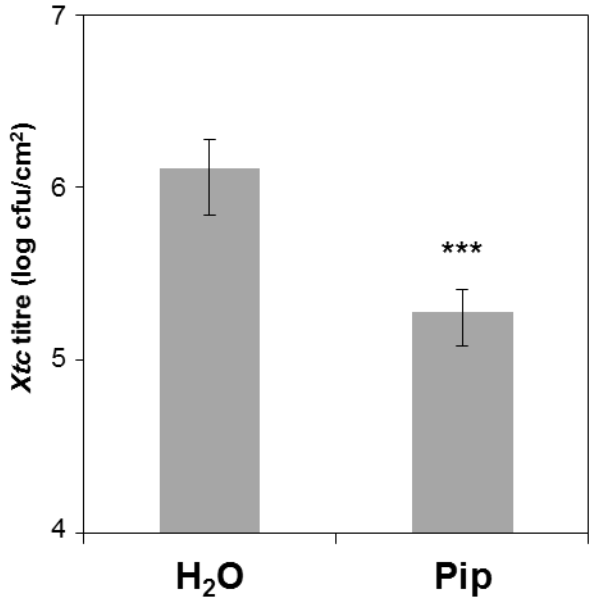

Figure 11. *Xtc* titres in pipecolic acid (Pip)-treated barley plants (GP). Pip (or H_2O as a control) was applied by soil drench and 3 days later, plants were infected with *Xtc* using syringe infiltration. Leaves were harvested to determine *Xtc* titres at 4 days after infection. Bars show one representative experiment plus/minus standard deviation with 5 plants per treatment. This experiment was performed 11 times, of which 10 disclose a similar result to the one shown above. Asterisks above bars indicate statistically significant difference from the control treatment (*t*-test; *** P<0.0005).

Thus, Pip accumulates in barley leaves and PEX after infection with *Psj* and induces resistance against *Xtc*, suggesting a possible role of Pip in barley immune responses, including in *Psj*-induced systemic or SAR-like resistance.

2.2.2 *Pseudomonas syringae* pv. *japonica* and pipecolic acid induce resistance in barley against powdery mildew

Barley is an important crop plant and yield losses due to phytopathogens are a realistic problem. Therefore, it was tested if *Psj* and Pip can induce resistance in barley against the agronomically relevant barley-specific powdery mildew pathogen *Bgh*. *Bgh* or powdery mildew of barley is an obligate biotrophic fungus that needs living host cells to thrive (Thordal-Christensen et al. 2000). To study barley immune responses to *Bgh* 3-week-old barley plants were first inoculated with *Psj* in the first true leaf or mock-treated. Five days later, (systemic) leaf 2 of the treated plants was inoculated with *Bgh*. Another 6 days later, the infected leaves were stained with DAF-FM DA to visualize *Bgh* (Figure 7 and Lenk et al. 2018). The resulting relative fluorescence intensities as obtained by imaging with a spinning disc confocal microscope reflected visual differences in *Bgh* infection levels (Figure 12A+B). Therefore, the DAF-FM DA

fluorescence intensities were used as a measure of fungal growth. First, *Bgh*-associated DAF-FM DA fluorescence was strongly reduced if the plants had been pre-treated with *Psj* (Figure 12C), with fluorescence of treated plants being circa 25% that of control plants. This reduction in fluorescence indicates a reduction of fungal mass and therefore an induction of systemic resistance to *Bgh* by *Psj*.

Second, it was tested if Pip likewise induces resistance to *Bgh* if exogenously applied. To this end, Pip was administered to barley plants by soil drench and the plants were subsequently infected with *Bgh*. The infected leaves were stained with DAF-FM DA at 6 dpi to measure fungal growth. As with *Psj*, the *Bgh*-associated relative DAF-FM DA fluorescence of Pip- and H_2O-treated plants corresponded to visual differences in disease symptoms caused by the fungus (Figure 12D+E). Fluorescence was reduced in Pip-pre-treated plants in comparison to the H_2O control (Figure 12F) to a similar level as seen with *Psj.* Taken together, the data suggest that Pip enhances barley resistance to *Bgh* and might be involved in *Psj*-induced resistance to *Bgh*.

Figure 12. Influence of *Psj* and Pip treatment of barley (GP) on resistance against *Bgh*. Barley was syringe-infiltrated with *Psj* or 10 mM $MgCl_2$ (M, mock) as a control as indicated and 5 days later, plants were infected with *Bgh* **(A+B+C)**. Pip (or H_2O as a control) was applied by soil drench and 3 days later, plants were infected with *Bgh* **(D+E+F)**. The second leaves of the inoculated plants were harvested at 6 days after infection. **(A+D)**: Photos of exemplary second leaves of plants pre-treated with *Psj* in their first leaves **(A)** or Pip **(D)**, taken at the day of the harvest. Ctrl denotes uninfected control plants. Scale bar: 20 mm. **(B+E)**: Leaf discs were cut out of the second leaves and stained with DAF-FM DA to determine *Bgh* propagation. Fluorescence was recorded with a spinning disc confocal microscope. Displayed are merged z-stack 3 × 3 tiled images of stained discs from one experiment, loaded in the first 8 columns of a 96-well plate. Enlarged: exemplary merged images of a single well, showing mock- (upper) and *Psj*-treated (lower) plants **(B)** or H_2O- (upper) and Pip-treated (lower) plants. **(E)**. Chlorophyll fluorescence is shown in red, DAF-FM DA fluorescence in green. Scale bar: 500 µm. **(C+F)**: Relative fluorescence of DAF-FM DA staining of *Bgh* in leaves of barley plants treated with *Psj* **(C)** or Pip **(F)**. Bars show one representative experiment plus/minus standard error. **(C)** was repeated 7 times, of which 5 experiments show similar results to the one presented above. **(F)** was repeated 4 times with similar results. Asterisks above bars indicate statistically significant difference from the control treatment [**(C)** *t*-test, * P<0.05; **(F)** *t*-test with Welch's correction, *** P<0.0005].

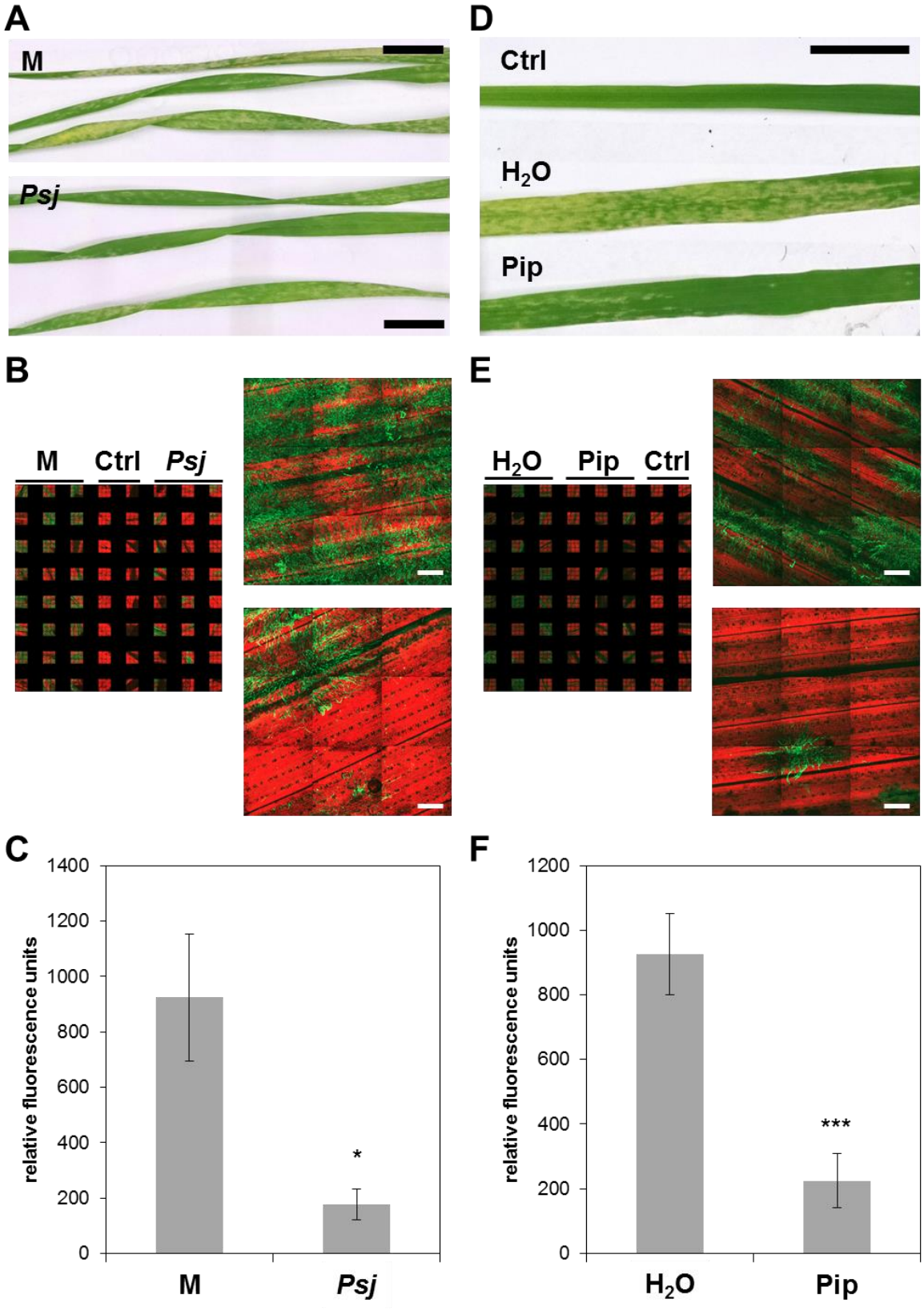
A
M
Psj
D
Ctrl
H2O
Pip
B
M
Ctrl
Psj
E
H2O
Pip
Ctrl
C
relative fluorescence units
1400
1200
1000
800
600
400
200
0
*
M
Psj
F
relative fluorescence units
1200
1000
800
600
400
200
0
***
H2O
Pip

2.2.3 *Pseudomonas syringae* pv. *japonica* but not pipecolic acid induces susceptibility in barley to *Pyrenophora teres*

SAR and SA induce resistance in *Arabidopsis* against (hemi)biotrophic bacteria and at the same time enhance susceptibility in *Arabidopsis* to the necrotrophic fungus *Alternaria brassicicola* (Spoel et al. 2007; Wittek et al. 2015). It is possible that a similar trade-off occurs in barley. To address this, *Psj*-infected or Pip-treated barley plants were inoculated with the necrotrophic fungus *P. teres*. *P. teres* is the causal agent of barley net blotch, a wide-spread disease that causes severe yield losses (Liu et al. 2011). In order to test for induced resistance against *P. teres*, 3-week-old barley plants were pre-treated with either *Psj* or Pip as described above and subsequently infected on (systemic) leaf 2 with *P. teres* by placing 5 spore-containing droplets on the leaf surface. Inoculated leaves were photographed at 4 dpi and the sizes of the developed necrosis and chlorosis were evaluated using ImageJ and the macro PIDIQ (Laflamme et al. 2016; Lenk et al. 2018). Since single experiments only showed tendencies, 6 and 9 experiments were combined to generate Figure 13A and B, respectively.

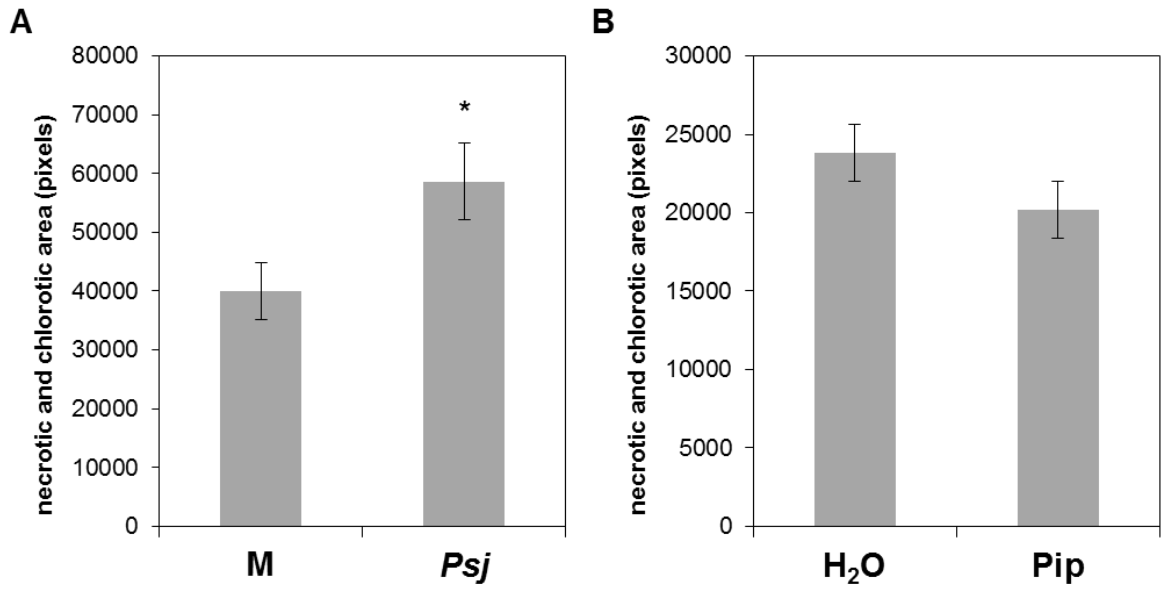

Figure 13. Size of necrotic and chlorotic area caused by *P. teres* on the leaves of barley (GP) treated with *Psj* (A) or Pip (B). (A) Barley was syringe-infiltrated with *Psj* or 10 mM $MgCl_2$ (M, mock) as a control in the first true leaf as indicated below the bars. Five days later, plants were infected in the second true leaf by applying droplets of a solution containing *P. teres* spores to the leaf surface. **(B)** Pip (or H_2O as a control) was applied by soil drench and 3 days later, plants were infected with *P. teres* spores in the second true leaf. **(A+B)** Leaves were photographed at 4 days after infection and necrotic and chlorotic area was measured using the ImageJ macro PIDIQ. Bars show merged experiments plus/minus standard error. **(A)** is merged from 6 experiments, **(B)** is merged from 9 experiments. Asterisk above bar indicates statistically significant difference from the control treatment [**(A)** Mann-Whitney test, * P<0.05].

Plants inoculated with *Psj* in the first true leaf developed significantly bigger *P. teres* lesions in their second true leaf than control plants (Figure 13A). This suggests the induction of systemic susceptibility, albeit relatively weak, to *P. teres* by *Psj*. In contrast, a pre-treatment of plants with Pip did not induce a significant change in the size of lesions caused by *P. teres* (Figure 13B). There rather seemed to be an opposite, but insignificant trend (P=0.0978) for slightly smaller *P. teres* lesions after Pip treatment of barley. Taken together, *Psj* induced systemic susceptibility to *P. teres* while Pip did not trigger the same adverse effect. Therefore, Pip might not be involved in the establishment of systemic susceptibility to *P. teres* induced by *Psj*.

2.2.4 Pipecolic acid- and bacteria-induced resistance do not share transcription factors

As next step, differential gene expression of candidate genes was analysed via qPCR in order to study possible parallels or differences between the mechanisms of bacteria- and Pip-induced systemic resistance in barley. Therefore, the transcript accumulation of two *ERF*s and two *WRKY* transcription factors previously associated with bacteria-induced systemic immunity in barley was monitored (Dey et al. 2014). Although up- or downregulation was observed in single experiments for some genes, the overall merged response revealed no clear effect of Pip on the expression of these genes (Figure 14).

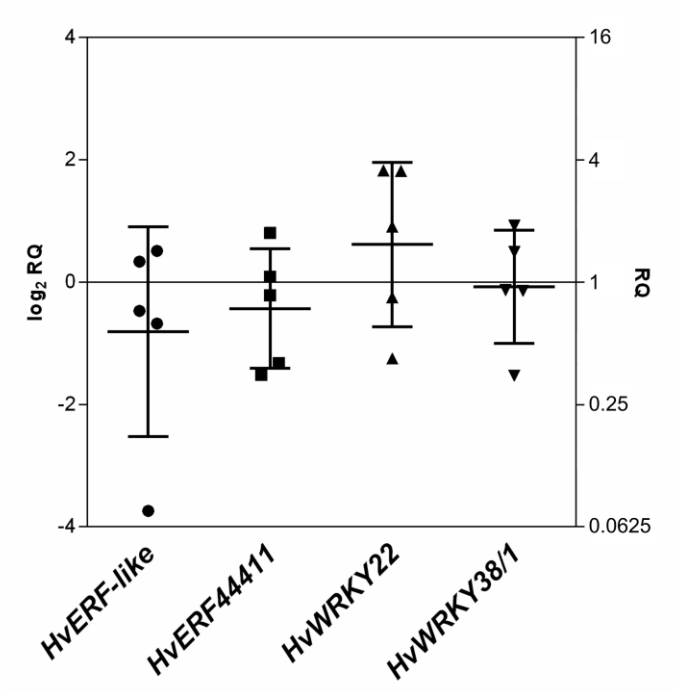

Figure 14. Gene expression in leaves of barley (GP) treated with Pip. Pip (or H_2O as a control) was applied by soil drench and 3 days later, gene expression in the second true leaf was determined. Gene expression is depicted as $\log_2$ of the transcript relative quantity (RQ). RQ of H_2O treated plants was set to 0; only data from Pip-treated plants is shown. Dots represent results from single experiments (5 in total); the middle line represents the average of 5 experiments, plus/minus standard deviation.

2.2.5 Pipecolic acid induces NO accumulation in barley

It was recently shown that Pip mediates resistance in *Arabidopsis* via the accumulation of NO (Wang et al. 2018). Here, it was tested if Pip also induces NO accumulation in barley. To this end, 3-week-old barley plants were treated with Pip and the NO content in leaves of the treated plants was monitored 3 days later by staining with the NO sensor DAF-FM DA.

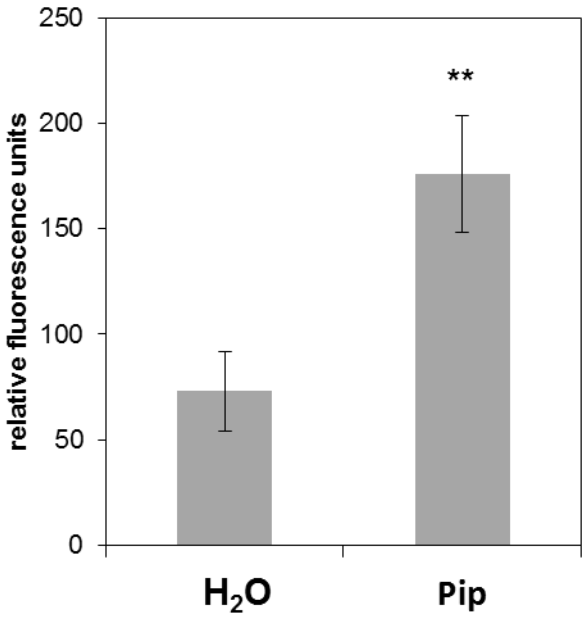

Figure 15. Relative fluorescence of DAF-FM DA staining to quantify NO content in leaves of Pip-treated barley plants. Pip (or H_2O as a control) was applied by soil drench and 3 days later, leaf discs were cut out and stained using DAF-FM DA. Fluorescence was recorded with a spinning disc confocal microscope. Bars show one experiment plus/minus standard error out of two experiments performed in the growth chamber; additional 4 experiments were performed in the greenhouse. All 6 experiments yielded similar results. Asterisk above bar indicates statistically significant difference from the control treatment (*t*-test; * P<0.005).

The fluorescence caused by DAF-FM DA was ~2-fold higher in plants pre-treated with Pip than in control plants (Figure 15). Thus, NO accumulates after Pip treatment of barley and this might lead to Pip-induced resistance in barley against *Xtc* and *Bgh.*

2.3 Establishment of the CRISPR/Cas technique in barley

2.3.1 Generation of CRISPR/Cas constructs for barley knockout mutants

In order to generate barley knockout mutants of the three *ERF*s and two *WRKY* transcription factors that had previously been associated with bacteria-induced systemic immunity in barley (Dey et al. 2014), the CRISPR/Cas system was employed. This method relies on the knowledge of exact target sequences, since parts of it are used to generate variable 20 nucleotide-long guides. These are expressed fused to invariable RNA scaffolds as gRNAs (guide RNAs), termed so because they “guide” the Cas9 protein to its target location. After recognition of the PAM (5’-NGG-3’) by *Streptococcus pyogenes* Cas9 and DNA-RNA heteroduplex formation, a

double-strand break is introduced. This is most frequently repaired by non-homologous end joining, resulting in a short insertion or deletion that will in most cases lead to a frameshift mutation and therefore a gene knockout (reviewed in Bortesi & Fischer, 2015). Since the barley cultivar Golden Promise is best transformed but the cultivar Morex is sequenced, the target genes were amplified from the target cultivar Golden Promise via PCR and cloned to be sequenced. The resulting sequences were searched for possible Cas9 cut sites using CRISPRdirect online (http://crispr.dbcls.jp/; Naito *et al.*, 2015). Two cut sites at a distance of 50-100 bp between each other were targeted in every gene of interest. In some circumstances, this results in the deletion of the sequence between the cut sites and thereby facilitates the recognition of mutations by PCR. For each target gene, at least two constructs were generated with two gRNAs each. Additionally, two constructs were cloned targeting two genes at the same time: *ERF-like* and *ERF4* (Table 1). These two genes show 77% identity on DNA level and 66% identity and 77% similarity on amino acid level.

Table 1. Target genes, gRNA (guide RNA) and vector combinations. The genes listed in this table were previously found to be associated with bacteria-induced resistance of barley using RNA sequencing (Dey et al. 2014). For detailed explanations regarding shuttle and recipient vectors, see Methods (6.5.8 Golden Gate cloning of CRISPR/Cas vectors).

gene	number of gRNAs	number of shuttle vectors	number of recipient vectors
ERF-like (MLOC_24530)	4	4	2
ERF4 (MLOC_73358)	4	4	3
ERF-like & *ERF4* (MLOC_24530 & 73358)	2 each and 2 for both	6	2
ERF44411 (MLOC_44411)	4	4	2
WRKY22 (MLOC_45055)	4	4	2
WRKY38/1 (MLOC_60890)	4	4	2

Genome editing vectors for monocots (pMGE) using the CRISPR/Cas system were designed and provided by Johannes Stuttmann, Institut für Biologie/Genetik, Martin-Luther-Universität Halle (Saale). The assembled CRISPR/Cas vector encodes (among others, see Figure 16) the Cas9 protein under control of the maize *Ubiquitin* promoter, which is a strong promoter in barley. In addition, the CRISPR/Cas vector contains two guide RNAs each under the control of a rice *U6* promoter, which is a RNA

polymerase III promoter. RNA polymerase III mostly transcribes non protein-coding genes and therefore catalyses transcription of DNA to RNA, but usually not translation of the latter (Dieci et al. 2007). In addition, the CRISPR/Cas vector contains a hygromycin resistance gene under the control of a 35S promoter for selection of transgenic plants.

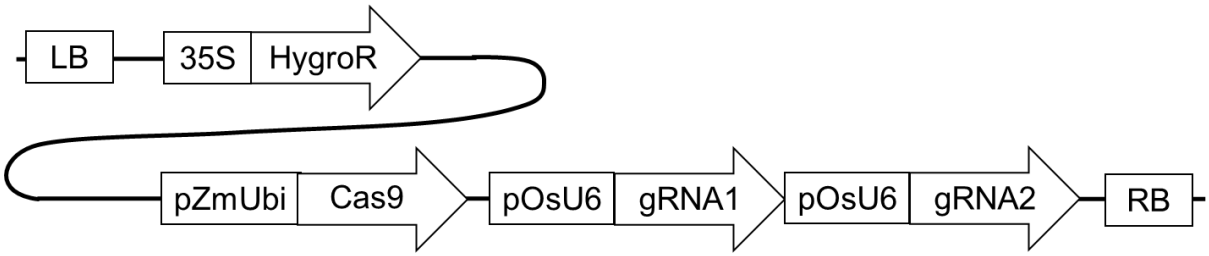

Figure 16. Schematic drawing of a CRISPR/Cas vector. Depicted are promoters and genes situated in between left border and right border sequences. LB: left border, pZmUbi: maize *Ubiquitin* promoter, pOsU6: rice *U6* promoter, RB: right border.

To test if these CRISPR/Cas constructs might be effective *in planta*, the seven CRISPR/Cas vectors targeting *ERF-like* and/or *ERF4* (recipient vectors in Table 1) were transiently expressed in barley protoplasts to assess the efficiency of the different gRNAs in the constructs. To this end, protoplasts were transformed with the individual CRISPR/Cas vectors and DNA was extracted from the protoplasts 2 days later using alkaline lysis and SDS. Subsequently, PCR was performed on the two target genes *ERF-like* and *ERF4*, replicating a region of about 500 bp length around the Cas9 target sites. Cas9-induced deletions of 50-100 bp would shorten the PCR product by this range, which can be visualised using agarose gel electrophoresis. PCR conditions were optimised to yield one clear band on wild type DNA; no smaller bands in addition to the wild type-sized band appeared after agarose gel electrophoresis of PCR performed on DNA from protoplasts transformed with CRISPR/Cas vectors (Figure 17).

Since it is possible that the desired mutation was not detected due to low abundance of the 50-100 bp deletion variant, a T7 Endonuclease I (T7EI) assay was performed to detect small insertions or deletions. T7EI recognises and specifically cleaves heteroduplex DNA. These heteroduplexes are formed by melting the PCR product (the same as above) and allowing it to re-anneal. If Cas9 has been active, wild type and mutant DNA will have been replicated. In some cases during double-strand formation after melting, one of the strands will carry a Cas9-induced mutation while the other

strand will not. These mismatches are recognised and cleaved by T7EI, resulting in additional, smaller size bands. After T7EI digestion, the reaction mixture was loaded on a 2% agarose gel and the DNA fragments were separated via electrophoresis. No additional bands were visible in samples from protoplasts transformed with the different CRISPR/Cas vectors (Figure 18). Since the formed smear also appears in the empty vector control, there is no proof of CRISPR/Cas activity in barley protoplasts.

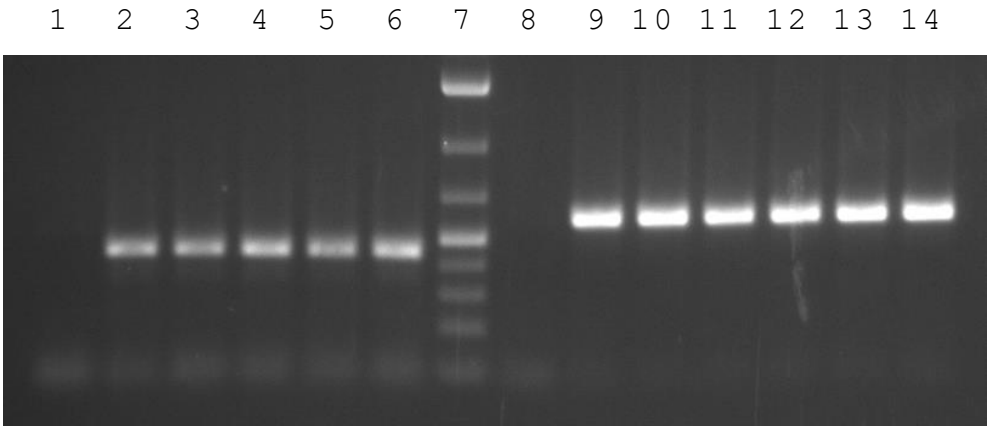

Figure 17. Agarose gel electrophoresis of PCR performed on protoplast DNA targeting *HvERF-like* and *HvERF4*. Protoplasts were isolated from leaves of barley (GP) plants and transformed with different vectors to express Cas9 and gRNAs. After 48 h, DNA was isolated and PCR was performed to replicate the target genes. On the left side the PCR product of *HvERF-like* is shown, next to it the DNA ladder and on the right side the PCR product of *HvERF4*. Lane 1: negative control without DNA, lane 2: DNA of protoplasts transformed with empty vector pMGE500, lane 3: pMGE500+gRNA1+3, lane 4: pMGE500+gRNA2+4, lane 5: pMGE500+gRNA9+10, lane 6 pMGE500+gRNA2+4+6+7, lane 7: 1 kb plus gene ruler (Thermo Fisher Scientific, bright bands correspond to 1500 and 500 bp), lane 8: negative control without DNA, lane 9: empty vector pMGE500, lane 10: pMGE500+gRNA5+7, lane 11: pMGE500+gRNA6+7, lane 12: pMGE500+gRNA6+8, lane 13: pMGE500+gRNA9+10, lane 14: pMGE500+gRNA2+4+6+7.

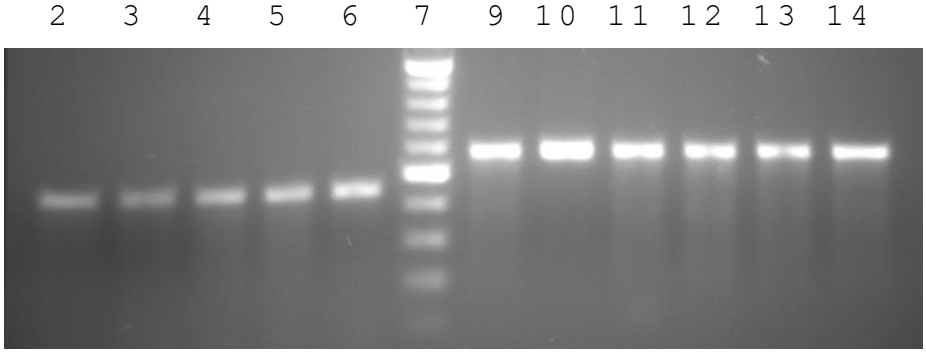

Figure 18. Agarose gel electrophoresis of T7EI assay performed on PCR of protoplast DNA replicating *HvERF-like* and *HvERF4*. PCR products shown in Figure 17 were digested with T7EI. Lane numbers correspond to those in Figure 17.

2.3.2 The fluorescence-based reporter system

In order to confirm the functionality of the CRISPR/Cas vectors to be used for the production of barley knockout mutants, a fluorescence-based reporter system was used. To this end, barley protoplasts were isolated and co-transformed with a CRISPR/Cas vector and a matching reporter vector (both vectors designed and provided by Johannes Stuttmann, Institut für Biologie/Genetik, Martin-Luther-Universität Halle (Saale)).

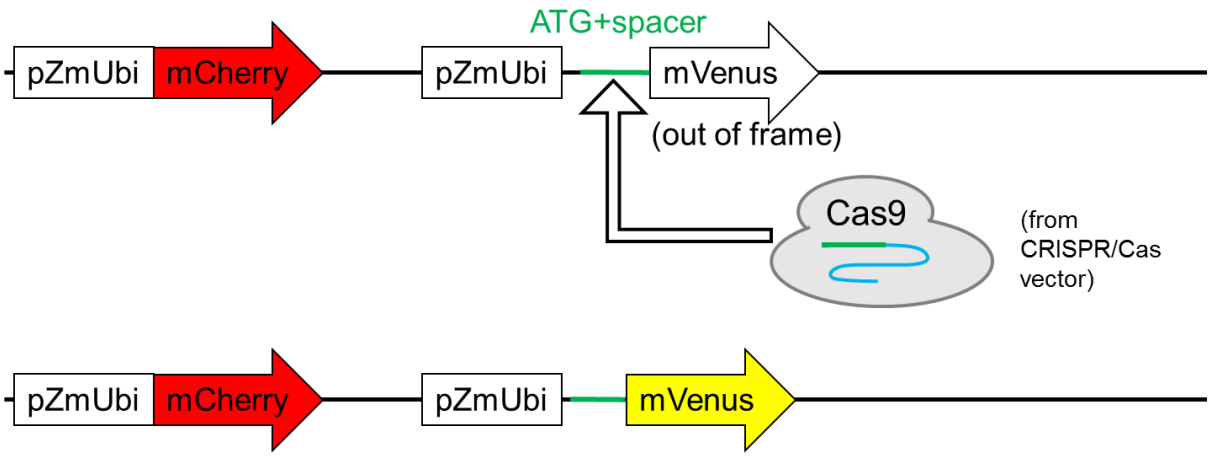

Figure 19. Fluorescence-based CRISPR/Cas reporter system. Depicted are promoters and genes encoding the fluorescent proteins mCherry and mVenus. Co-expression with a CRISPR/Cas vector encoding the Cas9 protein and a gRNA targeting the spacer in the *mVenus* sequence leads to small insertions or deletions in the spacer, bringing the *mVenus* sequence back in frame.

The reporter vector contains the target or CRISPR/Cas reporter (see Figure 19). It encodes mCherry under the control of the maize *Ubiquitin* promoter, which is a strong promoter in barley. mCherry is expressed at a high level in protoplasts containing the reporter vector and therefore serves as a marker for transformed cells. In addition, the vector encodes an out-of-frame mVenus, also under control of the maize *Ubiquitin* promoter. The *mVenus* sequence is brought out-of-frame due to the addition of a variable spacer sequence between its first and second base triplet so that no functional mVenus protein is expressed. Co-transformation of a matching CRISPR/Cas vector leads to expression of the Cas9 protein and a gRNA targeting the *mVenus* spacer sequence. The Cas9 protein will create double-strand breaks in the spacer sequence; their repair will lead to small insertions or deletions in the spacer. In some cases (e.g. a 1 bp deletion or 2 bp insertion), this will bring the *mVenus* sequence back in frame so that functional mVenus protein is expressed and yellow fluorescence can be detected (see Figure 19).

A test of the fluorescence-based reporter system was performed using a target sequence in the reporter vector that is not encoded in the barley genome, so that the matching gRNA on the CRISPR/Cas vector would not lead to double-strand breaks in the barley genome which might interfere with the assay. This gRNA was termed control gRNA. In Figure 20, photos of the experiment are shown; in the upper panels, mCherry fluorescence can be observed in all vector combinations containing the reporter vector. This indicates successful transformation events and expression of genes encoded on the vectors. The CRISPR/Cas vector does not encode a fluorescent protein, therefore only autofluorescence of chloroplasts is visible. The lower panels show mVenus fluorescence. No fluorescence was visible if either the reporter or the CRISPR/Cas vector were transformed alone, indicating that the frameshift in the mVenus sequence was not spontaneously reverted. mVenus fluorescence was only observed if the guide sequence of the gRNA on the CRISPR/Cas vector and the target sequence on the reporter vector were matching. If a different CRIPSR/Cas vector with a gRNA not matching the target sequence was used, no mVenus fluorescence was detected. Likewise, if a different reporter vector with a target sequence not matching the gRNA was co-transformed, no mVenus fluorescence was observed.

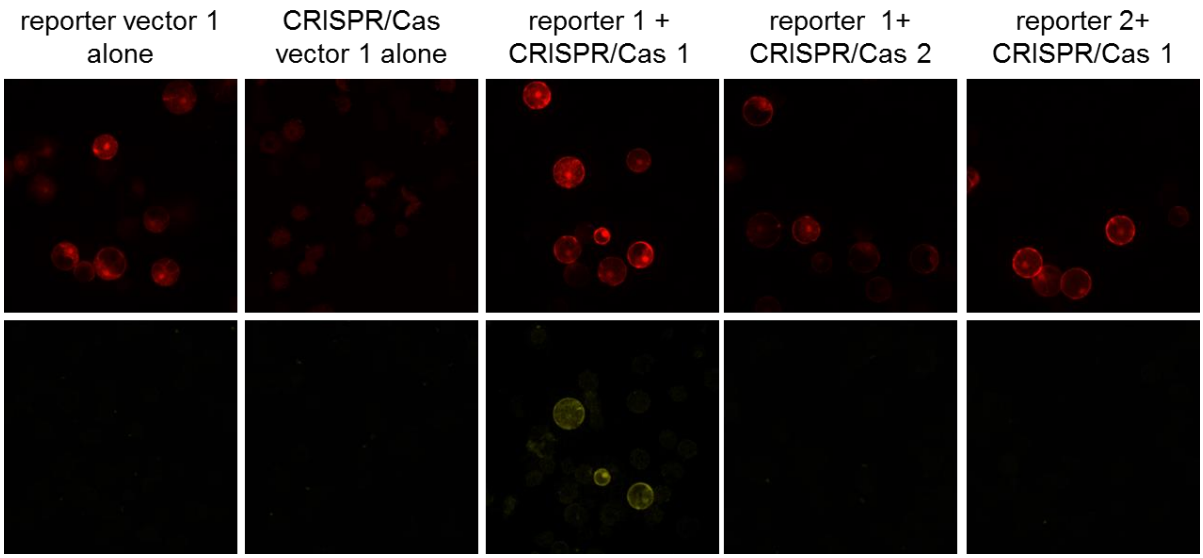

Figure 20. Fluorescent reporter experiment in barley protoplasts. The upper panels show mCherry fluorescence, the lower panels that of mVenus in the same section. Protoplasts were transformed with the vector(s) indicated above each column. Reporter vector 1 corresponds to pJOG541+527.1, CRISPR/Cas vector 1 to pMGE527 (encoding the control gRNA), CRISPR/Cas vector 2 corresponds to pMGE500+22+24, reporter vector 2 corresponds to pJOG541+24. Pictures were taken three days after transformation.

Yellow fluorescence was detected in barley protoplasts if they were transformed with the correct combination of CRISPR/Cas and matching reporter vectors (Figure 20). Thus, Cas9-induced mutations could be observed using the fluorescence-based reporter system and the CRISPR/Cas vectors were functional in barley protoplasts.

Since the spacer sequence in the reporter vector is variable, the reporter system can be used to compare the mutagenesis rates of different gRNAs. Using this technique, it is possible to find the most efficient gRNA for a given target gene. This was done as part of a bachelor thesis comparing CRISPR/Cas vectors with ten different gRNAs, all targeting one or two of our barley target genes possibly involved in systemic resistance (*HvERF-like* or/and *HvERF4*). In order to exclude variations due to varying transformation rates, the same vector expressing the control gRNA was transformed in each experiment. Negative controls with non-matching CRISPR/Cas and reporter vectors were always included and displayed no mutations. The mutagenesis rates of the different gRNAs showed marked differences, varying between circa 2 and 25% (see Figure 21, experiments performed by Veronika Wolf). Since the vector backbone was the same for all tested vectors containing the different gRNAs, the observed differences in efficiency should be due to the different gRNA sequences.

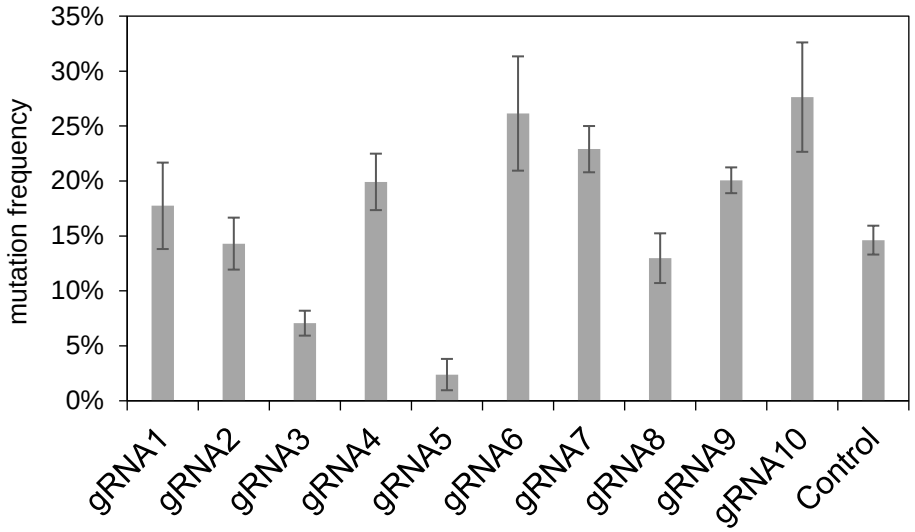

Figure 21. Mutation rates induced by different gRNAs. Protoplasts were transformed with CRISPR/Cas vectors expressing different gRNAs plus the corresponding reporter vector. The mutation rate was calculated as the percentage of mVenus-positive protoplasts among all transformed protoplasts (mCherry-positive). At least 100 protoplasts were counted per gRNA. Error bars depict standard error. The counting was repeated 3 times, except for gRNA 5, 7, and 8, which were counted 2 times. The control gRNA was tested 16 times. All experiments were done by Veronika Wolf.

2.3.3 Mutation detection in transgenic barley

Meanwhile, some of the CRISPR/Cas constructs were used to generate stable transgenic barley lines (Imani and Kogel, Justus-Liebig-University, Gießen). Due to problems with hygromycin selection, transgenic plants were generated without a selecting agent and transgene presence was confirmed via PCR.

CRISPR/Cas vectors were designed to create two cut sites at a distance of 50-100 bp between each other in the gene of interest. As noted above, this can result in the deletion of the sequence between the cut sites and thereby facilitate the recognition of mutations via PCR. Therefore, DNA from confirmed transgenics was used for PCR around the CRISPR/Cas target sites. All PCRs yielded wild type-sized bands (see Figure 22 and Figure 23), meaning no deletions were detected.

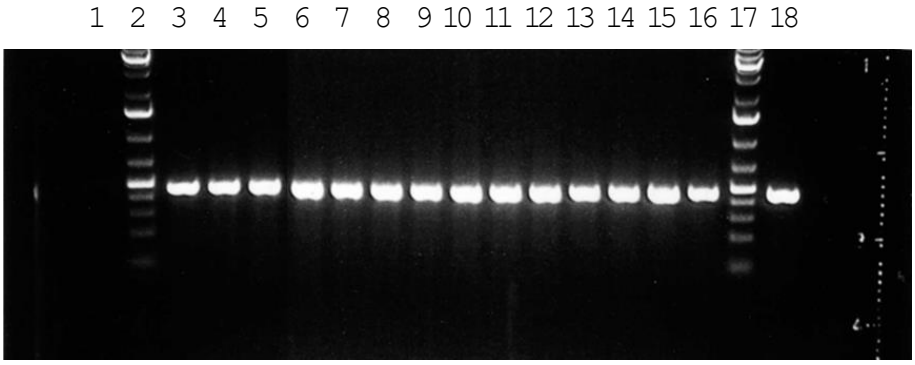

Figure 22. PCR around the target sites in MLOC_60890 (*WRKY38/1*) of plants expressing gRNAs 33+35. Lane 1: negative control without DNA, lane 2: 1 kb plus gene ruler (Thermo Fisher Scientific, bright bands correspond to 5000, 1500, and 500 bp), lane 3-16: transgenic lines, lane 17: 1 kb plus gene ruler, lane 18: wild type DNA.

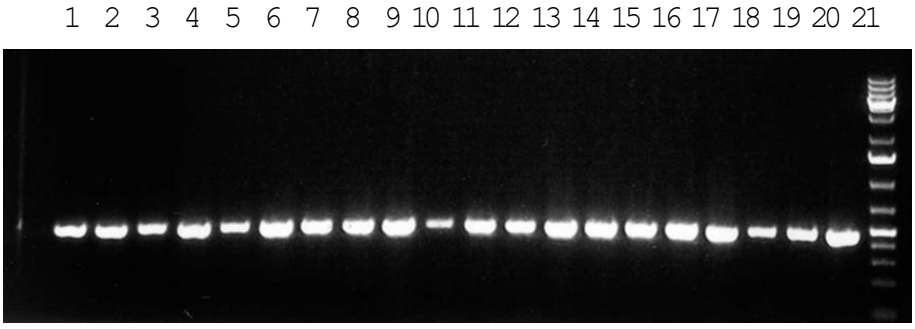

Figure 23. PCR around the target sites in MLOC_60890 (*WRKY38/1*) of plants expressing gRNAs 34+36. Lane 1-20: transgenic lines, lane 21: 1 kb plus gene ruler (Thermo Fisher Scientific, bright bands correspond to 5000, 1500, and 500 bp).

Since it is possible that the desired mutation was not detected due to low abundance of the 50-100 bp deletion variant, a T7EI assay was performed to detect frameshift

mutations (induced by one rather than two gRNAs). The PCR products shown above (Figure 22 and Figure 23) were digested with T7EI, the reaction mixture was loaded on a 2% agarose gel and the DNA fragments were separated via electrophoresis. Most of the samples showed only one band, meaning there was no mutation detectable (see Figure 24 and Figure 25). For one line expressing gRNAs 34 and 36, an additional smaller band was visible, confirming the presence of a heterozygous mutation in the target gene *WRKY38/1* of this line (see Figure 25, marked with a white arrow).

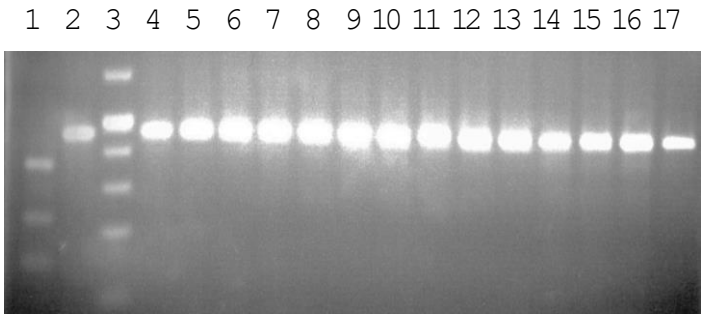

Figure 24. T7EI assay around the target sites in MLOC_60890 (*WRKY38/1*) of plants expressing gRNAs 33+35. Lane 1: positive control, lane 2: negative control (wild type DNA), lane 3: 1 kb plus gene ruler (Thermo Fisher Scientific, bright band corresponds to 500 bp), lane 4-17: transgenic lines.

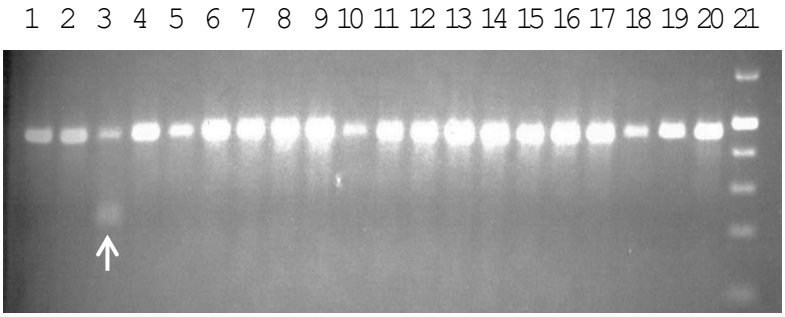

Figure 25. T7EI assay around the target sites in MLOC_60890 (*WRKY38/1*) of plants expressing gRNAs 34+36. Lane 1-20: transgenic lines, lane 21: 1 kb plus gene ruler (Thermo Fisher Scientific, bright band corresponds to 500 bp).

This line and all other, non-mutant T_0 lines were self-fertilised to generate T_1 seeds. Ten T_1 seeds of each T_0 plant were sown and again tested for mutations via PCR and T7EI assay. For none of these lines a variant with a deletion between two gRNA cut sites was detected.

The descendants of the mutated T_0 line all showed mutations in a T7EI assay, which would not be expected for a heterozygous mutation, meaning that Cas9 was still active and generating new mutations. Sequencing of the target gene revealed mostly biallelic or homozygous mutations, which were most often insertions of 1 bp. Both types of

mutations have the same effect with both alleles being mutated, the difference being that in biallelic mutants both alleles show different mutations, while in homozygous mutants, both alleles have the same mutation. In addition, different homozygous mutations (i.e., either an insertion of T or G in both alleles) were observed, which cannot be explained by Mendelian inheritance, meaning that new mutations were created by an active Cas9. Consequently, all the lines with mutations had retained the *Cas9*-containing transgene. Nevertheless, mutant lines for *WRKY38/1* with both alleles knocked-out have been generated in the T_1 generation.

The descendants of the lines with constructs targeting other *WRKY* genes or *ERF*s showed no mutations in the T_0 generation. In the T_1 generation, they behaved in one of two ways. Either there were no mutations detectable in any of the descendants, or all descendants had mutations. For *ERF-like* (MLOC_24530), the latter was the case. All tested lines showed mutations, as visible after T7EI assay (Figure 26).

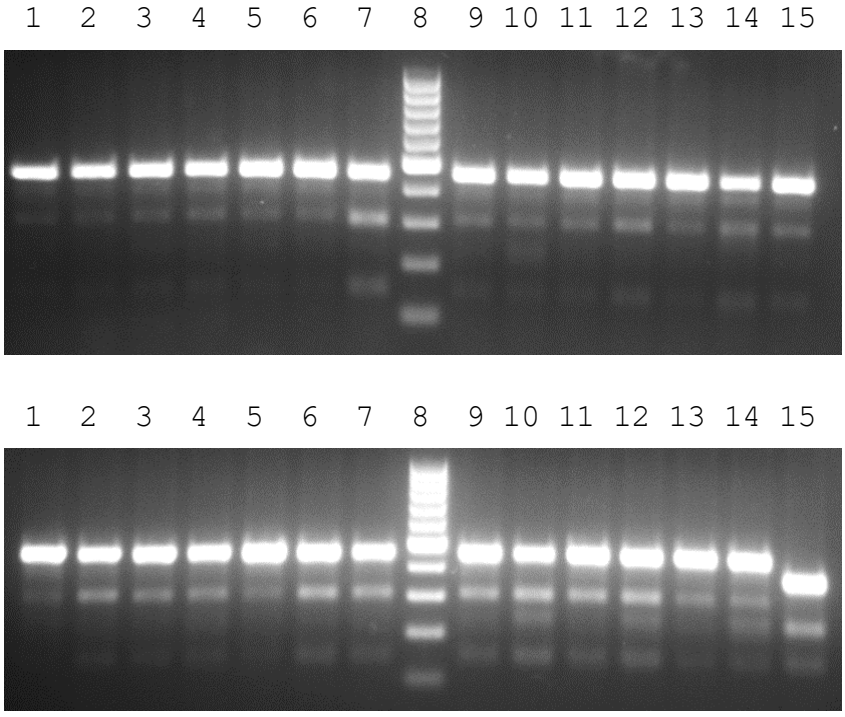

Figure 26. T7EI assay around the target sites in MLOC_24530 (*ERF-like*) of plants expressing gRNAs1+3. Upper gel: Lane 1-7 and 9-15: transgenic lines, lane 8: 100 bp gene ruler (Thermo Fisher Scientific, bright band corresponds to 500 bp). Lower gel: Lane 1-7 and 9-14: transgenic lines, lane 8: 100 bp gene ruler (Thermo Fisher Scientific, bright band corresponds to 500 bp), lane 15: positive control for T7EI assay.

Interestingly, different mutations can be seen on the gel: While all lines had mutations in the target of gRNA1 (shown by the presence of a 300 bp band), some lines had

additional mutations in the target of gRNA3 (shown by the presence of a 240 bp band). Five lines with a high probability of having mutations in both alleles were sequenced. Of these, 4 lines were homozygous, all of them with an insertion of 1 bp, either T or A. Since one of these lines had a second mutation downstream in the sequence that might have brought the frameshift back in frame, only 3 lines were selected as frameshift and knockout mutants. The *Cas9*-containing transgene was still present in all lines. Nevertheless, homozygous mutants for *ERF-like* were created within one generation from lines that had no mutations in T_0 with a mutation rate of 100% from T_0 to T_1.

In conclusion, 7 *wrky38/1* knockout lines were generated, 2 of them biallelic and 5 of them homozygous. For *ERF-like*, 3 homozygous mutant lines were generated. For the other target genes, either no transgenic plants were available carrying the corresponding CRISPR/Cas constructs or more than 100 lines have been tested negatively.

The mutant T_1 lines have been cultivated to produce T_2 seeds and phytopathological experiments have been performed using plants grown from these seeds (experiments were performed by Claudia Knappe). Results from these experiments are preliminary and should be interpreted with caution, as the control seeds of wild type plants were not produced under the same conditions as the mutant seeds. Therefore, seed batch effects cannot be excluded.

Six *wrky38/1* lines have been tested for Pip-induced resistance against *Xtc* (all experiments were performed by Claudia Knappe). Of these lines, only one (#30) mounted a Pip-induced resistance response to *Xtc* (Figure 27). Whereas the other five mutants did not respond to Pip treatment with elevated resistance to *Xtc,* some of these mutant lines appeared to have a higher basal resistance against *Xtc* as seen in the titres after H_2O control treatments. These experiments will be repeated to answer the question if *WRKY38/1* plays roles in basal and Pip-induced resistance against *Xtc*. The *Xtc* titres in H_2O-treated plants were different in the mutants as compared to wild type plants for three lines. The same titres in H_2O-treated mutant plants also did not always significantly differ from the *Xtc* titres in Pip-treated wild type plants. Nevertheless, in five out of six mutant lines Pip did not induce a reduction in growth of an *Xtc* inoculum. In summary, these preliminary data suggest that it is possible that

WRKY38/1 contributes to, but is not essential for basal resistance and Pip-induced resistance in barley.

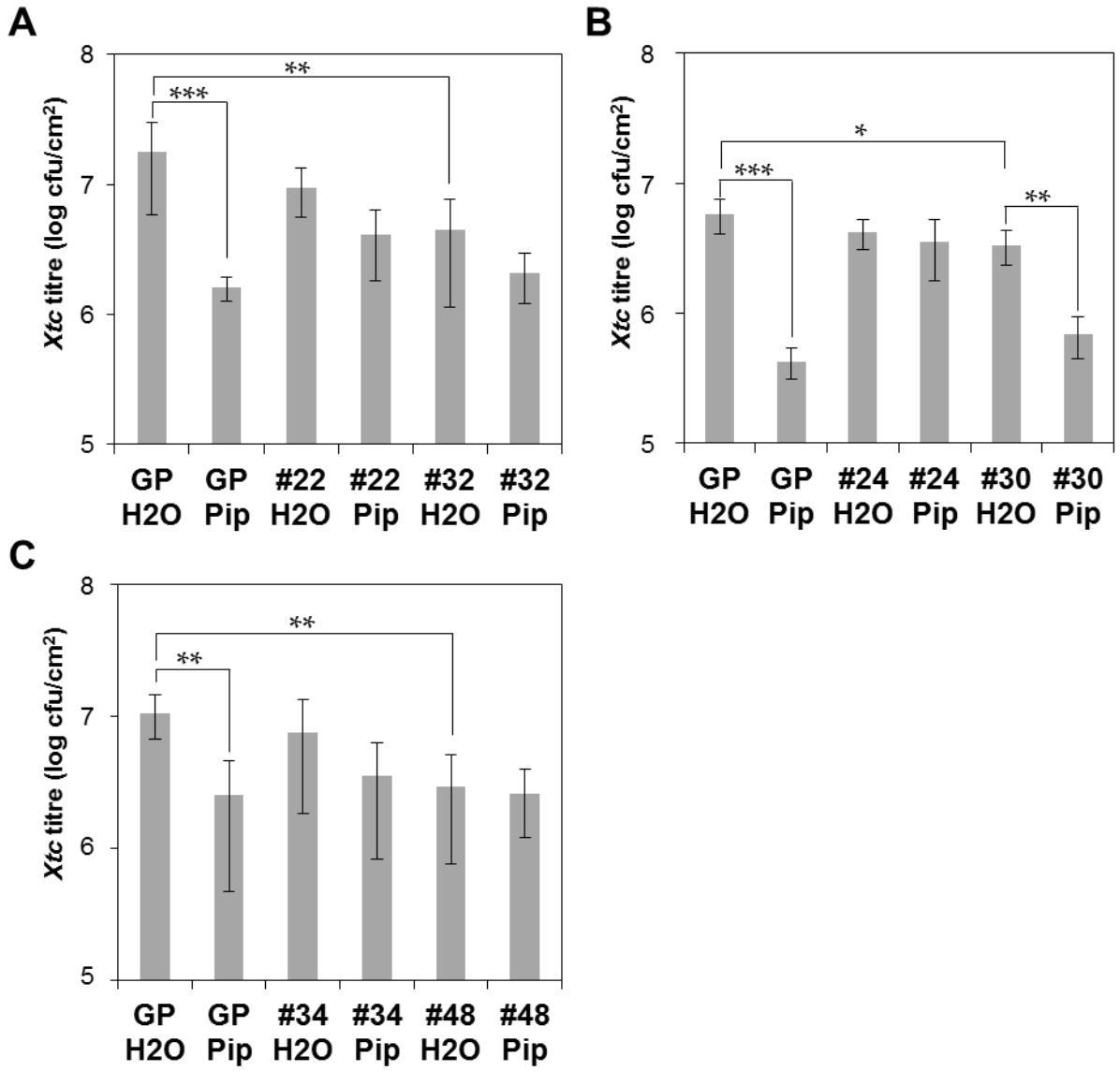

Figure 27. *Xtc* titres in Pip-treated transgenic barley lines mutated in *WRKY38/1*. Pip (or H_2O as a control) was applied by soil drench and 3 days later, plants were infected with *Xtc* using syringe infiltration. Leaves were harvested to determine *Xtc* titres at 4 days after infection. Bars show results from one preliminary experiment plus/minus standard deviation with 4-5 plants per treatment. Asterisks above bar indicate statistically significant difference from the control treatment (ANOVA with Sidak's post-hoc test comparing H_2O-treated GP and mutant plants as well as H_2O and Pip treatments of one particular line; * P<0.05, ** P<0.005, *** P<0.0005). Experiments were performed by Claudia Knappe.

In summary, the CRISPR/Cas technique was successfully established in barley plants and several knockout mutants were generated for the genes *ERF-like* and *WRKY38/1*.

3 Discussion

3.1 Induced resistance in barley

3.1.1 Salicylic acid has differential effects on pathogens with different lifestyles

The aim of this work was to report on the role of SA, Fol, AzA, and Pip on barley defence against pathogens with different lifestyles. The four tested compounds are involved in *Arabidopsis* SAR and known for inducing resistance to (hemi)biotrophic pathogens in the model plant. In contrast, it has been reported that a local application of SA does not induce systemic resistance to the hemibiotrophic bacterium *Xtc* in barley (Dey et al. 2014). In order to find out if SA is involved in (systemic) defence responses in barley, inoculations with two additional pathogens were performed.

Although a local application of SA did not affect growth of the hemibiotrophic bacterium *Xtc* in the systemic tissue (Dey et al. 2014), the same treatment reduced disease burden of the biotrophic fungal pathogen *Bgh* in the systemic leaves by approximately 50% (Figure 9). There might also be a local effect of SA on *Bgh* propagation, for which a clear, but statistically insignificant trend was observed. Thus, SA might enhance the resistance of barley to the powdery mildew pathogen *Bgh.* Similar to SA, its functional analogue BTH does not affect barley resistance to *Xtc* (Dey et al. 2014), but induces resistance to *Bgh* (Beßer et al. 2000). Additionally, NPR1, the master regulator of SA responses in *Arabidopsis* (Fu and Dong 2013; Klessig et al. 2018; Pajerowska-Mukhtar et al. 2013), is important for barley defence responses against *Bgh*, but not against *Xtc* (Dey et al. 2014), further supporting a possible role of SA in barley defence against *Bgh* but not *Xtc*. Previous studies had reported only a minor effect on *Bgh*, if any, after SA treatment of barley plants (Beßer et al. 2000; Kogel et al. 1995). The relatively robust effect of SA on systemic *Bgh* propagation in barley observed in this study can have one or more of three reasons. First, the apparent difference in *Bgh* burden between SA- and mock-treated plants might be exaggerated by the method used for evaluation of the *Bgh* infections. While other studies count pustules (Beßer et al. 2000; Dey et al. 2014; Torres et al. 2017) or interaction sites (Delventhal et al. 2014; Jain et al. 2004), this study used the fluorescent dye DAF-FM DA to quantify fungal material. It is known that barley produces NO as part of the plants early defence

responses against *Bgh* (Prats et al. 2005). Additionally, at certain stages of its life cycle the fungus itself produces NO (Prats et al. 2008). However, it seems unlikely that this NO interferes with our quantification. The production of NO is very short-lived and happens mostly in early defence responses and early life stages of *Bgh*, whereas in this study, the fungus was stained with DAF-FM DA at 6 dpi, a relatively late stage of the infection, at which time *Bgh* displays significant hyphal growth (Figure 7). Second, previous studies used soil-drench treatment for SA application (Beßer et al. 2000; Kogel et al. 1995) while in this study, syringe-infiltration of leaves was used. Finally, and perhaps most importantly, plant age differed between both prior and the current studies. In Beßer et al. (2000) and Kogel et al. (1995), seedlings of 5 or 7 days of age were used while this study worked with 3-week-old plants. It is known that plant age can positively affect plant resistance against *Bgh* (Lin and Edwards 1974). In support of this hypothesis, robust effects of SA and the other tested compounds were observed on *Bgh* propagation and *Xtc* growth in 3-week-old plants, but not in 2-week-old plants (Wenig and Vlot, unpublished data). Comparing our data to those presented in (Beßer et al. 2000; Kogel et al. 1995), it is possible that SA more effectively enhances barley resistance to *Bgh* if applied directly to the leaves rather than the soil and/or if applied to 3-week-old rather than younger plants.

Although SA locally enhances the susceptibility of *Arabidopsis* plants to a necrotrophic fungal pathogen (Spoel et al. 2007; Wittek et al. 2015), it had no effect on *P. teres* lesion sizes either locally or systemically in barley (Figure 10 and Supplemental Figure 1). Thus, the trade-off between plant defence responses to biotrophic and necrotrophic pathogens that is observed in *Arabidopsis* does not appear to influence growth of the necrotrophic fungus in SA-treated barley plants.

In summary, SA appears to induce systemic resistance against *Bgh* in barley but likely does not contribute to resistance against *Xtc* or *P. teres*.

3.1.2 Folic acid has differential effects against bacteria and fungi with similar lifestyles

Fol application is known to induce local and systemic resistance to hemibiotrophic bacteria in *Arabidopsis* (Wittek et al. 2015). This effect is dependent on SA biosynthesis and signalling and on the SAR-associated compound G3P. Similar to SA, Fol application triggers local susceptibility to necrotrophic *A. brassicicola* (Wittek et al.

2015). Here, barley was infiltrated or sprayed with Fol and the effects on local and systemic propagation of bacterial and fungal barley pathogens were monitored.

In contrast to SA, Fol application enhanced barley susceptibility to *Xtc* both systemically and to a lesser extent also in the local treated tissue (Figure 5 and Figure 6). In *Arabidopsis*, Fol enhances resistance, probably through the SA pathway (Wittek et al. 2015). SA and Fol differentially affected *Xtc* growth in barley, which was not affected by SA (Dey et al. 2014) and was enhanced (rather than reduced) by Fol. It is conceivable that *Xtc* can take up Fol, which is a precursor of compounds needed for nucleotide biosynthesis (Schnell et al. 2004). Such supplementation could directly enhance bacterial growth, mimicking the induction of plant susceptibility. However, because the effect of Fol application on *Xtc* growth was stronger in the systemic compared to the local, treated tissue (Figure 5 and Figure 6), the data argue in favour of a Fol-induced effect on plant immunity or susceptibility.

Similar to SA, application of Fol enhanced barley resistance to *Bgh* both locally and systemically but did not affect the response of the plants to *P. teres* (Figure 8, Figure 9, and Figure 10). Again, the effects of SA and Fol on *Bgh* propagation were more pronounced in tissues that were systemic to site of SA/Fol treatment than in the treated leaves themselves. Although direct effects of the compounds on fungal growth cannot be excluded, the data argue in favour of SA- and Fol-induced plant defence mechanisms affecting *Bgh* propagation in barley. Importantly, Fol-related compounds can promote plant yield (Song et al. 2013), whereas SA causes cell death at high concentrations (Klessig et al. 2018; Miura and Tada 2014). Thus, although adverse effects on barley susceptibility to hemibiotrophic bacteria such as *Xtc* should be considered, Fol could be used as an alternative to SA or BTH (Beßer et al. 2000) to enhance the resistance of barley to the economically relevant powdery mildew pathogen *Bgh.*

3.1.3 Azelaic acid moderately affects barley defence responses

Application of AzA to *Arabidopsis* confers local and systemic resistance to hemibiotrophic bacteria (Cecchini et al. 2015; Jung et al. 2009; Yu et al. 2013). AzA primes *Arabidopsis* to accumulate higher SA levels more quickly after a subsequent infection (Jung et al. 2009). Similar to Fol-induced responses in *Arabidopsis* (Wittek et al. 2015), AzA-mediated SAR depends on SA (Jung et al. 2009). In the course of this

project, it was found that AzA influences pathogen propagation in barley very similarly to Fol. Whereas Fol locally and systemically enhanced *Xtc* growth, AzA did the same only in the local treated tissue and not systemically (Figure 5B and Figure 6). Nevertheless, this similarity in the effects of Fol and AzA on barley susceptibility to *Xtc* argues for a possible interference of these compounds with the barley defence response to *Xtc* rather than for direct effects of either compound on bacterial growth. Furthermore, in contrast to its effect on *Xtc* growth, AzA reduced *Bgh* propagation systemically but not locally (Figure 9). In this case, the systemic response induced by AzA is similar to the responses induced by SA and Fol, which also appear to induce systemic resistance to *Bgh*. Similar to SA and Fol, AzA application did not have an influence on fungal growth of *P. teres* (Figure 10 and Supplemental Figure 1), neither in local treated nor in systemic tissues.

In *Arabidopsis*, SAR appears to be regulated by two parallel signalling pathways that are interdependent. One of these pathways depends on SA, the other one on AzA, G3P, ROS, NO, and Pip (Gao et al. 2015; Wang et al. 2018; Wendehenne et al. 2014). While the SA pathway seems to be effective in barley at least against *Bgh* (Beßer et al. 2000 and Figure 9), the function of the other pathway, if existent in barley, is still unclear. Since SA did not affect barley resistance to *Xtc* while both Fol and to a minor extent AzA enhanced susceptibility rather than immunity to this hemibiotrophic pathogen, it is possible that Fol and AzA influenced an SA-independent immune pathway. Such a pathway might rely on JA and/or ABA, which are positively associated with barley defence against *Xtc* (Dey et al. 2014).

Since AzA induced systemic resistance to *Bgh* (Figure 9) this SAR-associated compound might well be an active defence compound in barley. Also, it cannot be excluded that the associated SAR pathway introduced above as the Pip, NO, ROS, AzA, and G3P pathway exists and is functional in barley (Wang et al. 2018; Wendehenne et al. 2014). In support of this hypothesis, AzA can be found in extracts of barley leaves and its accumulation is induced after pathogen inoculation (Bauer, Dey, Knappe, Lange, and Vlot; unpublished results). Factors required for AzA function in *Arabidopsis* are (1) the lipid transfer proteins AZI1 and DIR1 and (2) G3P accumulation (Jung et al. 2009; Yu et al. 2013; Cecchini et al. 2015). The barley genome encodes several lipid transfer proteins (Molina et al. 1993). Some of them are involved in systemic resistance induced by application of non-pathogenic

Pseudomonas fluorescens to barley roots (Petti et al. 2010) while others were shown to directly inhibit growth of bacterial and fungal pathogens (Molina et al. 1993). A BLAST search for AZI1 and DIR1 homologues in barley identified no obvious homology candidates. Homology was restricted to the lipid transfer domain found in both proteins. To (2), not much is known about the role of G3P in barley, but in wheat, it has been observed that G3P levels rise after infection with *Puccinia striiformis* and *Blumeria graminis* f. sp. *tritici* (Li et al. 2016; Yang et al. 2013). Therefore, a function of G3P in defence responses of wheat is possible. If this were also the case for the related species barley, it would further support the hypothesis that the Pip, NO, ROS, AzA, and G3P pathway (Wang et al. 2018; Wendehenne et al. 2014) of SAR exists in barley.

3.1.4 Pipecolic acid induces resistance against biotrophic pathogens and might induce processes similar to those induced in *Arabidopsis*

PEX of barley infiltrated with *Psj* increased *PR1* expression when infiltrated into leaves of *Arabidopsis* (Supplemental Figure 2, experiments performed by Claudia Knappe). This data suggests that both plant species share common signals in defence induction. It is possible that these signals are associated with SA signalling, the hallmark phytohormone associated with SAR in *Arabidopsis* (Klessig et al. 2018; Vernooij et al. 1994; Vlot et al. 2009). It has already been shown that SA induces the resistance of barley against *Bgh* and it was shown here that *Psj*-induced systemic resistance also acts against *Bgh* (Figure 12A-C; Beßer et al. 2000; Kogel et al. 1995; Lenk et al. 2018). However, *Psj* neither enhances SA accumulation in barley nor is the resulting systemic immunity against *Xtc* dependent on *HvNPR1* (Dey et al. 2014). In addition, SA did not enhance the resistance of barley against *Xtc*, while Fol and AzA appeared to raise the susceptibility of barley to *Xtc* (Dey et al. 2014; Figure 5 and Figure 6). Therefore, it seems logical that signalling components other than SA are induced during *Psj*-triggered systemic immunity in barley. Here, it was shown that these signalling components might include Pip.

Pip application to barley induced resistance to the hemibiotrophic bacterium *Xtc* (Figure 11), comparable to resistance induction in *Arabidopsis* to *Pseudomonas syringae* pv. *maculicola* (Návarová et al. 2012; Wang et al. 2018). Since Pip (1) phenocopies the effect of a *Psj* pre-treatment inducing resistance against *Xtc* and (2) accumulates after infection with *Psj*, it might be an important signalling molecule

also during barley SAR. The role of Pip in induced resistance of barley was further studied using inoculations with additional pathogens. Resistance to *Bgh* was triggered by pre-treatment with *Psj* as well as Pip (Figure 12). Thus, Pip-induced resistance is functional in barley against the biotrophic fungus *Bgh*. The data further suggest that bacteria-induced resistance against *Bgh* might be associated with Pip.

Psj- and Pip-induced responses varied against the necrotrophic fungus *P. teres*. While *Psj* induced systemic susceptibility, an application of Pip did not significantly change the size of lesions caused by *P. teres* (Figure 13). In *Arabidopsis*, pre-treatment with *Pseudomonas syringae* pv. *tomato*, SA, or Fol induces local, but not systemic susceptibility against necrotrophic *A. brassicicola* (Spoel et al. 2007; Wittek et al. 2015). This happens due to negative crosstalk between SA and JA, with *P. syringae* pv. *tomato*-induced SA inhibiting JA-mediated defence against *A. brassicicola*. Apparently, the SA level in systemic tissues of *Arabidopsis* is not sufficient to down-regulate JA signalling (Spoel et al. 2007). In barley on the other hand, there seem to be changes in the systemic leaves after *Psj* infection that enhance *P. teres* growth (Figure 13A), suggesting antagonistic effects of *Psj* on systemic responses of barley to biotrophic and necrotrophic pathogens. Such antagonistic cross talk between defence responses against biotrophic and necrotrophic pathogens has previously been observed. Barley plants with a mutation in *Mlo* are completely resistant to the biotrophic fungus *Bgh* (Büschges et al. 1997). At the same time, *mlo* plants display increased susceptibility to necrotrophic *Fusarium graminearum* (Jansen et al. 2005b). In addition, infiltration of *mlo* plants with culture filtrates from necrotrophic *Bipolaris sorokiniana* resulted in increased symptoms and necrosis, which was correlated with increased H_2O_2 levels (Kumar et al. 2001). Increased accumulation of H_2O_2, in turn, has been linked to increased resistance to *Bgh* (Hückelhoven et al. 1999). Therefore, it is possible that H_2O_2 accumulation is associated with both enhanced resistance to biotrophic pathogens and enhanced susceptibility to necrotrophic pathogens in barley. It would be of interest to study the H_2O_2 levels after treatment of barley with *Psj* or Pip. If H_2O_2 or other ROS accumulate, this would be an additional hint at the presence and functionality of the Pip, NO, ROS, AzA, and G3P pathway of SAR in barley (Wang et al. 2018; Wendehenne et al. 2014).

Interestingly, enhanced *P. teres* growth after a local *Psj* infection was independent of Pip, since Pip did not significantly affect the size of necrosis and chlorosis. If at all, Pip

might reduce the size of *P. teres* lesions rather than increasing them, but this trend was not significant across multiple biologically independent experiments (Figure 13B). Nevertheless, additional signals other than Pip might be released after *Psj* inoculation and move systemically to affect defence against *P. teres*. Because SA and AzA applications did not affect the size of *P. teres* lesions on barley (Figure 10 and Supplemental Figure 1), it does not seem likely that these signalling compounds are involved in *Psj*-induced susceptibility to *P. teres*. Because ABA and MeJA applications similarly to *Psj* induce resistance in barley to *Xtc* accompanied with enhanced expression of *ERF* and *WRKY* transcription factors (Dey et al. 2014), it seemed possible that these compounds are also involved in *Psj*-induced susceptibility to *P. teres*. However, the application of ABA or MeJA did not induce susceptibility to *P. teres* when applied at the same concentrations that induce resistance against *Xtc* (Dey et al. 2014; Supplemental Figure 3). It is possible that either other concentrations are needed or several compounds need to work in concert during *Psj*-induced susceptibility to *P. teres*. Alternatively, different compounds not yet identified might have caused the increased size of *P. teres* lesions.

Although Pip might be associated with *Psj*-induced resistance against *Xtc* and *Bgh*, it did not induce the same transcription factors that inoculation with *Psj* activates. A set of four *ERF* and *WRKY* transcriptions factor transcripts is induced during *Psj*-induced immunity and also by application of ABA and MeJA (Dey et al. 2014). The same transcription factors were analysed after Pip application. Pip had no significant influence on the expression of the SAR-responsive transcription factors (Figure 14). Since single experiments showed inconclusive up- as well as downregulation of genes, a slight effect cannot be completely excluded. It is also possible that Pip works via a different set of genes altogether, or that Pip induces a segment of SAR-responsive genes that is not yet known. In *Arabidopsis*, Pip also does not induce a large number of genes compared to an infection with bacteria for resistance induction (Hartmann et al. 2018; Wang et al. 2018). A similar case has been described for barley and the root colonizing fungus *Piriformospora indica*. *P. indica* induces tolerance to salt stress as well as resistance to *Bgh* and *F. culmorum* (Waller et al. 2005), but only induces very subtle expression changes in a small number of genes (Molitor et al. 2011; Waller et al. 2008). This transcriptional change becomes stronger after a challenge infection with *Bgh*, as *P. indica*-inoculated plants show an earlier and faster

induction of defence gene expression (Molitor et al. 2011; Waller et al. 2008). Therefore, *P. indica* inoculation seems to resemble induced systemic resistance (ISR), a process in which non-pathogenic rhizobacteria confer resistance to aerial plant parts (Pieterse et al. 2014; van Loon et al. 1998). ISR is characterised by a low number of differentially regulated genes in the non-challenged state, but prepares the plant to better combat a subsequent infection, seen in a faster induction of gene expression (Pieterse et al. 2014; Verhagen et al. 2004). Therefore, ISR is another example for priming in addition to SAR (Gamir et al. 2014; Gourbal et al. 2018; Hilker et al. 2016; Pieterse et al. 2014).

Pip plays a crucial role in priming of plants during SAR (Zeier 2013). Priming of defence mechanisms such as the accumulation of camalexin or the up-regulation of defence-related transcripts during SAR is completely abolished in *ald1* plants defective in Pip biosynthesis (Bernsdorff et al. 2016; Návarová et al. 2012). Furthermore, the exogenous application of Pip also primes plants for quicker and more efficient defence activation, such as camalexin and transcript accumulation, which resembles priming during SAR (Bernsdorff et al. 2016; Návarová et al. 2012). *PR1* transcript accumulation, for example, does not appear to be robustly induced by Pip, but its accumulation is exaggerated in response to infection if the plants had been treated/'primed' with Pip before the infection (Bernsdorff et al. 2016; Návarová et al. 2012). SA is required in addition to Pip for full establishment of priming during SAR (Bernsdorff et al. 2016). Although Pip differentially regulates a much lower number of genes compared to a SAR-inducing infection, it up- and down-regulates mainly genes that are also up- and down-regulated during SAR (Hartmann et al. 2018; Wang et al. 2018). Considering the relatively low number of gene expression changes induced by Pip application to *Arabidopsis* and the findings that Pip primes rather than induces *PR1* transcript accumulation, it is possible that Pip induces relatively few gene expression changes in barley as well.

This study uncovered several parallels between induced resistance in *Arabidopsis* and barley. Therefore, it would be interesting to compare transcriptional responses of barley to known SAR and Pip-responsive genes in *Arabidopsis*, although it might prove difficult to find the correct homologous genes in barley. For treatments with Pip, it might also be advantageous to monitor differential expression after the challenge infection, since Pip is a priming agent and does not have a strong impact on gene expression

before the infection, but rather amplifies transcriptional changes afterwards (Bernsdorff et al. 2016; Návarová et al. 2012).

Since it has recently been shown in *Arabidopsis* that Pip induces resistance via accumulation of NO (Wang et al. 2018), it was tested if this is also the case in barley. The data suggest that that soil-drench application of Pip induces NO accumulation in barley leaves (Figure 15). This draws an interesting parallel between *Arabidopsis* and barley. Other molecular mechanisms induced by Pip in *Arabidopsis* are ROS, AzA, and G3P (see above, and Wang et al. 2018). Similarly to Pip, accumulation of AzA is induced after inoculation of barley leaves with *Psj* (Bauer, Dey, Knappe, Lange, and Vlot; unpublished results). Therefore, two of the compounds that Pip induces in *Arabidopsis*, NO and AzA (Wang et al. 2018), are induced in barley either after inoculation (AzA) or Pip application (NO). Although the data do not allow conclusions on direct signalling connections between these compounds, the findings from this work that Pip enhances NO accumulation and immunity in barley against (hemi)biotrophic pathogens provide further support to the hypothesis postulated above that the Pip, NO, ROS, AzA, and G3P pathway exists in barley and is active in systemic immunity. It would be interesting to also investigate the other *Arabidopsis* signals in this pathway, i.e. NO, ROS, AzA, and G3P, both after *Psj* infection and after Pip application in barley and do a time-course analysis to see in which order the different compounds accumulate.

In *Arabidopsis*, Pip is further converted by FMO1 to its active form NHP (Chen et al. 2018; Hartmann et al. 2018). Whether this is also the case for barley has not been investigated yet. According to a BLAST search, the barley genome encodes several proteins with similarity to *Arabidopsis* FMO1. Therefore, it is possible that Pip is converted to NHP in barley, as is the case in *Arabidopsis* (Chen et al. 2018; Hartmann et al. 2018). It would be interesting to see if barley plants produce NHP and react to its application by defence activation, which would uncover further parallels in induced resistance between model and crop plants.

Taken together, whereas Pip and bacteria-induced (systemic) resistance might differ in the genes activated for defence induction, Pip induces NO accumulation in barley leaves, which is one of the proposed molecular mechanisms by which Pip confers resistance in *Arabidopsis* (Wang et al. 2018).

3.1.5 Parallels and differences of induced defence mechanisms between *Arabidopsis* and barley

Taking all data together, induced resistance in barley to *Xtc* seems only partially similar to induced defence responses in *Arabidopsis*. The compounds SA and AzA, which induce resistance in *Arabidopsis* to hemibiotrophic bacteria (Breitenbach et al. 2014; Jung et al. 2009), did not affect systemic defence against *Xtc* in barley (Dey et al. 2014 and Figure 5). Fol, another compound inducing resistance in *Arabidopsis* (Wittek et al. 2015), even induced systemic susceptibility to *Xtc* (Figure 5). Conversely, Pip induced resistance to *Xtc* (Figure 11), similar to its effect in *Arabidopsis* (Návarová et al. 2012; Wang et al. 2018). Therefore, it seems that the SA-dependent SAR pathway might not function in defence against *Xtc*. It is possible that the Pip, NO, ROS, AzA, and G3P pathway (Wang et al. 2018; Wendehenne et al. 2014) is involved in induced resistance against *Xtc*. This is not only supported by Pip application inducing resistance to *Xtc* (Figure 11) but also by Pip accumulation after *Psj* inoculation (Bauer, Dey, Knappe, Lange, and Vlot; unpublished results), suggesting that Pip is naturally involved in induced resistance responses of barley. Pip accumulation after inoculation is also observed in *Arabidopsis* (Návarová et al. 2012). In addition, Pip application induced NO accumulation in barley (Figure 15), a response also seen in *Arabidopsis* (Wang et al. 2018). AzA, another compound involved in the same pathway, accumulated after inoculation of barley with *Psj* (Bauer, Dey, Knappe, Lange, and Vlot; unpublished results). Since three players of the Pip, NO, ROS, AzA, and G3P pathway (Wang et al. 2018; Wendehenne et al. 2014), namely Pip, NO, and AzA accumulate in barley, either after inoculation or Pip application, this provides a strong hint that this pathway exists in barley and is functional in resistance induction.

Furthermore, systemic resistance in barley to the biotrophic fungus *Bgh* was induced by the application of the SAR-related compounds SA, Fol, AzA, and Pip, respectively (Figure 8, Figure 9, and Figure 12). These responses closely resemble induced resistance in *Arabidopsis* (Breitenbach et al. 2014; Jung et al. 2009; Návarová et al. 2012; Wittek et al. 2015). Consequently, it is possible that both SAR pathways exist in barley and might function in defence against *Bgh*. Whether these two pathways truly exist in barley can only be established with additional experiments, but the data presented in this study provide strong hints for the presence and functionality of induced resistance pathways from *Arabidopsis* in barley. In contrast, none of the

compounds had an effect on growth of the necrotrophic fungus *P. teres* (Figure 10, Figure 13, and Supplemental Figure 1).

In summary, there is evidence for transferability of knowledge concerning at least some defence-related signalling pathways from the model plant *Arabidopsis* to the cereal crop plant barley. Transferability depends, as so often, on the exact compounds and pathogens of interest. Defence against *Bgh* had most parallels to induced resistance of *Arabidopsis*; in defence against *Xtc,* the SA branch of SAR might not be functional. In addition, the resistance-inducing mechanism of Pip by induction of NO accumulation seems to occur in both plant species (Wang et al. 2018). Importantly, the data show that Fol- and AzA-induced resistance is a double-edged sword that can at the same time induce resistance and susceptibility against different pathogens (*Bgh* and *Xtc*), similar to what has been shown in *Arabidopsis* with SA and Fol (Spoel et al. 2007; Wittek et al. 2015). In addition, Fol and AzA differentially influence the responses of *Arabidopsis* and barley to host-adapted hemibiotrophic bacterial pathogens. Conversely, Pip induced resistance against both *Xtc* and *Bgh*. Therefore, Pip might be an interesting candidate compound for chemically-induced plant protection.

3.2 Establishment of the CRISPR/Cas technique in barley

3.2.1 CRISPR/Cas in protoplasts

CRISPR/Cas vectors were cloned targeting *ERF* and *WRKY* genes potentially related to SAR-like resistance in barley in order to create knockout mutants. No mutations were detected in DNA isolated from transformed barley protoplasts (Figure 17 and Figure 18). This might be caused by the presence of many different mutations in the protoplast DNA, so that no single mutation existed at a number high enough for detection.

Therefore, a fluorescence-based reporter system was used to show that the vectors are functional in barley protoplasts, which was proven by the presence of mVenus-positive protoplasts (Figure 20). These can only occur if the out-of-frame *mVenus* sequence in the reporter vector has been mutated to bring *mVenus* back in frame (Figure 19), indicating Cas9-induced mutations. Similar reporter systems have been published for other plant species (Jiang et al. 2014; Mao et al. 2013; Ordon et al. 2017) or human cells (Højland Knudsen et al. 2018; Ramakrishna et al. 2014).

Mutagenesis rates were shown to vary widely for the tested gRNAs (Figure 21). gRNA5, displaying the lowest mutation efficiency (about 2%), contained the highest number of possible consecutive base pair formations (6) within the guide region (variable region) of the gRNA (Supplemental Table 2). This means that the 20 bp-long guide sequence can partially pair with itself and/or with the conserved gRNA scaffold (80 bp) (Supplemental Figure 4). The guide region is responsible for double-strand break initiation by forming a DNA/RNA heteroduplex with the target DNA (Jinek et al. 2012). However, if the guide region has many consecutive interactions with other gRNA base pairs, it might form a quite stable hairpin, which prevents DNA/RNA hybridisation, so that a lower number of double-strand breaks is formed. Alternatively, the interaction between the gRNA and Cas9 might be destabilised by a change in the secondary structure of the gRNA. In support of this hypothesis, it has been shown that gRNA structure has an impact on the mutation rate of Cas9 (Thyme et al. 2016; Xu et al. 2017). The gRNAs with the lowest number of base pairings (2) in the guide region, gRNA9 and gRNA10 belonged to the gRNAs with higher mutation efficiencies. On the other hand, gRNA6 and gRNA7 also induced high mutation rates, but have a medium number of base pairings (4). gRNA3, which also supports 4 base pairings in the guide region, showed a much lower mutation rate. This suggests that the number of base pairings in the guide region of the gRNA can be an indicator for mutagenesis efficiency, but only for “higher” numbers of base pairings indicating lower mutagenesis efficiencies, with about 6 pairings being the threshold. Lower numbers of base pairings do not correlate well with mutagenesis efficiency. Interestingly, the same result has been found by Liang et al. 2016 and Ma et al. 2015, both stating that 6 or more base pairs in the guide region of a gRNA will lead to the gRNA being inefficient. Additional rules and guidelines for design of efficient gRNAs have been established in human or animal cells (Doench et al. 2014, 2016; Liu et al. 2016; Xu et al. 2015). Unfortunately, it seems that these rules do not apply in plants, since previous studies found no strict correlation between predicted and in planta activity of gRNAs (Johnson et al. 2015; Ordon et al. 2017).

For the two gRNAs, for which both protoplast and plant data are available, the mutagenesis rates calculated from the protoplast experiments (Figure 21) reflected the mutagenesis rates seen in stably transformed barley plants (Figure 26). In T_1, all of the tested plant lines had mutations at the target site of gRNA1, but only a small

proportion of the lines had a mutation in the target site of gRNA3 (4 out of 27). A similar pattern could be seen in the fluorescent reporter system (Figure 21), with gRNA1 having a higher mutation rate than gRNA3 (18% versus 7%). Interestingly, gRNA1 was not among the most efficient gRNAs in protoplast experiments although in stable plants, it reached a mutation rate of 100% from the T_0 to the T_1 generation. This shows that mutation rates calculated from protoplast experiments underestimate the actual mutation frequency. First of all, the fluorescence-based reporter system can only display certain mutation events: All mutations that do not restore the frame of the *mVenus* sequence are invisible. Second, CRISPR/Cas-generated mutations accumulate with time (Brinkman et al. 2018). In stably transformed plants, there is more time for Cas9 to induce mutations (several weeks) and therefore mutations will accumulate over this period of time, whereas protoplasts were inspected after 2 to 3 days, which is far less time to accumulate mutations. In summary, one should not dismiss a gRNA with a low mutation frequency in protoplasts, because its actual rate of mutation induction might be much higher. Still, the protoplast experiments can help to choose the most efficient among a group of gRNAs and are a simple and quick tool to do so. The fluorescence-based reporter system used in this work can be applied in other monocot species (e.g. maize or wheat) and with a few changes in dicots as well. In plants more amenable to *Agrobacterium*-mediated transformation, the fluorescent reporter system can be simplified and used without protoplasts, by infiltration of *Agrobacterium* carrying the CRISPR/Cas and reporter constructs into plant leaves (Jiang et al. 2013).

3.2.2 CRISPR/Cas in stable transgenic lines

The CRISPR/Cas vectors targeting *ERF* and *WRKY* genes were used for the generation of stable barley knockout mutants (Jafargholi Imani and Karl-Heinz Kogel, Justus-Liebig-Universität, Gießen). A first batch of plants expressing gRNAs to knockout *WRKY38/1* was tested for mutations in the target sequence. The desired Cas9-induced deletions of 50-100 bp could not be proven via PCR, probably because this is a very rare event. In order to find smaller mutations like frameshifts, a T7EI assay was employed. One T_0 line with a heterozygous mutation in the target sequence of *WRKY38/1* was detected (Figure 25), showing that the CRISPR/Cas vectors were active in barley plants. More lines with additional mutations in *WRKY38/1* were found in the T_1 generation, showing that the Cas9 protein and gRNAs were constantly

expressed from the transgene. This means that mutations should accumulate with proceeding plant age and generation. Indeed, for CRISPR/Cas in *Arabidopsis*, PCR-detectable deletions became more frequent from one generation to the next (Ordon et al. 2017). In a recent publication, a low number of deletion events (6.7%) between two gRNA target sites was observed in barley T_1 plants (Kapusi et al. 2017). In the same publication, a mutation rate of 78% was reported in the T_0 generation. Since our mutation rates were much lower (1 line out of 69, corresponding to circa 1.4%), the number of deletion events between two gRNA target sites will be lower as well, explaining why none were detected in the course of this work. In comparison to the three publications studying CRISPR/Cas in barley, the mutation rates achieved in this work were lower. Published mutation rates in T_0 were reported to be 10 or 23% (Lawrenson et al. 2015), 78% (Kapusi et al. 2017), and 77% (Kumar et al. 2018), respectively. This may be due to differences in the vectors encoding the CRISPR/Cas components. All systems, including ours, use the maize *Ubiquitin* promoter to drive expression of *Streptococcus pyogenes* Cas9. Kapusi et al. (2017) is the only study working with a wild type Cas9; in the other publications and in this work, Cas9 with human codon usage was used. This might have had an effect on mutagenesis, since the mutation rates reported by Kapusi et al. (2017) are the highest of all publications (78%), although the human Cas9 sequence used by Kumar et al. (2018) reached a mutation rate of 77% as well. Another study reported similar mutagenesis efficiencies of Cas9 optimised for either *Arabidopsis* or human codon usage in *Nicotiana benthamiana* leaves (Johnson et al. 2015). Therefore, the use of a human Cas9 in plants does not seem disadvantageous. Other differences between the CRISPR/Cas systems in barley include the gRNAs themselves and the promoters driving their expression. Unfortunately, Kapusi et al. (2017) did not specify the gRNA scaffold sequence they used. Lawrenson et al. (2015) and Kumar et al. (2018) used the same gRNA scaffold as this work. The biggest difference lies in the promoters that were used to drive gRNA expression: Lawrenson et al. (2015) used the *U6* promoter from wheat, producing the lowest mutation rates of the three publications. Kapusi et al. (2017) used the rice *U6* promoter and achieved very high mutation rates. Interestingly, the same promoter was used in this work, albeit with a much lower mutagenesis efficiency. Thus, there must be additional factors influencing the mutation rate, for example the choice of the target DNA and therefore the variable part of the gRNA. Kumar et al. (2018) optimised the vectors used in this work for mutagenesis of barley.

After identification of the barley *U3* promoter, they proved that it is expressed at a higher level than the rice *U3* promoter. The CRISPR/Cas vector system with the barley *U3* promoter produced 77% mutant lines in the T_0 generation, some of them already biallelic loss-of-function lines. In the T_1 generation, the barley promoter variety reached a mutation rate of 100%, while the vector system relying on the rice *U3* promoter only showed 70% efficiency. Due to the high mutation efficiency of the construct encoding the barley *U3* promoter, homozygous and Cas9-free plants were generated already in the T_1 generation, making this vector system a promising candidate for further mutagenesis projects in barley.

Several T_1 lines were detected with mutations in *ERF-like* whose progenitor T_0 lines did not show mutations (Figure 26). Interestingly, all of the T_1 lines tested showed mutations, indicating a strong increase in CRISPR/Cas9 efficiency. These lines also showed a phenotype during cultivation with a prolonged vegetative growth phase and low seed production. Therefore, it is possible that *ERF-like* plays a role in the reproductive phase of barley, which limits reproduction and seed production in the knockout mutant.

The stable T_1 barley mutants generated in this study were grown for seed production, and T_2 seeds were generated. T_2 plants will be tested again for the presence of mutations, although in theory, all should have either homozygous or biallelic mutations according to Mendelian inheritance. In homozygous or biallelic T_2 mutants, it will be evaluated if the *Cas9*-containing transgene is still present. Cas9 stays active over the course of generations and continues to produce double-strand breaks and mutations. Therefore, and because Cas9 allows for some mismatches between the gRNA and the target DNA sequence, mutations in DNA regions other than the target DNA could arise and accumulate. These so-called off-target mutations are undesirable, which is why *Cas9* should be segregated out after having done its ‘target’ job. If the T_1 plants were heterozygous for the *Cas9*-containing transgene and if the transgene has only integrated into the genome once, it should be feasible to segregate out the *Cas9*-containing transgene. Therefore, transgene-free homozygous or biallelic knockout mutants will be selected in the T_2 generation.

The results of experiments performed with the knockout mutants are very preliminary and therefore to be interpreted with caution (Figure 27, experiments performed by Claudia Knappe). Only 1 out of 6 mutant lines responded to Pip treatment with

enhanced resistance to *Xtc*; in the other 5 lines, Pip did not affect growth of *Xtc* (Figure 27). Notably, some of the mutant lines showed increased basal resistance with reduced *Xtc* titres in H_2O-treated control plants, which could be caused either by differences in how well the mutants can be infiltrated or by an increased resistance against *Xtc*. The experiments should be repeated and *Xtc* growth curves should be generated including *in planta Xtc* titre determinations on the day of the infiltration to exclude an infiltration effect. Nevertheless, the preliminary data suggest that *WRKY38/1* might contribute to Pip-induced and possibly basal resistance in barley.

4 Outlook

4.1 Induced resistance in barley

Chemically induced resistance is an interesting mechanism of plant protection that exploits the plant's own defence capacities. This poses an advantage over pesticides, which simply kill phytopathogens but can also have harmful side effects on other organisms. Several chemical compounds known from SAR in *Arabidopsis*, namely SA, Fol, AzA, and Pip, were used in this work and shown to be partially effective in barley defence against *Xtc* and/or *Bgh*. It would be interesting to find out how these compounds unfold their function in barley and what signalling pathways are employed against the different pathogens. Especially for Pip, quite detailed knowledge about molecular mechanisms and their sequence of action is known from *Arabidopsis*. Therefore, it should be investigated if the mechanisms induced, the sequence of signals, and the genes expressed after Pip application to barley resemble that in *Arabidopsis*. In order to find barley genes that are induced by Pip application and lead to resistance, RNA sequencing is the method of choice. Results should uncover transferability of well-researched induced resistance mechanisms from model to crop plants and help to protect the latter from pathogens, thereby minimising crop yield loss.

A lot of work remains to be done until resistance-inducing compounds like Fol or Pip can be used in agronomy. First, it is important to investigate if the induction of defence has a cost for the plant. In crop plants, this could manifest as yield loss due to allocation of resources to defence instead of growth (Huot et al. 2014). Interestingly, this was not the case for a precursor of Fol applied to pepper plants. In this case, the SA analogue BTH induced yield loss, whereas the folate precursor was shown to even enhance yield (Song et al. 2013), which makes Fol an interesting candidate for induced resistance in crop plants. Second, it should be investigated if the protection of crop plants from one pathogen via induced resistance leaves them vulnerable to other pathogens. In this work, this was the case for Fol, which induced resistance to *Bgh* but susceptibility to *Xtc*. Therefore, any promising compound inducing resistance to a certain pathogen should be tested against several other pathogens of the same host in order to be sure that no detrimental consequences exist. Finally, investigations need to be made if chemically-induced resistance is feasible in crop plants. Points to

be addressed are e.g. the level of protection provided, the duration of the protective effect, the number of necessary reapplications, the costs of application, and the feasibility of large-scale production of the compound in question.

4.2 CRISPR/Cas in barley

Although CRISPR/Cas is widely used for genome-editing of plants, gRNA activity prediction tools exist for animal systems (Doench et al. 2014, 2016), but not for plants so far. Furthermore, there seems to be no strict correlation between predicted and *in planta* activity (Ordon et al. 2017). Some rules for gRNA design in plants have been established, but they are less extensive than their animal counterparts (Liang et al. 2016). Therefore, it would be interesting to continue using the reporter system presented in this work for evaluation of gRNA efficiency, in particular in barley and other cereal crops, trying to find a correlation between mutagenesis rates and certain nucleotide motives or positions of the target sequence in the genome of barley. Since many possible target sites for CRISPR/Cas can be found in one gene of interest, this evaluation will be helpful to select the most efficient gRNA for a maximal number of knockout mutants. This will also increase the number of deletion events between 2 gRNAs, thereby facilitating the detection of mutations by PCR. It would also be interesting to test bigger target fragments in the reporter vector than the 20 bp used in this work. This would help to determine if the region surrounding the target DNA has an influence on the mutation rate of a certain gRNA. In order to use our fluorescent reporter system to address these questions, it would be helpful to automate and accelerate the evaluation. Different options for this are automated microscopy, use of a plate reader, or flow cytometry.

As to the stable knockout lines, if new lines for the other candidate transcription factors will be generated, this should be done using the optimised vectors with higher gRNA expression and mutation efficiency (Kumar et al. 2018). In the meantime, there have also been reports about Cas9 or Cas9-like enzymes that cause less off-target mutations, which is also a very desirable trait for genome editing purposes (Kleinstiver et al. 2016; Zaidi et al. 2017). Off-target mutations are mutations introduced by Cas9 at DNA regions other than the intended target. How frequent these are in plants is not well-researched yet, since they are not always easy to find. Additional mutations can

make analysis of phenotypes very difficult, since they might be (partially) caused by an off-target mutation and not the on-target mutation.

The role of the mutagenized *ERF* and *WRKY* transcription factors during resistance of barley should be further investigated in the near future. This could be done using the knockout mutants generated in this project. Additional experiments are needed to understand the role of the candidate *ERF*s and *WRKY*s in barley induced resistance. First experiments using the SAR compound Pip are underway, but more experiments using other SAR inducers could elucidate the effect of the genes in the signalling pathways associated with each compound. In addition, the experiments could be performed using different pathogens in order to see if the genes are involved in pathogen-specific induced defence mechanisms.

It would also be interesting to investigate the role of *ERF* and *WRKY* transcription factors in resistance of other plant species. These could be crop plants closely related to barley, e.g. wheat. In addition, such crops could include dicotyledonous species, since it was shown that induced resistance of barley and *Arabidopsis* share several compounds and signalling pathways. For more distantly related plant species, it might prove difficult to find orthologous genes due to diversification after the last common ancestor of monocots and dicots. Indeed, for the sequences of *Hv*ERF-like, *Hv*ERF4, and *Hv*ERF44411, similarities to *Arabidopsis* are mostly restricted to the conserved AP2 DNA-binding domain and little or nothing of the rest of the sequence. For *Hv*WRKY38/1, the closest hit was *At*WRKY40 with an identity of 36% and similarity of 49% of amino acids covering 97% of the sequence. This gene has been implied to be involved in PAMP signalling (Birkenbihl et al. 2017). Therefore, it would be interesting to investigate the role of *At*WRKY40 in induced resistance of *Arabidopsis*.

In addition, more details about the *ERF*s and *WRKY*s should be investigated. First, one important point would be to find the DNA targets and thus the genes regulated by the transcription factors. In order to find these targets, either a DNA pulldown of naked DNA or chromatin immunoprecipitation could be used. Second, it would be interesting to see if the *ERF*s and *WRKY*s are transcriptional activators or repressors. This could be resolved using tools such as the protoplasts transactivation system, which relies on transcription factors activating luciferase expression as a readout (Wehner et al. 2011). Third, transcription factors never work on their own, but in complexes of several transcription factors and cofactors interacting with each other (Spitz and Furlong

2012). Therefore, it would be interesting to find proteins interacting with the ERFs and WRKYs investigated in this work. This could be done in a screening system such as yeast two-hybrid or directly *in planta* by co-immunoprecipitation of interacting proteins.

Furthermore, CRISPR/Cas could be used in barley to create knockout mutants of genes involved in induced defence signalling. Knockout mutants are readily available and widely used in the model plant *Arabidopsis* in order to investigate if a certain gene is involved in a certain process (O'Malley et al. 2015). Since in the course of this work, many connections were made between induced resistance responses in barley and *Arabidopsis*, it would be interesting to find barley genes homologous to *Arabidopsis* SAR-related genes. Considering that best transferability seems to apply to the Pip, NO, ROS, AzA, and G3P branch of SAR, genes involved in this pathway should be mutagenised and examined for induced resistance responses (Chanda et al. 2011; Ding et al. 2016; Hartmann et al. 2018; Návarová et al. 2012; Wang et al. 2014, 2018). This could further confirm indications found in the course of this work that suggest possible parallels between systemic defence signalling in *Arabidopsis* and barley.

5 Material

5.1 Plants

Barley experiments were performed with cultivars Golden Promise (GP) and Barke. *Arabidopsis* experiments were performed with ecotype Columbia-0 (Col-0).

5.2 Bacteria and fungi

Table 2. Bacteria and fungi used in this work.

Species	Strain	Source
Blumeria graminis f. sp. *hordei*	Swiss field isolate CH4.8	Dr. Patrick Schweizer (Leibniz-Institut für Pflanzengenetik und Kulturpflanzenforschung, Gatersleben, Germany)
Escherichia coli	NEB5-alpha	New England Biolabs (Ipswich, USA)
	DB3.1	Dr. Christian Lindermayr
Pseudomonas syringae pv. *japonica*	LMG5659	Laboratory of Microbiology UGent collection of the Belgian Coordinated Collections of Microorganisms
Pyrenophora teres	Field isolate	Günther Bahnweg (Helmholtz Zentrum München, Neuherberg, Germany)
Xanthomonas translucens pv. *cerealis*	LMG7393	Laboratory of Microbiology UGent collection of the Belgian Coordinated Collections of Microorganisms

5.3 Kits

Table 3. Kits used in this work.

Kit	Company	Application
illustra Plant DNA extraction kit Phytopure	illustra/GE Healthcare, (Buckinghamshire, UK)	Nucleon Resin included in the kit was used for DNA extraction
Nucleo spin plant II kit	Macherey-Nagel (Düren, Germany)	DNA preparation from protoplasts

Kit	Company	Application
QIAGEN plasmid midi kit	QIAGEN (Hilden, Germany)	preparation of plasmid DNA for protoplast transformation
QIAprep spin miniprep kit	QIAGEN (Hilden, Germany)	small scale preparation of plasmid DNA
QIAquick gel extraction kit	QIAGEN (Hilden, Germany)	gel extraction of DNA
QIAquick PCR purification kit	QIAGEN (Hilden, Germany)	PCR purification of DNA
SensiMix SYBR Low-Rox Kit	Bioline Reagents (London, United Kingdom)	qPCR

5.4 Chemicals

Chemicals not specifically listed in this table were purchased from either Merck (Darmstadt, Germany), Roth (Karlsruhe, Germany), or Sigma-Aldrich (St. Louis, USA).

Table 4. Chemicals used in this work.

Chemical	Manufacturer
ABA (abscisic acid)	Sigma-Aldrich (St. Louis, USA)
AzA (azelaic acid)	Sigma-Aldrich (St. Louis, USA)
CTAB (cetyltrimethylammoniumbromid)	Sigma-Aldrich (St. Louis, USA)
DAF-FM DA (4-Amino-5-Methylamino-2',7'-Difluorofluorescein Diacetate)	Sigma-Aldrich (St. Louis, USA) or Santa Cruz Biotechnology (Dallas, USA)
Fol (folic acid)	Roth (Karlsruhe, Germany)
Gamborg's B5 basal salt mixture	Sigma-Aldrich (St. Louis, USA)
MeJA (methyl jasmonate)	Sigma-Aldrich (St. Louis, USA)
MES [2-(N-morpholino)ethanesulfonic acid]	Roth (Karlsruhe, Germany)
Pip (pipecolic acid)	Sigma-Aldrich (St. Louis, USA)
SA (salicylic acid)	Roth (Karlsruhe, Germany)
Silwet	Lehle Seeds (Texas, USA)
Tween-20	Calbiochem (San Diego, USA)

5.5 Enzymes

Table 5. Enzymes used in this work

Enzyme	Manufacturer
Cellulase Onozuka R-10	Serva (Heidelberg, Germany)
Driselase Basidiomycetes sp.	Sigma-Aldrich (St. Louis, USA
Fast Digest restriction enzymes	Thermo Fisher Scientific (Waltham, USA)
Macerozyme R-10	Serva (Heidelberg, Germany)
MangoTaq DNA polymerase	Bioline Reagents (London, United Kingdom)
Phire Hot Start II DNA polymerase	Thermo Fisher Scientific (Waltham, USA)
Phusion high fidelity polymerase	New England Biolabs (Ipswich, USA)
SuperScript II reverse transcriptase	Invitrogen/Thermo Fisher Scientific (Waltham, USA)
T4 DNA ligase	Thermo Fisher Scientific (Waltham, USA)
T7 Endonuclease I (T7EI)	New England Biolabs (Ipswich, USA)

5.6 Buffers and solutions

Table 6. Buffers and solutions used in this work.

Buffer/solution	Composition	Application
CTAB solution	100 mM Tris, 20 mM EDTA, 1.4 M NaCl, 2% (w/v) CTAB, pH 8.0, autoclave	isolation of genomic DNA
DAF-FM DA buffer	5 µM DAF-FM DA, 50 mM MES-KOH pH 5.7, 1 mM $CaCl_2$, 0.25 mM KOH	DAF-FM DA staining for NO or *Bgh* detection
gDNA isolation buffer (NTES)	250 mM NaCl, 200 mM Tris pH 8, 25 mM EDTA, 0.5% SDS	quick isolation of genomic DNA
Infection solution for fungi	0.85 g KH_2PO_4, 0.1 g glucose, 1 µl Tween 20 in 100 ml H_2O, pH 6.0	suspension of fungal spores
Mock buffer	10 mM $MgCl_2$	control treatment for infiltration
RNA extraction buffer	3.05 g ammonium thiocyanate, 9.44 g guanidinium thiocyanate, 5 ml glycerol, 3.33 ml 3 M sodium acetate pH 5.2, 40 ml H_2O, adjust pH to 5.0, 38 ml Roti-Aqua-Phenol	RNA extraction
TAE (Tris-acetate-EDTA) buffer	40 mM Tris, 1 mM EDTA, 0.1% (v/v) glacial acetic acid	gel electrophoresis

Buffer/solution	Composition	Application
Protoplast buffers:		
Digestion solution (all solutions for protoplasts were filtered using 0.45 µm filters)	0.45 M mannitol, 10 mM MES pH 5.7, 10 mM $CaCl_2$, 3.1 g/l Gamborg's B5, 0.5% cellulose, 0.5% macerozyme, 0.5% driselase centrifuge for 4 min at 2,000 rpm to remove non-dissolved enzymes	release of protoplasts from barley leaves
W5 solution	154 mM NaCl, 125 mM $CaCl_2$, 5 mM KCl, 2 mM MES pH 5.7	washing of protoplasts
MMG solution	0.4 M mannitol, 15 mM $MgCl_2$, 2 mM MES pH 5.7	pre-transformation buffer
PEG solution	40% (w/v) PEG 4000, 0.2 M mannitol, 0.1 M $CaCl_2$	transformation of protoplast
WI solution	0.5 M mannitol, 20 mM KCl, 4 mM MES pH 5.7	storage of protoplasts

5.7 Media

The components used for media were purchased from Roth (Karlsruhe, Germany) unless stated otherwise.

Table 7. Media and their compositions.

Medium	Composition	Application
LB	10 g tryptone 5 g yeast extract 10 g NaCl ad 1 l H_2O, adjust pH to 7 15 g agar-agar	growth of *E. coli*
LMG	15 g tryptone from casein 5 g soy peptone 5 g NaCl ad 1 l H_2O, adjust pH to 7.3 18 g agar-agar	growth of *Xtc*
Malt	24 g malt extract (Merck, Darmstadt, Germany) 12 g agar-agar ad 800 ml H_2O	growth and maintenance of *P. teres*
NB	8 g Nutrient Broth No. 4 (Fluka Analytical/ Sigma-Aldrich, St. Louis, USA) 15 g agar-agar ad 1 l H_2O	growth of *Xtc*

Medium	Composition	Application
NYGA	5 g proteose peptone 3 g yeast extract 20 ml glycerol ad 1 l H_2O, adjust pH to 7 18 g agar-agar	growth of *Pst*
Oat	10 g rolled oats (Alnatura, Germany) 7.5 g agar-agar ad 500 ml H_2O	growth and sporulation of *P. teres*
SOC outgrowth medium (New England Biolabs Ipswich, USA)	2% Vegetable Peptone 0.5% Yeast Extract 10 mM NaCl 2.5 mM KCl 10 mM MgCl2 10 mM MgSO4 20 mM Glucose	growth of *E. coli* after heat shock

5.8 Antibiotics

Antibiotics were purchased from Roth (Karlsruhe, Germany)

Table 8. Antibiotics and their concentrations.

Antibiotic	Final concentration
Ampicillin	100 µg/ml
Hygromycin	100 µg/ml
Kanamycin	50 µg/ml

5.9 DNA ladders

DNA ladders were purchased from Thermo Fisher Scientific (Waltham, USA).

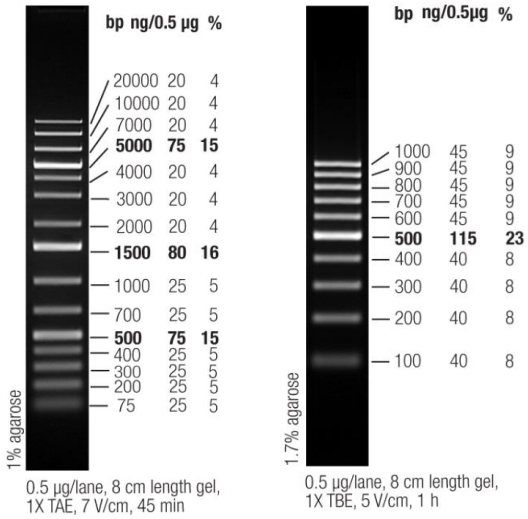

Figure 28. DNA ladders used in this work. Left panel: 1 kb plus gene ruler, right panel: 100 bp gene ruler. Adapted from the respective user guides (Thermo Fisher Scientific, Waltham, USA).

5.10 Primers

Primers were obtained from Metabion (Planegg, Germany).

Table 9. Primers for sequencing.

Name	Sequence 5' → 3'	Description
M13f	GTTTTCCCAGTCACGAC	sequencing primer for final vectors with 4 gRNAs
JS1057	CATCAGACAAACCGGCCAG	sequencing primer for final vectors with 4 gRNAs
M13 rev (-29)	CAGGAAACAGCTATGACC	sequencing primer for shuttle vectors
ML 40	TGGTGCAGATCAGCTTCAGG	sequencing primer for reporter vectors

Table 10. Primers for detection of mutations.

Name	Sequence 5' → 3'	Description	T_m (°C)
ML 21	GCCTTATCCTGGGCGCTAC	forward primer for *HvERF-like*	65
ML 22	CGAGTCCAAGGTGCTGTTGC	reverse primer for *HvERF-like*	65
ML 23	CAGATCCTGCACGCCATCC	forward primer for *HvERF4*	65
ML 24	GGGTGCGAAACGGGGTAG	reverse primer for *HvERF4*	65
ML 50	CTCTCACTCGGAACTCGGAA	forward primer for *HvWRKY38/1*	56.5
ML 52	CTCCGACTCAAGAACCGCAA	reverse primer for *HvWRKY38/1*	56.5

Table 11. Primers for detection of transgene presence.

Name	Sequence 5' → 3'	Description	T_m (°C)
ML 56	TACGCCGGATACATTGACGG	hCas9 in pMGE500 F	67
ML 57	GATTTGCGAGTCATCCACGC	hCas9 in pMGE500 R	67
ML 60	ACCGCAAGGAATCGGTCAAT	hygromycin resistance in pMGE500 F	61
ML 61	ATTTGTGTACGCCCGACAGT	hygromycin resistance in pMGE500 R	61

Table 12. Primers used for qPCR.

Name	Sequence 5' → 3'	Target gene
Hv EF1α F	GTCATTGATGCTCCTGGTCA	*HvEF1α*
Hv EF1α R	CTGCTTCACACCAAGAGTGA	*HvEF1α*
24530F4	CCGTACTTCTTCTACGAACA	*HvERF-like*
24530R4	CGGTTCAGATCCAGATCAAA	*HvERF-like*
Hv 44411_1 F	GAGGAAGAGCAGAGCGACAC	*HvERF44411*
Hv 44411_1 R	ATCGATCCTGGCAATAAACG	*HvERF44411*
60890 2F	GTGAAGGACGGGTACCAATG	*HvWRKY38/1*
60890 2R	GTCGCCACGAGTATGGTCTT	*HvWRKY38/1*
45055 2F	AGAGCACTACCCGTTCTCCA	*HvWRKY22*
45055 2R	GACACCACCTCGTCCAACTC	*HvWRKY22*
Ubiquitin F	AGATCCAGGACAAGGAGGTATTC	*AtUbq10*
Ubiquitin R	CGCAGGACCAAGTGAAGAGTAG	*AtUbq10*
PR1 F	CTACGCAGAACAACTAAGAGGCAAC	*AtPR1*
PR1 R	TTGGCACATCCGAGTCTCACTG	*AtPR1*

5.11 Vectors

Table 13. Used vectors and their features.

vector	features	source
pENTR/D-TOPO	Kan^r, TOPO cloning site	Invitrogen/Thermo Fisher Scientific (Waltham, USA)
pMGE500	Kan^r, *in planta* hygromycin resistance, pZmUbi::Cas9	J. Stuttmann, University Halle
pMGE501	Amp^r, pOsU6:: insertion site for gRNA + gRNA scaffold	J. Stuttmann, University Halle
pMGE503	Amp^r, pOsU6:: insertion site for gRNA + gRNA scaffold	J. Stuttmann, University Halle
pMGE505	Amp^r, pOsU6:: insertion site for gRNA + gRNA scaffold	J. Stuttmann, University Halle
pMGE508	Amp^r, pOsU6:: insertion site for gRNA + gRNA scaffold	J. Stuttmann, University Halle
pMGE509	Amp^r, pOsU6:: insertion site for gRNA + gRNA scaffold	J. Stuttmann, University Halle
pMGE527	Kan^r, *in planta* hygromycin resistance, pZmUbi::Cas9, pOsU6::control-gRNA	J. Stuttmann, University Halle

vector	features	source
pJOG541	Kan^r, pZmUbi::mCherry, pZmUbi:: insertion site for gRNA target + mVenus (out of frame)	J. Stuttmann, University Halle

5.12 Devices and instruments

Table 14. Devices and instruments used in this work.

Instrument	Type	Company
Camera	Nikon DC300	Minato (Tokyo, Japan)
Centrifuges	Heraeus Fresco 21	Thermo Fisher Scientific (Waltham, USA)
	Heraeus Pico 17	
	Centrifuge 5415 D	Eppendorf (Hamburg, Germany)
	Centrifuge 5810 R	
Gel electrophoresis chamber	PerfectBlue Horizontal Minigelsystems	Peqlab/VWR (Radnor, USA)
Gel station	BIO-Print M1 gel documentation system	Vilber Lourmat (Eberhardzell, Germany)
Homogenizer	Silamat S6	Ivoclar Vivadent, (Ellwangen, Germany)
Microscope	Zeiss Axio Observer. Z1	Zeiss (Oberkochen, Germany)
PCR cycler	Mastercycler nexus	Eppendorf (Hamburg, Germany)
Photometer	NanoDrop ND-1000	Nanodrop Technologies/Thermo Fisher Scientific (Waltham, USA)
Power supply	PowerPac 200 and 300	Bio-Rad (Hercules, USA)
qPCR cycler	Applied Biosystems 7500 Fast Real-Time PCR system (ABI 750 Fast)	Applied Biosystems, Freiburg, Germany
Robot arm	KiNEDx robot (Model KX-300-660-SSU)	Peak Analysis & Automation, Inc. (Farnborough, UK) set up by Analytik Jena (Jena, Germany)
Rotator	intelli-mixer rotator with vortexer	Neolab (Heidelberg, Germany)
Ultracentrifuge	Sorvall Evolution RC	Sorvall/Thermo Fisher Scientific (Waltham, USA)

5.13 Software and web applications

Table 15. Software and web applications used in this work.

Software	Version/source	Application
7500 Fast System SDS Software	Version 1.3.1.21	qPCR control and raw data generation
Camera Control Pro 2	Version 2.0.0	camera control software
CRISPRdirect online	https://crispr.dbcls.jp/ (Naito et al. 2015)	gRNA design
CyBio Application Studio/CyBio Feeder for Zeiss Microscope	Version 1.10	control of robot arm
GraphPad	GraphPad Prism 7 for Windows (version 7.04)	statistics and graph design
ImageJ	Version 1.52d	image editing and analysis
Microsoft Office	Excel, PowerPoint, Word, 2016	data analysis and graph design
mfold Web server	http://unafold.rna.albany.edu/?q=mfold/RNA-Folding-Form2.3 (Zuker 2003)	simulation of RNA folding
Primer BLAST	https://www.ncbi.nlm.nih.gov/tools/primer-blast (Ye et al. 2012)	primer design for qPCR
ZEN2	Blue edition, Version 2.0.0.0	control of microscope

6 Methods

6.1 Plant treatments

6.1.1 Plants and growth conditions

Barley [*Hordeum vulgare* L. cultivar 'Golden Promise' (GP) or 'Barke'] seeds were sterilised in 1.2% sodium hypochlorite for 3 min with 25 inversions per min. Subsequently, seeds were rinsed 3 times with water for 10 min with 25 inversions per min and then sown (Einheitserde classic CL-T, Bayerische Gärtnerei-genossenschaft was used for infiltration experiments and protoplasts; Floradur Anzuchtsubstrat B Seed, Floragard, mixed 5+1 with sand was used for soil-drench applications). Plants for DAF staining and both *Xtc* and *P. teres* infections were either grown in a greenhouse with additional lights HQI-TS 400W/D (Osram) using a day-night cycle of 12 h with 24 °C during the day and 20 °C during the night or in a climate chamber with 14 h light and 10 h darkness at a temperature of 20 °C (day)/18 °C (night). Chamber-grown plants inoculated with *Xtc* were transferred to a climate chamber with 14 h light and 10 h darkness at a temperature of 29 °C (day)/19 °C (night). Plants for *Bgh* infections were grown in climate chambers with 14 h light and 10 h darkness at a temperature of 20 °C (day)/18 °C (night). For experiments with transgenic barley, plants were grown in a climate chamber at 14 h light and 10 h darkness at a temperature of 24 °C (day)/18 °C (night).

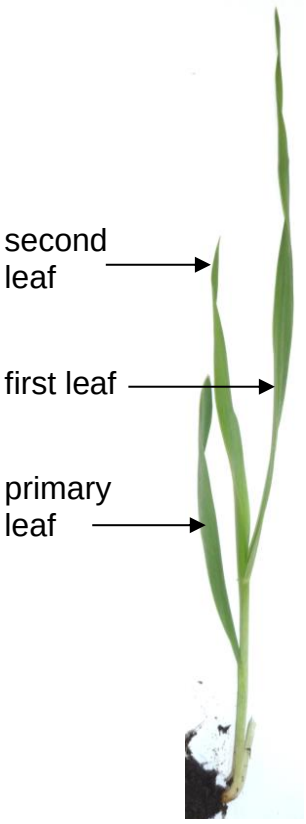

Figure 29. Overview of the leaf architecture in a 2-week-old barley plant.

Arabidopsis thaliana plants were grown on soil (Floradur Anzuchtsubstrat B Seed, Floragard) mixed with silica sand at a ratio of 5+1 and kept at 10 h light and 14 h darkness at a temperature of 22 °C (day)/18 °C (night).

6.1.2 Syringe-infiltration application of chemical compounds

Stock solutions of each chemical compound were freshly prepared for each experiment (for suppliers, see Table 4). SA was dissolved at 4 M and ABA as well as

MeJA at 400 mM in 100% methanol. Fol was dissolved at 1 M and AzA at 2 M in 50% MeOH. For plant treatments, the substances were diluted to 1 mM SA (Wittek et al. 2015; Görlach et al. 1996), 100 µM ABA or MeJA (Dey et al. 2014), 50 or 500 µM Fol (Wittek et al. 2015), and 1 mM AzA (Jung et al. 2009; Cecchini et al. 2015) in 10 mM $MgCl_2$. 0.025% MeOH in 10 mM $MgCl_2$ served as the mock treatment. To monitor systemically induced resistance, the first true leaves of 3-week-old barley plants (6 plants per treatment) were infiltrated with the different compounds or the mock solution using a needleless syringe. Five days after the primary treatment, the second leaves of the treated plants were infected with either *Xtc*, *Bgh*, or *P. teres* (see below). To monitor local induced resistance against *Xtc*, 4-week-old barley plants were sprayed with 1 mM SA, 500 µM Fol, 1 mM Aza, or 0.05% MeOH (as mock treatment) in 0.01% Tween-20. To monitor local induced resistance against *Bgh*, 1 mM SA, 500 µM Fol, and 1 mM AzA in 10 mM $MgCl_2$ were syringe-infiltrated into the first true leaves of 3-week-old barley plants. 0.025% MeOH in 10 mM $MgCl_2$ served as the mock treatment. To monitor local induced resistance against *P. teres*, the second true leaves of 3-week-old barley plants were syringe-infiltrated with the compounds. The treated leaves were inoculated with *Xtc* 1 day after treatment, with *Bgh* 5 days after treatment, or with *P. teres* 1 day after treatment.

6.1.3 Soil-drench application of pipecolic acid

Pip (Table 4) was dissolved at 0.75 mM in H_2O. Pip was applied by soil drench at an amount of 30 µmol per plant. The same volume of H_2O served as mock treatment. Pre-treated plants were infected in the second true leaves with *Xtc*, *Bgh*, or *P. teres* 3 days later (see below).

6.2 Pathogen infections

6.2.1 Infection with *Pseudomonas syringae* pv. *japonica*

For infection, *Psj* (Table 2) was grown on LMG medium (Table 7) over night at 28 °C. Bacteria were subsequently resuspended in 1 ml 10 mM $MgCl_2$. The concentration of the bacterial suspension was adjusted to ~10^6 colony forming units (cfu)/ml in 10 mM $MgCl_2$ using a photometer (assuming the formula: OD_{600} of 0.2 equals ~10^8 cfu/ml). Leaves of 3–6 barley plants were subsequently inoculated with the resulting *Psj*

suspension by infiltration using a needleless syringe. The infected plants were covered with a plastic hood and then inoculated with *Xtc*, *Bgh*, or *P. teres* 5 days later.

6.2.2 Infection with *Xanthomonas translucens* pv. *cerealis*

For infection, *Xtc* (Table 2) was grown on LMG medium (Table 7) over night at 28 °C. Bacterial solutions were prepared as described for *Psj* above, but with a concentration of 10^5 cfu/ml. Leaves of 3–6 barley plants were infiltrated with the *Xtc* suspension using a needleless syringe. The infected plants were covered with a plastic hood and kept in the green house for 4 days, after which bacterial titres were determined. To this end, three 6 mm leaf discs were punched out of the lower leaf half of each *Xtc*-infected leaf. These were shaken at 600 rpm for 1 h at room temperature in 500 µl 10 mM $MgCl_2$ with 0.01% Silwet. The resulting suspension was diluted with 10 mM $MgCl_2$ in five serial 1:10 steps. Twenty µl of each dilution were spotted on LMG or NB plates. The plates were incubated for four days at room temperature and *Xtc* colonies were counted in the appropriate dilution steps to calculate the bacterial titre according to the formula:

$$\frac{cfu}{cm^2} = colony\ count \times dilution\ factor \times \frac{V_{total}}{V_{spotted}} \div leaf\ disc\ area$$

$$with\ leaf\ disc\ area\ for\ 3\ discs = leaf\ disc\ radius^2 \times \pi \times 3$$

6.2.3 Infection with *Blumeria graminis* f. sp. *hordei*

Bgh (Table 2) propagation and inoculation was performed essentially as described in (Delventhal et al. 2017). In short, a pot containing 12 10-day-old seedlings was infected with *Bgh* one week prior to each experiment. Six hours prior to the start of an experiment, these plants were shaken in order to remove old conidia and provide a uniform inoculum for the experiment (Nair and Ellingboe 1962). Pre-treated plants were subsequently inoculated with spores from the prepared *Bgh*-infected plants in an inoculation tower (Delventhal et al. 2017) at an inoculation density of ~30 spores/mm^2. The inoculated plants were placed back in the climate chamber for 6 days after which *Bgh* propagation was evaluated using DAF-FM DA staining (see below).

6.2.4 Infection with *Pyrenophora teres*

P. teres (Table 2) was grown on oat plates (Table 7) for ~one week at room temperature in the dark and then transferred to light for at least 2 weeks. Two ml of infection solution for fungi (Table 6) were pipetted onto the *P. teres* plates and spores

were scratched off the agar using an inoculation loop. The spore suspension was subsequently pipetted into a 5 ml tube and vortexed. After determining the spore concentration under a binocular, the spore suspension was diluted to 65-110 spores per µl. Infections were performed on 6 cm-long segments of a leaf, at a distance of 1.5 centimetres from the leaf base. Five 3 µl droplets of spore suspension were pipetted alternatingly on each side of the leaf midrib. The drops were left to dry for ~1 h and the plants (6 plants per treatment) were then covered with a plastic hood. Necrotic lesions caused by *P. teres* were measured 4 days after infection using the ImageJ macro PIDIQ (Laflamme et al. 2016). The macro was modified to measure brown necrotic lesions caused by *P. teres.* These modifications were restricted to the values used for colour characterisation; the values for lesion measurements were as follows: hue 0-52, saturation 150-255, brightness 0-150 or hue 0-45, saturation 150-255, brightness 0-255.

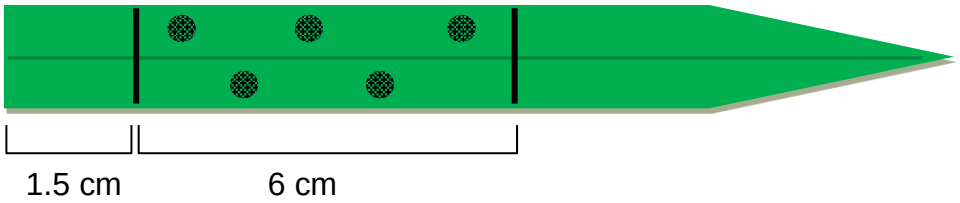

Figure 30. Schematic depiction of an infection with *P. teres* spores on a barley leaf.

6.3 DAF staining

Four leaf discs (6 mm) were cut out of the distal halves of each first (local/compound-treated) and second (systemic) true leaf of the treated plants. The discs were incubated with 5 µM DAF-FM DA in MES buffer (Table 6) for 45 min in the dark and then vacuum-infiltrated. Subsequently, the leaf discs were placed in light (45 V lamp) for 1 h and 45 min and afterwards distributed on 96-well plates (1 leaf disc per well, 20–24 discs from 6 plants per treatment) with the wells filled evenly to the rim with 1% phytoagar. Fluorescence of appropriate *z*-stacks was visualised using the 5x objective of an inverse spinning disc confocal microscope. Chlorophyll was excited using a laser with 561 nm and detected using a bandpass 629/62 filter; DAF-FM DA was excited using a laser with 488 nm and detected using a bandpass 525/50 filter (Foissner et al. 2000). The 96-well plates were transferred to the microscope with a KiNEDx Robot. The robot and the visualisation as well as evaluation were controlled by the softwares CyBio Application Studio/CyBio Feeder for Zeiss Microscope and ZEN2 (Table 15).

Fluorescence intensities were normalised to those of uninfected barley plants (background fluorescence) of the same age in case of *Bgh* staining with DAF-FM DA. In case of NO staining with DAF-FM DA, fluorescence intensities were normalised to those of untreated barley plants of the same age.

6.4 Protoplast isolation and transformation

The isolation protocol is based on (Zhang et al. 2011), with modifications by Reinhard Pröls (Chair for Plant Pathology, TUM).

Barley (*Hordeum vulgare*) cultivar “Golden Promise” seeds were sterilised in 1.2% sodium hypochlorite for 3 min with 25 inversions per min. Subsequently, seeds were rinsed three times with sterile water for 10 min with 25 inversions per min. Sixteen seeds were sawn per pot and grown in a plant chamber in 14 h light with 20°C and 10 h dark at 18°C and 70% humidity. The upper surface of the primary leaves (Figure 29) of 7-10 day-old barley seedlings was cut but not cut through transversally close to the leaf tip. The latter was then pulled downward on the side of the lower leaf surface to peel off the lower epidermis. The leafs were floated with the exposed mesophyll on 10 ml digestion solution (Table 6) in a petri dish for 3 h in the dark with occasional gentle rotation. Ten ml of W5 solution (Table 6) were added, followed by gentle shaking for 10 sec. The protoplast suspension was then filtered through 40 µm nylon cell sieves into a tube and centrifuged for 3 min at 1,000 rpm and room temperature. The supernatant was discarded using a pipette and 10 ml W5 solution were added. Twenty µl protoplast suspension were added in a tube with 80 µl W5 solution and trypan blue, mixed gently and incubated for 5 min at room temperature. Ten µl of stained cells were placed in a Fuchs-Rosenthal counting chamber and the number of unstained cells was counted in 16 small squares. The protoplast concentration was calculated as follows:

protoplast number in 16 small squares × dilution factor × 5,000 = protoplasts/ml

Protoplasts were then diluted to 2.5 × 10^6 cells/ml in MMG solution (Table 6). For transformation, 10 µg of plasmid DNA were mixed with 100 µl of protoplasts in a 2 ml tube. After adding 110 µl of freshly prepared PEG solution (Table 6), the solution was mixed and incubated at room temperature for 10-20 min in the dark. 440 µl W5 solution were slowly added, mixed by gentle inversions and centrifuged for 3 min at 1,000 rpm.

The protoplast pellets were resuspended in 2 ml WI solution (Table 6), transferred to 6-well-plates and incubated in the dark for 24-60 h at room temperature.

6.5 Molecular biological methods

6.5.1 DNA isolation from plants

Frozen plant material was ground in liquid nitrogen, 500 µl chloroform and 500 µl CTAB solution (Table 6) plus 1% β-mercaptoethanol were added and the samples were shaken at 1,400 rpm/8°C/15 min. Then, the samples were centrifuged at 13,300 rpm/4°C/10 min. The supernatant (approx. 600 µl) was transferred to a new tube and 100 µl Nucleon Resin (Table 3) and 500 µl chloroform were added. Samples were shaken and centrifuged as above. The supernatant (approx. 500 µl) was transferred to a new tube supplemented with 250 µl isopropanol. Samples were mixed, incubated on ice for 10 min and centrifuged as above. The supernatant was decanted, 1 ml of 70% ethanol/0.1 M sodium acetate was added to the pellet and the samples were incubated for 5 min at room temperature. The pellet was washed first with 80% ethanol, then with 100% ethanol and subsequently dried for circa 10 min below a clean bench at room temperature. In order to dissolve the pellet, 50-100 µl H_2O was added and the samples were shaken at 800 rpm/ 8°C/20 min.

6.5.2 Quick DNA isolation for genotyping

The protocol was kindly provided by Sebastian Scholz (Chair for Plant Developmental Biology, TUM).

Frozen plant tissue was disrupted using a homogenizer, 400 µl of gDNA extraction buffer (Table 6) were added and mixed by inverting the tubes. The samples were centrifuged at 13,000 rpm/3 min, then 300 µl of supernatant were transferred to new tubes containing 300 µl isopropanol, mixed by inverting and incubated for 3 min at room temperature. The samples were centrifuged at 13,000 rpm/8 min, the supernatant was discarded and 500 µl 70% ethanol were added. The tubes were centrifuged at 13,000 rpm/2 min, the supernatant was discarded, the pellets were dried and resuspended in 100 µl 5 mM Tris/HCl pH 8.5.

6.5.3 RNA isolation from plants

Frozen plant material was ground in liquid nitrogen and RNA was isolated using phenol-extraction (Table 6) according to (Logemann et al. 1987). Quality and concentration of RNA samples were determined by measuring the absorption at 260 nm and 280 nm using a spectrophotometer.

6.5.4 cDNA synthesis

cDNA was synthesised from 1.5 µg of RNA using SuperScriptII reverse transcriptase (Table 5) following the manufacturer's instructions (Invitrogen/Thermo Fisher Scientific).

6.5.5 Reverse transcription quantitative PCR

RT-qPCR was performed with the SensiMix SYBR Low ROX kit on a 7500 Fast qPCR system (Table 3) according to the manufacturers' instructions (Bioline and Applied Biosystems). cDNA was used as template to quantify gene expression. Expression was normalised to the reference gene *HvEF1α* for barley or *AtUbq10* for *Arabidopsis*.

6.5.6 PCR

Phusion high fidelity polymerase was used for the replication of the target genes to be sequenced and for cloning. Phire Hot Start II DNA polymerase was used for genotyping. MangoTaq was used for genotyping and all other purposes (Table 5).

12.5 µl sterile H_2O	10 µl Phire II master mix	8.6 µl sterile H_2O
5 µl 5x buffer	2 µl 5 µM forward primer	4 µl 5x buffer
0.5 µl dNTPs	2 µl 5 µM reverse primer	1 µl 50 mM $MgCl_2$
0.75 µl DMSO/formamide	0.6 µl formamide	0.4 µl dNTPs
2.5 µl 5 µM forward primer	0.5 µl DNA	0.6 µl DMSO/formamide
2.5 µl 5 µM reverse primer	4.4 µl H_2O	2 µl 5 µM forward primer
0.25 µl Phusion polymerase	19.5 µl	2 µl 5 µM reverse primer
24 µl	+ 0.5 µl template DNA	0.4 µl MangoTaq
+ 1 µl template DNA		19 µl
		+ 1 µl template DNA
temperature profile:	temperature profile:	temperature profile:
98°C – 2 min	98°C – 5 min	95°C – 1 min 30 sec
98°C – 15 sec	98°C – 15 sec	95°C – 20 sec
xx°C – 7-10 sec	56.6°C – 5 sec	xx°C – 3-5 sec
72°C – 30 sec per kb	72°C – 15 sec	72°C – 30 sec per kb
72°C – 10 min	72°C – 1 min	72°C – 10 min
10°C – hold	10°C – hold	10°C – hold

steps 2-4 were repeated 29-34 times	steps 2-4 were repeated 39 times	steps 2-4 were repeated 29-39 times

6.5.7 Gateway cloning

DNA fragments were cloned into pENTR/D-TOPO (Table 13) according to the manufacturer's instructions (Invitrogen).

6.5.8 Golden Gate Cloning of CRISPR/Cas vectors

Genome editing vectors for monocots (pMGE, Table 13) using the CRISPR/Cas system were designed and provided by Johannes Stuttmann, Institut für Biologie/Genetik, Martin-Luther-Universität Halle (Saale). Shuttle vector sequences and promoters as well as genes encoded on the recipient vector were published in (Kumar et al. 2018). The recipient vector backbone corresponds to the vectors published in (Ordon et al. 2017).

Two cut sites at a distance of 50-100 bp between each other were targeted in every gene of interest. In some circumstances, this results in the deletion of the sequence between the cut sites and thereby facilitates the recognition of mutations by PCR. For each target gene, at least two constructs were generated with two gRNAs each. Additionally, two constructs were cloned targeting two genes at the same time: *ERF-like* and *ERF4.*

gRNA sequences of 20 nucleotides length were designed using CRISPRdirect online (Naito *et al.*, 2015) and introduced into shuttle vectors as hybridised oligonucleotides. BsaI and BpiI restriction enzyme recognition sites and stretches of multiple thymidines had to be avoided in the gRNA sequences. A cloning overhang of GTTG was attached to the sequence at the 5' end of the forward oligonucleotide and AAAC at the 5' end of the reverse oligonucleotide (Supplemental Table 3). In case of a gRNA sequence starting with G, only GTT was added to the forward oligonucleotide and the last nucleotide at the 3' end of the reverse oligonucleotide was omitted. This lead to 24- or 23-base pair-long oligonucleotide sequences for gRNA insertion. These were hybridised by heating a tube with the following content to 98°C for 5 min and subsequent slow cooling.

5 µl 100 µM forward oligonucleotide
5 µl 100 µM reverse oligonucleotide
40 µl H_2O

The annealed oligonucleotides were diluted 1:100 to get a final concentration of 100 fmol/µl and cloned into the appropriate shuttle vector. For one gRNA to be cloned in the final vector, shuttle vector pMGE516 was used, for two gRNAs pMGE501 and 505 and for 4 gRNAs pMGE501, 503, 509, and 508. The reaction mix for shuttle vector cloning was as follows:

20 fmol shuttle vector (≈ 60 ng)
200 fmol hybridised oligonucleotides (= 2 µl)
1 µl 10x ligation buffer
1 µl 10x bovine serum albumin (1 mg/ml)
0.5 µl BpiI
0.5 µl T4 DNA ligase (5 U/µl)
ad 10 µl H_2O

The reaction mix was incubated for 30 cycles of alternately 2 min 37°C and 5 min 16°C, with two subsequent inactivation steps for 10 min at 50°C and 80°C, respectively. The ligated vector was transformed in chemically competent *E. coli*, which were then plated on LB containing ampicillin and incubated at 37°C over night. Two colonies were picked to each inoculate 5 ml of LB medium with ampicillin and grown at 37°C over night. DNA was extracted using the Qiagen Miniprep Kit (Table 3) according to the manufacturer's instructions, a restriction enzyme digest was performed using PvuII (Table 5) and correct insertion was verified by sequencing with the M13 rev (-29) primer provided by Eurofins. Correct shuttle vectors were assembled with the final vector pMGE500 in the following reaction mix:

20 fmol pMGE500 (≈ 200 ng)
20 fmol shuttle vector (≈ 40 ng)
2 µl 10x Ligation buffer
2 µl 10x bovine serum albumin (1 mg/ml)
1 µl BsaI
1 µl T4 DNA ligase (5 U/µl)
ad 20 µl H_2O

The reaction mix was incubated for 50 cycles of alternately 2 min 37°C and 5 min 16°C, with two subsequent inactivation steps for 10 min at 50°C and 80°C, respectively. The ligated vector was transformed in chemically competent *E. coli*, which were then plated on LB containing kanamycin and incubated at 37°C over night. Two colonies were picked to each inoculate 5 ml of LB medium with kanamycin and grown at 37°C over night. DNA was extracted using the Qiagen Miniprep Kit (Table 3) according to the manufacturer's instructions. A restriction enzyme digest was

performed using HincII and XhoI (for two shuttle vectors to be inserted) or HincII and XbaI (for one or four shuttle vectors to be inserted) according to the manufacturer's instructions and correct insertion was verified by sequencing with the M13f primer (Table 9) for a one and two shuttle vector insertion and additionally JS1057 for a four shuttle vector insertion. Verified vectors were isolated in bigger scale using the Qiagen Plasmid Midi Kit (Table 3) according to the manufacturer's instructions.

6.5.9 Golden Gate Cloning of reporter vectors

Reporter vectors for monocots (pJOG541, Table 13) were designed and provided by Johannes Stuttmann, Institut für Biologie/Genetik, Martin-Luther-Universität Halle (Saale). The vector backbone corresponds to the one published by Ordon et al. (2018). New oligonucleotides were ordered as spacer sequences. They were designed to be identical to the variable parts of the corresponding gRNAs to be tested. The cloning overhang of the forward oligonucleotide was changed to ATTG and that of the reverse oligo to CCCT (Supplemental Table 4). Oligonucleotides were annealed and diluted as described above (6.5.8 Golden Gate Cloning of CRISPR/Cas vectors). A cut/ligation reaction was set up as follows:

20 fmol reporter vector (≈ 150 ng)
200 fmol hybridised oligonucleotides (= 2 µl)
1 µl 10x ligation buffer
1 µl 10x bovine serum albumin (1 mg/ml)
0.5 µl BsmBI (Thermo Scientific, Waltham, USA)
0.5 µl T4 DNA ligase (5 U/µl) (Fermentas, St Leon-Rot, Germany)
ad 10 µl H_2O

All further steps were performed as described above (6.5.8 Golden Gate Cloning of CRISPR/Cas vectors) except for digestion, which was done using BamHI and EcoRI and sequencing, for which ML 40 (Table 9) was used.

6.5.10 Transformation of *Escherichia coli*

A tube containing chemically competent *E. coli* (Table 2) was thawed on ice water, an appropriate amount of DNA or cloning reaction was added and mixed by carefully stirring with the pipette tip. The mixture was incubated for 30 min on ice water, subsequently heat shocked for 30 sec at 42°C and rested for 5 min on ice water again. 250 µl of SOC medium (Table 7) were added and the tube was shaken at 37°C for 1 h at 200 rpm. Two aliquots of 30 µl and 270 µl were plated on LB medium (Table 7) containing the appropriate antibiotic (Table 8) and incubated at 37°C over night.

6.5.11 T7EI assay

A region of circa 500 bp around the CRISPR/Cas target sites was replicated via PCR (see above) and used to form DNA heteroduplexes. For detection of mutations, the following mixtures were used:

heterozygous mutations		**homozygous mutations**	
5 µl	PCR reaction of transgenic line	5 µl	PCR reaction of transgenic line
2 µl	10x NEB2 buffer	5 µl	PCR reaction of wild type
12 µl	H_2O	2 µl	10x NEBuffer 2
		12 µl	H_2O

The reaction mix was put in a thermomixer, heated at 95 °C for 5 min and then slowly cooled to allow double-strand formation (95-85 °C: -1.5 °C/sec, 85-25 °C: -0.1 °C/sec). 1 µl T7EI (10 units/µl) (Table 5) was added to each tube, mixed, spinned down and incubated at 37 °C for 15 min. The digestion products were separated on a 2% agarose gel using electrophoresis.

6.6 Statistics

Data were analyzed in GraphPad Prism 7 for Windows. In order to test for Gaussian distribution, experiments with up to 6 replicates per sample were analysed using the Shapiro-Wilk normality test and experiments with more replicates were analysed using the D'Agostino–Pearson normality test, both with $\alpha = 0.01$. If the normality assumption failed, data with only positive values were $\log_2$ transformed and data with negative and positive values were transformed according to the formula: $Y=\log_2[Y+1-\min(Y)]$, where min(Y) denotes the lowest measured value within the experiment. Outliers were removed using Grubbs' test with $\alpha = 0.05$. If it was necessary to assure normal data distribution, the Grubbs' outlier test was repeated (a maximum of 2 Grubbs' outlier tests were performed per data set).

For normal data with two groups, an *F*-test was used to compare variances. If the P value of the *F*-test was 0.05 or higher, an unpaired two-tailed *t*-test was conducted. If the P value of the *F*-test was below 0.05, an unpaired two-tailed *t*-test with Welch's correction was conducted. For non-normal data, the non-parametric two-tailed Mann-Whitney test was used.

For normal data with more than two groups, one-way ANOVA with Geisser-Greenhouse correction ($P<0.05$) and a subsequent Dunnett's or Sidak's post-hoc test

with α=0.05 was conducted. Dunnet's post-hoc test was used for comparisons to one control group; Sidak's post-hoc test was used for comparisons between chosen group pairings.

In case of single experiments repeatedly showing tendencies but insignificant results, data from several experiment were merged and analysed together.

For qPCR analysis, average ΔCt values for each single gene from several experiments were collected and analysed using either an unpaired two-tailed *t*-test (with or without Welch's correction) in the case of 2 groups (meaning one gene, treated and untreated) or a one-way ANOVA in the case of more than 2 groups (several genes, treated and untreated). Since 5 one-way ANOVAs had to be conducted to analyse 5 repeats, α was reduced to α = 0.01. As post-hoc test, Sidak's multiple comparisons test was used with α = 0.05.

7 References

Ahmed, S. M., Liu, P., Xue, Q., Ji, C., Qi, T., Guo, J., Guo, J., and Kang, Z. 2017. TaDIR1-2, a Wheat Ortholog of Lipid Transfer Protein AtDIR1 Contributes to Negative Regulation of Wheat Resistance against *Puccinia striiformis* f. sp. *tritici*. Front. Plant Sci. 8:521

Armijo, G., Salinas, P., Monteoliva, M. I., Seguel, A., García, C., Villarroel-Candia, E., Song, W., van der Krol, A. R., Álvarez, M. E., and Holuigue, L. 2013. A Salicylic Acid–Induced Lectin-Like Protein Plays a Positive Role in the Effector-Triggered Immunity Response of Arabidopsis thaliana to Pseudomonas syringae Avr-Rpm1. Mol. Plant-Microbe Interact. 26:1395–1406

Balmer, D., De Papajewski, D. V., Planchamp, C., Glauser, G., and Mauch-Mani, B. 2013a. Induced resistance in maize is based on organ-specific defence responses. Plant J. 74:213–225

Balmer, D., Planchamp, C., and Mauch-Mani, B. 2013b. On the move: Induced resistance in monocots. J. Exp. Bot. 64:1249–1261

Barrangou, R., Fremaux, C., Deveau, H., Richards, M., Boyaval, P., Moineau, S., Romero, D. A., and Horvath, P. 2007. CRISPR provides acquired resistance against viruses in prokaryotes. Science. 315:1709–1712

Beckers, G. J. M., and Spoel, S. H. 2006. Fine-tuning plant defence signalling: Salicylate versus jasmonate. Plant Biol. 8:1–10

Belhaj, K., Chaparro-Garcia, A., Kamoun, S., Patron, N. J., and Nekrasov, V. 2015. Editing plant genomes with CRISPR/Cas9. Curr. Opin. Biotechnol. 32:76–84

Bernsdorff, F., Doering, A.-C., Gruner, K., Schuck, S., Bräutigam, A., and Zeier, J. 2016. Pipecolic acid orchestrates plant systemic acquired resistance and defense priming via salicylic acid-dependent and independent pathways. Plant Cell. 28:102–129

Beßer, K., Jarosch, B., Langen, G., and Kogel, K.-H. 2000. Expression analysis of genes induced in barley after chemical activation reveals distinct disease resistance pathways. Mol. Plant Pathol. 1:277–286

Birkenbihl, R. P., Kracher, B., and Somssich, I. E. 2017. Induced Genome-Wide Binding of Three *Arabidopsis* WRKY Transcription Factors during Early MAMP-Triggered Immunity. Plant Cell. 29:20–38

Bortesi, L., and Fischer, R. 2015. The CRISPR/Cas9 system for plant genome editing and beyond. Biotechnol. Adv. 33:41–52

Breitenbach, H. H., Wenig, M., Wittek, F., Jorda, L., Maldonado-Alconada, A. M., Sarioglu, H., Colby, T., Knappe, C., Bichlmeier, M., Pabst, E., Mackey, D., Parker, J. E., and Vlot, A. C. 2014. Contrasting Roles of the Apoplastic Aspartyl Protease APOPLASTIC, ENHANCED DISEASE SUSCEPTIBILITY1-DEPENDENT1 and LEGUME LECTIN-LIKE PROTEIN1 in *Arabidopsis* Systemic Acquired Resistance,. Plant Physiol. 165:791–809

Brinkman, E. K., Chen, T., de Haas, M., Holland, H. A., Akhtar, W., and van Steensel, B. 2018. Kinetics and Fidelity of the Repair of Cas9-Induced Double-Strand DNA Breaks. Mol. Cell. 70:801–813.e6

Büschges, R., Hollricher, K., Panstruga, R., Simons, G., Wolter, M., Frijters, A., van Daelen, R., van der Lee, T., Diergaarde, P., Groenendijk, J., Töpsch, S., Vos, P., Salamini, F., and Schulze-Lefert, P. 1997. The barley Mlo gene: a novel control element of plant pathogen resistance. Cell. 88:695–705

Cecchini, N. M., Steffes, K., Schläppi, M. R., Gifford, A. N., and Greenberg, J. T. 2015. *Arabidopsis* AZI1 family proteins mediate signal mobilization for systemic defence priming. Nat. Commun. 6:7658

Champigny, M. J., Isaacs, M., Carella, P., Faubert, J., Fobert, P. R., and Cameron, R. K. 2013. Long distance movement of DIR1 and investigation of the role of DIR1-like during systemic acquired resistance in *Arabidopsis*. Front. Plant Sci. 4:230

Chanda, B., Xia, Y., Mandal, M. K., Yu, K., Sekine, K. T., Gao, Q. M., Selote, D., Hu, Y., Stromberg, A., Navarre, D., Kachroo, A., and Kachroo, P. 2011. Glycerol-3-phosphate is a critical mobile inducer of systemic immunity in plants. Nat. Genet. 43:421–429

Chaturvedi, R., Venables, B., Petros, R. A., Nalam, V., Li, M., Wang, X., Takemoto, L. J., and Shah, J. 2012. An abietane diterpenoid is a potent activator of systemic acquired resistance. Plant J. 71:161–172

Chen, Y.-C., Holmes, E. C., Rajniak, J., Kim, J.-G., Tang, S., Fischer, C. R., Mudgett, M. B., and Sattely, E. S. 2018. N-hydroxy-pipecolic acid is a mobile metabolite that induces systemic disease resistance in *Arabidopsis*. Proc. Natl. Acad. Sci. U. S. A. 115:E4920–E4929

Chen, Z., Silva, H., and Klessig, D. 1993. Active oxygen species in the induction of plant systemic acquired resistance by salicylic acid. Science. 262:1883–1886

Conrath, U., Beckers, G. J. M., Flors, V., García-Agustín, P., Jakab, G., Mauch, F., Newman, M.-A., Pieterse, C. M. J., Poinssot, B., Pozo, M. J., Pugin, A., Schaffrath, U., Ton, J., Wendehenne, D., Zimmerli, L., and Mauch-Mani, B. 2006. Priming: Getting Ready for Battle. Mol. Plant-Microbe Interact. 19:1062–1071

Cui, J., Bahrami, A. K., Pringle, E. G., Hernandez-Guzman, G., Bender, C. L., Pierce, N. E., and Ausubel, F. M. 2005. *Pseudomonas syringae* manipulates systemic plant defenses against pathogens and herbivores. Proc. Natl. Acad. Sci. 102:1791–1796

Dean, R., Van Kan, J. A. L., Pretorius, Z. A., Hammond-Kosack, K. E., Di Pietro, A., Spanu, P. D., Rudd, J. J., Dickman, M., Kahmann, R., Ellis, J., and Foster, G. D. 2012. The Top 10 fungal pathogens in molecular plant pathology. Mol. Plant Pathol. 13:414–430

Delventhal, R., Falter, C., Strugala, R., Zellerhoff, N., and Schaffrath, U. 2014. Ectoparasitic growth of *Magnaporthe* on barley triggers expression of the putative barley wax biosynthesis gene *CYP96B22* which is involved in penetration resistance. BMC Plant Biol. 14:26

Delventhal, R., Rajaraman, J., Stefanato, F. L., Rehman, S., Aghnoum, R., McGrann, G. R. D., Bolger, M., Usadel, B., Hedley, P. E., Boyd, L., Niks, R. E., Schweizer, P., and Schaffrath, U. 2017. A comparative analysis of nonhost resistance across the two *Triticeae* crop species wheat and barley. BMC Plant Biol. 17:232

Dey, S., Wenig, M., Langen, G., Sharma, S., Kugler, K. G., Knappe, C., Hause, B., Bichlmeier, M., Babaeizad, V., Imani, J., Janzik, I., Stempfl, T., Huckelhoven, R., Kogel, K.-H., Mayer, K. F. X., and Vlot, A. C. 2014. Bacteria-Triggered Systemic Immunity in Barley Is Associated with WRKY and ETHYLENE RESPONSIVE FACTORs But Not with Salicylic Acid. Plant Physiol. 166:2133–2151

Dieci, G., Fiorino, G., Castelnuovo, M., Teichmann, M., and Pagano, A. 2007. The expanding RNA polymerase III transcriptome. Trends Genet. 23:614–622

Ding, P., Rekhter, D., Ding, Y., Feussner, K., Busta, L., Haroth, S., Xu, S., Li, X., Jetter, R., Feussner, I., and Zhang, Y. 2016. Characterization of a Pipecolic Acid Biosynthesis Pathway Required for Systemic Acquired Resistance. Plant Cell. 28:2603–2615

Ding, Y., Sun, T., Ao, K., Peng, Y., Zhang, Y., Li, X., and Zhang, Y. 2018. Opposite Roles of Salicylic Acid Receptors NPR1 and NPR3/NPR4 in Transcriptional Regulation of Plant Immunity. Cell. 173:1454–1467.e10

Doench, J. G., Fusi, N., Sullender, M., Hegde, M., Vaimberg, E. W., Donovan, K. F., Smith, I., Tothova, Z., Wilen, C., Orchard, R., Virgin, H. W., Listgarten, J., and Root, D. E. 2016. Optimized sgRNA design to maximize activity and minimize off-target effects of CRISPR-Cas9. Nat. Biotechnol. 34:184–191

Doench, J. G., Hartenian, E., Graham, D. B., Tothova, Z., Hegde, M., Smith, I., Sullender, M., Ebert, B. L., Xavier, R. J., and Root, D. E. 2014. Rational design of highly active sgRNAs for CRISPR-Cas9-mediated gene inactivation. Nat. Biotechnol. 32:1262–1267

Durner, J., Shah, J., and Klessig, D. F. 1997. Salicylic acid and disease resistance in plants. Trends Plant Sci. 2:266–274

Foissner, I., Wendehenne, D., Langebartels, C., and Durner, J. 2000. In vivo imaging of elicitor-induced nitric oxide burst in tobacco. Plant J. 23:817–824

Fu, Z. Q., and Dong, X. 2013. Systemic Acquired Resistance: Turning Local Infection into Global Defense. Annu. Rev. Plant Biol. 64:839–863

Fu, Z. Q., Yan, S., Saleh, A., Wang, W., Ruble, J., Oka, N., Mohan, R., Spoel, S. H., Tada, Y., Zheng, N., and Dong, X. 2012. NPR3 and NPR4 are receptors for the immune signal salicylic acid in plants. Nature. 486:228–232

Gamir, J., Sánchez-Bel, P., and Flors, V. 2014. Molecular and physiological stages of priming: how plants prepare for environmental challenges. Plant Cell Rep. 33:1935–1949

Gao, Q.-M., Zhu, S., Kachroo, P., and Kachroo, A. 2015. Signal regulators of systemic acquired resistance. Front. Plant Sci. 6:228

Gao, Q. M., Kachroo, A., and Kachroo, P. 2014. Chemical inducers of systemic immunity in plants. J. Exp. Bot. 65:1849–1855

Garcia-Seco, D., Chiapello, M., Bracale, M., Pesce, C., Bagnaresi, P., Dubois, E., Moulin, L., Vannini, C., and Koebnik, R. 2017. Transcriptome and proteome analysis reveal new insight into proximal and distal responses of wheat to foliar infection by *Xanthomonas translucens*. Sci. Rep. 7:10157

Glazebrook, J. 2005. Contrasting Mechanisms of Defense Against Biotrophic and Necrotrophic Pathogens. Annu. Rev. Phytopathol. 43:205–227

Görlach, J., Volrath, S., Knauf-Beiter, G., Hengy, G., Beckhove, U., Kogel, K., Oostendorp, M., Staub, T., Ward, E., Kessmann, H., and Ryals, J. 1996. Benzothiadiazole, a Novel Class of Inducers of Systemic Acquired Resistance, Activates Gene Expression and Disease Resistance in Wheat. Plant Cell. 8:629–643

Gourbal, B., Pinaud, S., Beckers, G. J. M., Van Der Meer, J. W. M., Conrath, U., and Netea, M. G. 2018. Innate immune memory: An evolutionary perspective. Immunol. Rev. 283:21–40

Gruner, K., Griebel, T., Návarová, H., Attaran, E., and Zeier, J. 2013. Reprogramming of plants during systemic acquired resistance. Front. Plant Sci. 4:252

Hartmann, M., Zeier, T., Bernsdorff, F., Reichel-Deland, V., Kim, D., Hohmann, M., Scholten, N., Schuck, S., Bräutigam, A., Hölzel, T., Ganter, C., and Zeier, J. 2018. Flavin Monooxygenase-Generated N-Hydroxypipecolic Acid Is a Critical Element of Plant Systemic Immunity. Cell. 173:456–469.e16

Henry, E., Yadeta, K. A., and Coaker, G. 2013. Recognition of bacterial plant pathogens: Local, systemic and transgenerational immunity. New Phytol. 199:908–915

Hilker, M., Schwachtje, J., Baier, M., Balazadeh, S., Bäurle, I., Geiselhardt, S., Hincha, D. K., Kunze, R., Mueller-Roeber, B., Rillig, M. C., Rolff, J., Romeis, T., Schmülling, T., Steppuhn, A., van Dongen, J., Whitcomb, S. J., Wurst, S., Zuther, E., and Kopka, J. 2016. Priming and memory of stress responses in organisms lacking a nervous system. Biol. Rev. 91:1118–1133

Højland Knudsen, C., Ásgrímsdóttir, E. S., Rahimi, K., Gill, K. P., Frandsen, S., Hvolbøl Buchholdt, S., Chen, M., Kjems, J., Febbraro, F., and Denham, M. 2018. A Modified Monomeric Red Fluorescent Protein Reporter for Assessing CRISPR Activity. Front. Cell Dev. Biol. 6:54

Hückelhoven, R., Fodor, J., Preis, C., and Kogel, K.-H. 1999. Hypersensitive Cell Death and Papilla Formation in Barley Attacked by the Powdery Mildew Fungus Are Associated with Hydrogen Peroxide but Not with Salicylic Acid Accumulation. Plant Physiol. 119:1251–1260

Hückelhoven, R., and Panstruga, R. 2011. Cell biology of the plant-powdery mildew interaction. Curr. Opin. Plant Biol. 14:738–746

Huot, B., Yao, J., Montgomery, B. L., and He, S. Y. 2014. Growth-defense tradeoffs in plants: A balancing act to optimize fitness. Mol. Plant. 7:1267–1287

Jain, S. K., Langen, G., Hess, W., Börner, T., Hückelhoven, R., and Kogel, K.-H. 2004. The white barley mutant *albostrians* shows enhanced resistance to the biotroph *Blumeria graminis* f. sp. *hordei*. Mol. Plant. Microbe. Interact. 17:374–382

Jansen, C., Korell, M., Eckey, C., Biedenkopf, D., and Kogel, K.-H. 2005a. Identification and transcriptional analysis of powdery mildew-induced barley genes. Plant Sci. 168:373–380

Jansen, C., von Wettstein, D., Schafer, W., Kogel, K.-H., Felk, A., and Maier, F. J. 2005b. Infection patterns in barley and wheat spikes inoculated with wild-type and trichodiene synthase gene disrupted *Fusarium graminearum*. Proc. Natl. Acad. Sci. 102:16892–16897

Jiang, W. Z., Yang, B., and Weeks, D. P. 2014. Efficient CRISPR/Cas9-mediated gene editing in *Arabidopsis thaliana* and inheritance of modified genes in the T2 and T3 generations. PLoS One. 9:e99225

Jiang, W., Zhou, H., Bi, H., Fromm, M., Yang, B., and Weeks, D. P. 2013. Demonstration of CRISPR/Cas9/sgRNA-mediated targeted gene modification in *Arabidopsis*, tobacco, sorghum and rice. Nucleic Acids Res. 41:e188

Jinek, M., Chylinski, K., Fonfara, I., Hauer, M., Doudna, J. A., and Charpentier, E. 2012. A programmable dual-RNA-guided DNA endonuclease in adaptive bacterial immunity. Science. 337:816–21

Johnson, R. A., Gurevich, V., Filler, S., Samach, A., and Levy, A. A. 2015. Comparative assessments of CRISPR-Cas nucleases' cleavage efficiency in planta. Plant Mol. Biol. 87:143–156

Jones, J. D. G., and Dangl, J. L. 2006. The plant immune system. Nature. 444:323–329

Jung, H. W., Tschaplinski, T. J., Wang, L., Glazebrook, J., and Greenberg, J. T. 2009. Priming in Systemic Plant Immunity. Science. 324:89–91

Kapusi, E., Corcuera-Gómez, M., Melnik, S., and Stoger, E. 2017. Heritable Genomic Fragment Deletions and Small Indels in the Putative ENGase Gene Induced by CRISPR/Cas9 in Barley. Front. Plant Sci. 8:540

Kesarwani, M., Yoo, J., and Dong, X. 2007. Genetic Interactions of TGA Transcription Factors in the Regulation of Pathogenesis-Related Genes and Disease Resistance in *Arabidopsis*. Plant Physiol. 144:336–346

Kinkema, M., Fan, W., and Dong, X. 2000. Nuclear Localization of NPR1 Is Required for Activation of *PR* Gene Expression. Plant Cell. 12:2339–2350

Kiyota, E., Pena, I. A., and Arruda, P. 2015. The saccharopine pathway in seed development and stress response of maize. Plant, Cell Environ. 38:2450–2461

Kleinstiver, B. P., Pattanayak, V., Prew, M. S., Tsai, S. Q., Nguyen, N. T., Zheng, Z., and Joung, J. K. 2016. High-fidelity CRISPR-Cas9 nucleases with no detectable genome-wide off-target effects. Nature. 529:490–495

Klessig, D. F., Choi, H. W., and Dempsey, D. A. 2018. Systemic Acquired Resistance and Salicylic Acid: Past, Present, and Future. Mol. Plant-Microbe Interact. 31:871–888

Klessig, D. F., Durner, J., Noad, R., Navarre, D. A., Wendehenne, D., Kumar, D., Zhou, J. M., Shah, J., Zhang, S., Kachroo, P., Trifa, Y., Pontier, D., Lam, E., and Silva, H. 2000. Nitric oxide and salicylic acid signaling in plant defense. Proc. Natl. Acad. Sci. 97:8849–8855

Kogel, K. H., Ortel, B., Jarosch, B., Atzorn, R., Schiffer, R., and Wasternack, C. 1995. Resistance in barley against the powdery mildew fungus (*Erysiphe graminis* f.sp. *hordei*) is not associated with enhanced levels of endogenous jasmonates. Eur. J. Plant Pathol. 101:319–332

Kojima, H., Urano, Y., Kikuchi, K., Higuchi, T., Hirata, Y., and Nagano, T. 1999. Fluorescent indicators for imaging nitric oxide production. Angew. Chemie - Int. Ed. 38:3209–3212

Komor, A. C., Badran, A. H., Liu, D. R., Guilinger, J. P., Bessen, J. L., Hu, J. H., Maeder, M. L., Joung, J. K., Chen, Z.-Y., Liu, D. R., and Al., E. 2017. CRISPR-based technologies for the manipulation of eukaryotic genomes. Cell. 168:20–36

Kumar, J., Hückelhoven, R., Beckhove, U., Nagarajan, S., and Kogel, K.-H. 2001. A Compromised Mlo Pathway Affects the Response of Barley to the Necrotrophic Fungus *Bipolaris sorokiniana* (Teleomorph: *Cochliobolus sativus*) and Its Toxins. Phytopathology. 91:127–133

Kumar, N., Galli, M., Ordon, J., Stuttmann, J., Kogel, K. H., and Imani, J. 2018. Further analysis of barley MORC1 using a highly efficient RNA-guided Cas9 gene-editing system. Plant Biotechnol. J. :doi: 10.1111/pbi.12924

Laflamme, B., Middleton, M., Lo, T., Desveaux, D., and Guttman, D. S. 2016. Image-Based Quantification of Plant Immunity and Disease. Mol. Plant-Microbe Interact. 29:919–924

Lawrenson, T., Shorinola, O., Stacey, N., Li, C., Østergaard, L., Patron, N., Uauy, C., and Harwood, W. 2015. Induction of targeted, heritable mutations in barley and *Brassica oleracea* using RNA-guided Cas9 nuclease. Genome Biol. 16:258

Lenk, M., Wenig, M., Mengel, F., Häußler, F., Vlot, A., Lenk, M., Wenig, M., Mengel, F., Häußler, F., and Vlot, A. C. 2018. *Arabidopsis thaliana* Immunity-Related Compounds Modulate Disease Susceptibility in Barley. Agronomy. 8:142

Li, J. F., Norville, J. E., Aach, J., McCormack, M., Zhang, D., Bush, J., Church, G. M., and Sheen, J. 2013. Multiplex and homologous recombination-mediated genome editing in *Arabidopsis* and *Nicotiana benthamiana* using guide RNA and Cas9. Nat. Biotechnol. 31:688–691

Li, Y., Song, N., Zhao, C., Li, F., Geng, M., Wang, Y., Liu, W., Xie, C., and Sun, Q. 2016. Application of glycerol for induced powdery mildew resistance in *Triticum aestivum* L. Front. Physiol. 7:1–13

Liang, G., Zhang, H., Lou, D., and Yu, D. 2016. Selection of highly efficient sgRNAs for CRISPR/Cas9-based plant genome editing. Sci. Rep. 6:1–8

Liang, Z., Chen, K., Li, T., Zhang, Y., Wang, Y., Zhao, Q., Liu, J., Zhang, H., Liu, C., Ran, Y., and Gao, C. 2017. Efficient DNA-free genome editing of bread wheat using CRISPR/Cas9 ribonucleoprotein complexes. Nat. Commun. 8:14261

Lim, G. H., Shine, M. B., de Lorenzo, L., Yu, K., Cui, W., Navarre, D., Hunt, A. G., Lee, J. Y., Kachroo, A., and Kachroo, P. 2016. Plasmodesmata Localizing Proteins Regulate Transport and Signaling during Systemic Acquired Immunity in Plants. Cell Host Microbe. 19:541–549

Lin, M. -R., and Edwards, H. H. 1974. Primary Penetration Process in Powdery Mildewed Barley Related to Host Cell Age, Cell Type, and Occurrence of Basic Staining Material. New Phytol. 73:131–137

Liu, X., Homma, A., Sayadi, J., Yang, S., Ohashi, J., and Takumi, T. 2016. Sequence features associated with the cleavage efficiency of CRISPR/Cas9 system. Sci. Rep. 6:19675

Liu, Z., Ellwood, S. R., Oliver, R. P., and Friesen, T. L. 2011. *Pyrenophora teres*: Profile of an increasingly damaging barley pathogen. Mol. Plant Pathol. 12:1–19

Logemann, J., Schell, J., and Willmitzer, L. 1987. Improved method for the isolation of RNA from plant tissues. Anal. Biochem. 163:16–20

van Loon, L. C., Bakker, P. A. H. M., and Pieterse, C. M. J. 1998. Systemic resistance induced by rhizosphere bacteria. Annu. Rev. Phytopathol. 36:453–483

van Loon, L. C., Rep, M., and Pieterse, C. M. J. 2006. Significance of Inducible Defense-related Proteins in Infected Plants. Annu. Rev. Phytopathol. 44:135–162

Ma, X., Zhang, Q., Zhu, Q., Liu, W., Chen, Y., Qiu, R., Wang, B., Yang, Z., Li, H., Lin, Y., Xie, Y., Shen, R., Chen, S., Wang, Z., Chen, Y., Guo, J., Chen, L., Zhao, X., Dong, Z., and Liu, Y. G. 2015. A Robust CRISPR/Cas9 System for Convenient, High-Efficiency Multiplex Genome Editing in Monocot and Dicot Plants. Mol. Plant. 8:1274–1284

Makandar, R., Nalam, V. J., Lee, H., Trick, H. N., Dong, Y., and Shah, J. 2012. Salicylic Acid Regulates Basal Resistance to Fusarium Head Blight in Wheat. Mol. Plant-Microbe Interact. 25:431–439

Malamy, J., Carr, J. P., Klessig, D. F., and Raskin, I. 1990. Salicylic Acid : A Likely Endogenous Signal in the Resistance Response of Tobacco to Viral Infection. Science. 250:1002–1004

Maldonado, A. M., Doerner, P., Dixon, R. A., Lamb, C. J., and Cameron, R. K. 2002. A putative lipid transfer protein involved in systemic resistance signalling in *Arabidopsis*. Nature. 419:399–403

Mao, Y., Zhang, H., Xu, N., Zhang, B., Gou, F., and Zhu, J. K. 2013. Application of the CRISPR-Cas system for efficient genome engineering in plants. Mol. Plant. 6:2008–2011

Mauch-Mani, B., Baccelli, I., Luna, E., and Flors, V. 2017. Defense priming: an adaptive part of induced resistance. Annu. Rev. Plant Biol. 68:435–455

Métraux, J. P., Signer, H., Ryals, J., Ward, E., Wyss-Benz, M., Gaudin, J., Raschdorf, K., Schmid, E., Blum, W., and Inverardi, B. 1990. Increase in salicylic acid at the onset of systemic acquired resistance in cucumber. Science. 250:1004–1006

Meuwly, P., Molders, W., Buchala, A., and Metraux, J.-P. 1995. Local and Systemic Biosynthesis of Salicylic Acid in Infected Cucumber Plants. Plant Phisiology. 109:1107–1114

Mishina, T. E., and Zeier, J. 2006. The *Arabidopsis* Flavin-Dependent Monooxygenase FMO1 Is an Essential Component of Biologically Induced Systemic Acquired Resistance. Plant Physiol. 141:1666–1675

Miura, K., and Tada, Y. 2014. Regulation of water, salinity, and cold stress responses by salicylic acid. Front. Plant Sci. 5:1–13

Molina, A., Segura, A., and García-Olmedo, F. 1993. Lipid transfer proteins (nsLTPs) from barley and maize leaves are potent inhibitors of bacterial and fungal plant pathogens. FEBS Lett. 316:119–122

Molitor, A., Zajic, D., Voll, L. M., Pons-Kühnemann, J., Samans, B., Kogel, K.-H., and Waller, F. 2011. Barley Leaf Transcriptome and Metabolite Analysis Reveals New Aspects of Compatibility and *Piriformospora indica* –Mediated Systemic Induced Resistance to Powdery Mildew. Mol. Plant-Microbe Interact. 24:1427–1439

Møller, B. L. 1974. Lysine Biosynthesis in Barley (*Hordeum vulgare* L.). Plant Physiol. 54:638–643

Morris, S. W., Vernooij, B., Titatarn, S., Starrett, M., Thomas, S., Wiltse, C. C., Frederiksen, R. A., Bhandhufalck, A., Hulbert, S., and Uknes, S. 1998. Induced Resistance Responses in Maize. Mol. Plant-Microbe Interact. 11:643–658

Mou, Z., Fan, W., and Dong, X. 2003. Inducers of plant systemic acquired resistance Regulate NPR1 function through redox changes. Cell. 113:935–944

Nair, K. R. S., and Ellingboe, A. H. 1962. A method of controlled inoculations with conidiospores of *Erysiphe graminis* var. *tritici*. Phytopathology. 52:714

Naito, Y., Hino, K., Bono, H., and Ui-Tei, K. 2015. CRISPRdirect: Software for designing CRISPR/Cas guide RNA with reduced off-target sites. Bioinformatics. 31:1120–1123

Návarová, H., Bernsdorff, F., Doring, A.-C., and Zeier, J. 2012. Pipecolic Acid, an Endogenous Mediator of Defense Amplification and Priming, Is a Critical Regulator of Inducible Plant Immunity. Plant Cell. 24:5123–5141

O'Malley, R. C., Barragan, C. C., and Ecker, J. R. 2015. A user's guide to the *Arabidopsis* T-DNA insertion mutant collections. Pages 323–342 in: Methods in Molecular Biology, Howard Hughes Medical Institute.

Ordon, J., Bressan, M., Kretschmer, C., Dall'Osto, L., Marillonnet, S., Bassi, R., and Stuttmann, J. 2018. Optimized Cas9 expression systems for highly efficient *Arabidopsis* genome editing facilitate isolation of complex alleles in a single generation. bioRxiv. :doi:10.1074/jbc.M109.058990

Ordon, J., Gantner, J., Kemna, J., Schwalgun, L., Reschke, M., Streubel, J., Boch, J., and Stuttmann, J. 2017. Generation of chromosomal deletions in dicotyledonous plants employing a user-friendly genome editing toolkit. Plant J. 89:155–168

Pajerowska-Mukhtar, K. M., Emerine, D. K., and Mukhtar, M. S. 2013. Tell me more: Roles of NPRs in plant immunity. Trends Plant Sci. 18:402–411

Pálfi, G., and Dézsi, L. 1968. Pipecolic acid as an indicator of abnormal protein metabolism in diseased plants. Plant Soil. 29:285–291

Panstruga, R., Parker, J. E., and Schulze-Lefert, P. 2009. SnapShot: Plant Immune Response Pathways. Cell. 136:978.e1-978.e3

Park, S. W., Kaimoyo, E., Kumar, D., Mosher, S., and Klessig, D. F. 2007. Methyl salicylate is a critical mobile signal for plant systemic acquired resistance. Science. 318:113–116

Penninckx, I. A., Eggermont, K., Terras, F. R., Thomma, B. P., De Samblanx, G. W., Buchala, A., Métraux, J. P., Manners, J. M., and Broekaert, W. F. 1996. Pathogen-induced systemic activation of a plant defensin gene in *Arabidopsis* follows a salicylic acid-independent pathway. Plant Cell. 8:2309–23

Petti, C., Khan, M., and Doohan, F. 2010. Lipid transfer proteins and protease inhibitors as key factors in the priming of barley responses to Fusarium head blight disease by a biocontrol strain of *Pseudomonas fluorescens*. Funct. Integr. Genomics. 10:619–627

Pieterse, C. M. J., Van der Does, D., Zamioudis, C., Leon-Reyes, A., and Van Wees, S. C. M. 2012. Hormonal Modulation of Plant Immunity. Annu. Rev. Cell Dev. Biol. 28:489–521

Pieterse, C. M. J., Zamioudis, C., Berendsen, R. L., Weller, D. M., Van Wees, S. C. M., and Bakker, P. A. H. M. 2014. Induced Systemic Resistance by Beneficial Microbes. Annu. Rev. Phytopathol. 52:347–375

Prats, E., Carver, T. L. W., and Mur, L. A. J. 2008. Pathogen-derived nitric oxide influences formation of the appressorium infection structure in the phytopathogenic fungus *Blumeria graminis*. Res. Microbiol. 159:476–480

Prats, E., Mur, L. A. J., Sanderson, R., and Carver, T. L. W. 2005. Nitric oxide contributes both to papilla-based resistance and the hypersensitive response in barley attacked by *Blumeria graminis* f. sp. *hordei*. Mol. Plant Pathol. 6:65–78

Ramakrishna, S., Cho, S. W., Kim, S., Song, M., Gopalappa, R., Kim, J. S., and Kim, H. 2014. Surrogate reporter-based enrichment of cells containing RNA-guided Cas9 nuclease-induced mutations. Nat. Commun. 5:3378

Riedlmeier, M., Ghirardo, A., Wenig, M., Knappe, C., Koch, K., Georgii, E., Dey, S., Parker, J. E., Schnitzler, J.-P., and Vlot, A. C. 2017. Monoterpenes Support Systemic Acquired Resistance within and between Plants. Plant Cell. 29:1440–1459

Robert-Seilaniantz, A., Grant, M., and Jones, J. D. G. 2011. Hormone Crosstalk in Plant Disease and Defense: More Than Just JASMONATE-SALICYLATE Antagonism. Annu. Rev. Phytopathol. 49:317–343

Schnell, J. R., Dyson, H. J., and Wright, P. E. 2004. Structure, Dynamics, and Catalytic Function of Dihydrofolate Reductase. Annu. Rev. Biophys. Biomol. Struct. 33:119–140

Seyfferth, C., and Tsuda, K. 2014. Salicylic acid signal transduction: the initiation of biosynthesis, perception and transcriptional reprogramming. Front. Plant Sci. 5:697

Shah, J., Chaturvedi, R., Chowdhury, Z., Venables, B., and Petros, R. A. 2014. Signaling by small metabolites in systemic acquired resistance. Plant J. 79:645–658

Shan, Q., Wang, Y., Li, J., Zhang, Y., Chen, K., Liang, Z., Zhang, K., Liu, J., Xi, J. J., Qiu, J. L., and Gao, C. 2013. Targeted genome modification of crop plants using a CRISPR-Cas system. Nat. Biotechnol. 31:686–688

Sharma, R., De Vleesschauwer, D., Sharma, M. K., and Ronald, P. C. 2013. Recent advances in dissecting stress-regulatory crosstalk in rice. Mol. Plant. 6:250–260

Shigenaga, A. M., and Argueso, C. T. 2016. No hormone to rule them all: Interactions of plant hormones during the responses of plants to pathogens. Semin. Cell Dev. Biol. 56:174–189

Song, G. C., Choi, H. K., and Ryu, C. M. 2013. The folate precursor para-aminobenzoic acid elicits induced resistance against Cucumber mosaic virus and *Xanthomonas axonopodis*. Ann. Bot. 111:925–934

Song, J. T., Lu, H., McDowell, J. M., and Greenberg, J. T. 2004. A key role for *ALD1* in activation of local and systemic defenses in *Arabidopsis*. Plant J. 40:200–212

Spitz, F., and Furlong, E. E. M. 2012. Transcription factors: From enhancer binding to developmental control. Nat. Rev. Genet. 13:613–626

Spoel, S. H., and Dong, X. 2012. How do plants achieve immunity? Defence without specialized immune cells. Nat. Rev. Immunol. 12:89–100

Spoel, S. H., Johnson, J. S., and Dong, X. 2007. Regulation of tradeoffs between plant defenses against pathogens with different lifestyles. Proc. Natl. Acad. Sci. 104:18842–18847

Spoel, S. H., Koornneef, A., Claessens, S., Korzelius, J., Van Pelt, J., Mueller, M., Buchala, A., Métraux, J., Brown, R., Kazan, K., Van Loon, L., Dong, X., and Pieterse, C. 2003. NPR1 Modulates Cross-Talk between Salicylate- and Jasmonate-Dependent Defense Pathways through a Novel Function in the Cytosol. Plant Cell. 15:760–770

Tada, Y., Spoel, S. H., Pajerowska-Mukhtar, K., Mou, Z., Song, J., Wang, C., Zuo, J., and Dong, X. 2008. Plant immunity requires conformational charges of NPR1 via S-nitrosylation and thioredoxins. Science. 321:952–956

Thordal-Christensen, H., Gregersen, P. L., and Collinge, D. B. 2000. The Barley/Blumeria (Syn. Erysiphe) Graminis Interaction. Pages 77–100 in: Mechanisms of Resistance to Plant Diseases, Springer Netherlands, Dordrecht.

Thyme, S. B., Akhmetova, L., Montague, T. G., Valen, E., and Schier, A. F. 2016. Internal guide RNA interactions interfere with Cas9-mediated cleavage. Nat. Commun. 7:11750

Torres, D. P., Proels, R. K., Schempp, H., and Hückelhoven, R. 2017. Silencing of *RBOHF2* Causes Leaf Age–Dependent Accelerated Senescence, Salicylic Acid Accumulation, and Powdery Mildew Resistance in Barley. Mol. Plant-Microbe Interact. 30:906–918

Vallelian-Bindschedler, L., Mösinger, E., Métraux, J. P., and Schweizer, P. 1998. Structure, expression and localization of a germin-like protein in barley (*Hordeum vulgare* L.) that is insolubilized in stressed leaves. Plant Mol. Biol. 37:297–308

Verhagen, B. W. M., Glazebrook, J., Zhu, T., Chang, H.-S., van Loon, L. C., and Pieterse, C. M. J. 2004. The Transcriptome of Rhizobacteria-Induced Systemic Resistance in *Arabidopsis*. Mol. Plant-Microbe Interact. 17:895–908

Vernooij, B., Friedrichya, L., Reist, R., Kolditzjawhar, R., Ward, E., Uknes, S., Kessmann, H., and Ryals, J. 1994. Salicylic Acid Is Not the Translocated Signal Responsible for Inducing Systemic Acquired Resistance but Is Required in Signal Transduction. Plant Cell. 6:959–965

Vlot, A. C., Dempsey, D. A., and Klessig, D. F. 2009. Salicylic Acid, a Multifaceted Hormone to Combat Disease. Annu. Rev. Phytopathol. 47:177–206

Vlot, A. C., Pabst, E., and Riedlmeier, M. 2017. Systemic Signalling in Plant Defence. eLS. John Wiley Sons, Ltd Chichester. :DOI: 10.1002/9780470015902.a0001322.pub3

Waller, F., Achatz, B., Baltruschat, H., Fodor, J., Becker, K., Fischer, M., Heier, T., Hückelhoven, R., Neumann, C., von Wettstein, D., Franken, P., and Kogel, K.-H. 2005. The endophytic fungus *Piriformospora indica* reprograms barley to salt-stress tolerance, disease resistance, and higher yield. Proc. Natl. Acad. Sci. 102:13386–13391

Waller, F., Mukherjee, K., Deshmukh, S. D., Achatz, B., Sharma, M., Schäfer, P., and Kogel, K. H. 2008. Systemic and local modulation of plant responses by *Piriformospora indica* and related *Sebacinales* species. J. Plant Physiol. 165:60–70

Wang, C., El-Shetehy, M., Shine, M. B., Yu, K., Navarre, D., Wendehenne, D., Kachroo, A., and Kachroo, P. 2014. Free Radicals Mediate Systemic Acquired Resistance. Cell Rep. 7:348–355

Wang, C., Liu, R., Lim, G.-H., Lorenzo, L. De, Yu, K., Zhang, K., Hunt, A. G., Kachroo, A., and Kachroo, P. 2018. Pipecolic acid confers systemic immunity by regulating free radicals. Sci. Adv. 4:eaar4509

Wang, X., Wang, Y., Liu, P., Ding, Y., Mu, X., Liu, X., Wang, X., Zhao, M., Huai, B., Huang, L., and Kang, Z. 2017. TaRar1 Is Involved in Wheat Defense against Stripe Rust Pathogen Mediated by YrSu. Front. Plant Sci. 8:156

Wehner, N., Hartmann, L., Ehlert, A., Böttner, S., Oñate-Sánchez, L., and Dröge-Laser, W. 2011. High-throughput protoplast transactivation (PTA) system for the analysis of *Arabidopsis* transcription factor function. Plant J. 68:560–569

Wendehenne, D., Gao, Q., Kachroo, A., and Kachroo, P. 2014. Free radical-mediated systemic immunity in plants. Curr. Opin. Plant Biol. 20:127–134

Wittek, F., Hoffmann, T., Kanawati, B., Bichlmeier, M., Knappe, C., Wenig, M., Schmitt-Kopplin, P., Parker, J. E., Schwab, W., and Vlot, A. C. 2014. *Arabidopsis* ENHANCED DISEASE SUSCEPTIBILITY1 promotes systemic acquired resistance via azelaic acid and its precursor 9-oxo nonanoic acid. J. Exp. Bot. 65:5919–5931

Wittek, F., Kanawati, B., Wenig, M., Hoffmann, T., Franz-Oberdorf, K., Schwab, W., Schmitt-Kopplin, P., and Vlot, A. C. 2015. Folic acid induces salicylic acid-dependent immunity in *Arabidopsis* and enhances susceptibility to *Alternaria brassicicola*. Mol. Plant Pathol. 16:616–622

Wu, Y., Yi, G., Peng, X., Huang, B., Liu, E., and Zhang, J. 2013. Systemic acquired resistance in Cavendish banana induced by infection with an incompatible strain of *Fusarium oxysporum* f. sp. *cubense*. J. Plant Physiol. 170:1039–1046

Wu, Y., Zhang, D., Chu, J. Y., Boyle, P., Wang, Y., Brindle, I. D., De Luca, V., and Després, C. 2012. The *Arabidopsis* NPR1 Protein Is a Receptor for the Plant Defense Hormone Salicylic Acid. Cell Rep. 1:639–647

Xu, H., Xiao, T., Chen, C. H., Li, W., Meyer, C. A., Wu, Q., Wu, D., Cong, L., Zhang, F., Liu, J. S., Brown, M., and Liu, X. S. 2015. Sequence determinants of improved CRISPR sgRNA design. Genome Res. 25:1147–1157

Xu, J., Lian, W., Jia, Y., Li, L., and Huang, Z. 2017. Optimized guide RNA structure for genome editing via Cas9. Oncotarget. 8:94166–94171

Yang, Y., Zhao, J., Liu, P., Xing, H., Li, C., Wei, G., and Kang, Z. 2013. Glycerol-3-phosphate metabolism in wheat contributes to systemic acquired resistance against *Puccinia striiformis* f. sp. *tritici*. PLoS One. 8:e81756

Yasuda, M., Ishikawa, A., Jikumaru, Y., Seki, M., Umezawa, T., Asami, T., Maruyama-Nakashita, A., Kudo, T., Shinozaki, K., Yoshida, S., and Nakashita, H. 2008. Antagonistic Interaction between Systemic Acquired Resistance and the Abscisic Acid-Mediated Abiotic Stress Response in *Arabidopsis*. Plant Cell. 20:1678–1692

Ye, J., Coulouris, G., Zaretskaya, I., Cutcutache, I., Rozen, S., and Madden, T. L. 2012. Primer-BLAST: a tool to design target-specific primers for polymerase chain reaction. BMC Bioinformatics. 13:134

Yu, K., Soares, J., Mandal, M. K., Wang, C., Chanda, B., Gifford, A. N., Fowler, J. S., Navarre, D., Kachroo, A., and Kachroo, P. 2013. A feed-back regulatory loop between glycerol-3-phosphate and lipid transfer proteins DIR1 and AZI1 mediates azelaic acid-induced systemic immunity. Cell Rep. 3:1266–1278

Zacharius, R. M., Thompson, J. F., and Steward, F. C. 1954. The Detection, Isolation and Identification of L(-)Pipecolic Acid in the Non-protein Fraction of Beans (*Phaseolus vulgaris*). J. Am. Chem. Soc. 76:2908–2912

Zaidi, S. S. e. A., Mahfouz, M. M., and Mansoor, S. 2017. CRISPR-Cpf1: A New Tool for Plant Genome Editing. Trends Plant Sci. 22:550–553

Zeier, J. 2013. New insights into the regulation of plant immunity by amino acid metabolic pathways. Plant, Cell Environ. 36:2085–2103

Zhang, Y., Su, J., Duan, S., Ao, Y., Dai, J., Liu, J., Wang, P., Li, Y., Liu, B., Feng, D., Wang, J., and Wang, H. 2011. A highly efficient rice green tissue protoplast system for transient gene expression and studying light/chloroplast-related processes. Plant Methods. 7:30

Zhu, Z., An, F., Feng, Y., Li, P., Xue, L., A, M., Jiang, Z., Kim, J.-M., To, T. K., Li, W., Zhang, X., Yu, Q., Dong, Z., Chen, W.-Q., Seki, M., Zhou, J.-M., and Guo, H. 2011. Derepression of ethylene-stabilized transcription factors (EIN3/EIL1) mediates jasmonate and ethylene signaling synergy in *Arabidopsis*. Proc. Natl. Acad. Sci. 108:12539–12544

Zipfel, C., and Felix, G. 2005. Plants and animals: A different taste for microbes? Curr. Opin. Plant Biol. 8:353–360

Zoeller, M., Stingl, N., Krischke, M., Fekete, A., Waller, F., Berger, S., and Mueller, M. J. 2012. Lipid Profiling of the *Arabidopsis* Hypersensitive Response Reveals Specific Lipid Peroxidation and Fragmentation Processes: Biogenesis of Pimelic and Azelaic Acid. Plant Physiol. 160:365–378

Zuker, M. 2003. Mfold web server for nucleic acid folding and hybridization prediction. Nucleic Acids Res. 31:3406–15

8 Supplement

Supplemental Figures

Supplemental Tables

8.1 Supplemental figures

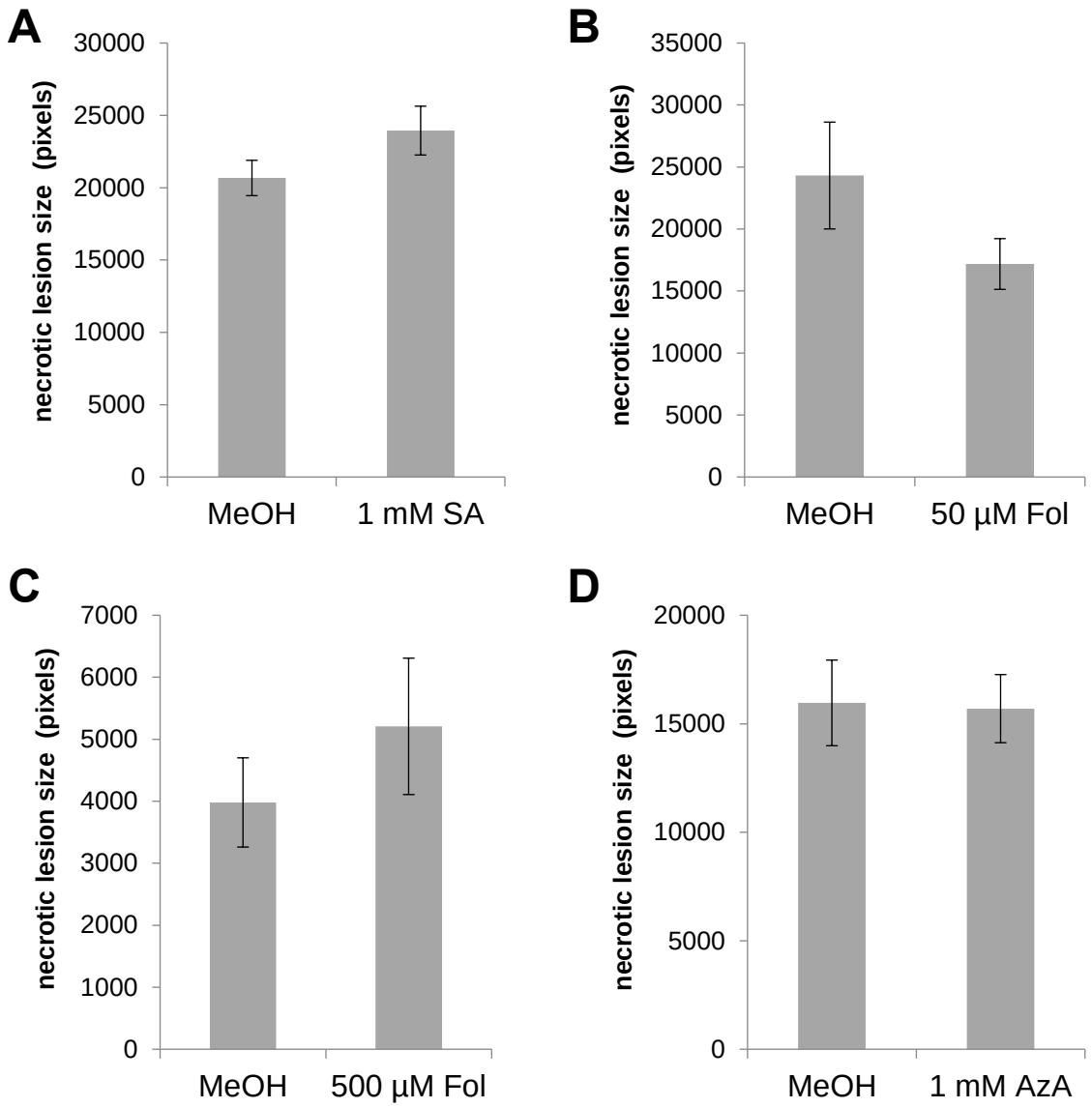

Supplemental Figure 1. Size of *P. teres* lesions on the systemic leaves of barley after local application of SA (A), 50 µM Fol (B), 500 µM Fol (C), or AzA (D). Barley cultivar GP plants were infiltrated in the first true leaf with 0.025% MeOH as control, 1 mM SA **(A)**, 50 µM Fol **(B)**, 500 µM Fol **(C)**, or 1 mM Aza **(D)** in 10 mM MgCl2 as indicated below the panels. Five days later, the second true leaves of the plants were inoculated with P. teres by pipetting droplets of a solution containing P. teres spores onto the leaf surface. The resulting necrotic lesions on leaf 2 were photographed at 4 dpi and measured using ImageJ. Bars represent the average of 10-51 replicates from 8 **(A)**, 9 **(B)**, 2 **(C**), and 8 **(D)** biologically independent experiments +/- standard error. Replicates were as follows: **(A)** MeOH and SA: 48 (8x6 replicates); **(B)** MeOH: 50 replicates (4x5 and 5x6 replicates), Fol: 51 (3x5 and 6x6 replicates); **(C)** MeOH: 10 (5+5 replicates), Fol: 10 (4+6 replicates); **(D)** MeOH and AzA: 45 (3x5 and 5x6 replicates).

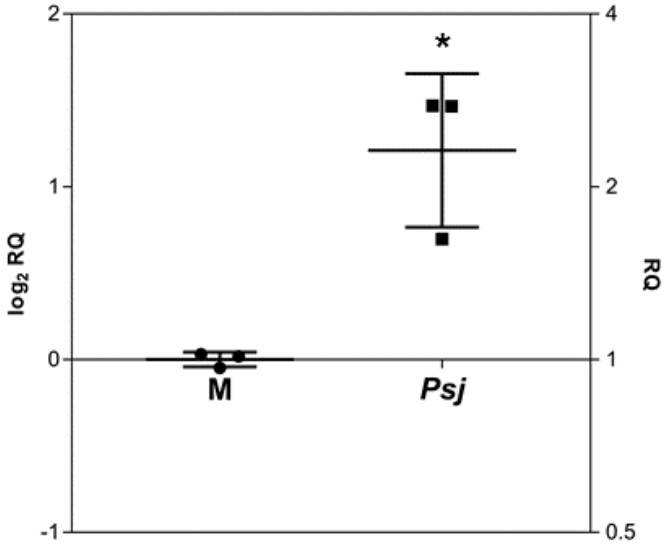

Supplemental Figure 2. PR1 expression in *Arabidopsis* leaves infiltrated with PEX from barley plants (Barke). Barley was syringe-infiltrated with *Psj* or 10 mM $MgCl_2$ (M, mock) as a control and after 2 days, PEX were collected from infected leaves. PEX of mock- and *Psj*-treated plants were infiltrated into leaves of *Arabidopsis* Col-0 and gene expression in these leaves was quantified after 1 day. Gene expression is depicted as log2 of the transcript relative quantity (RQ). Dots represent results from single experiments (3 in total); the middle line represents the average of 3 experiments, plus/minus standard deviation. Asterisk above bar indicates statistically significant difference from the control treatment (t-test with Welch's correction, * P<0.05). The experiment was performed by Claudia Knappe.

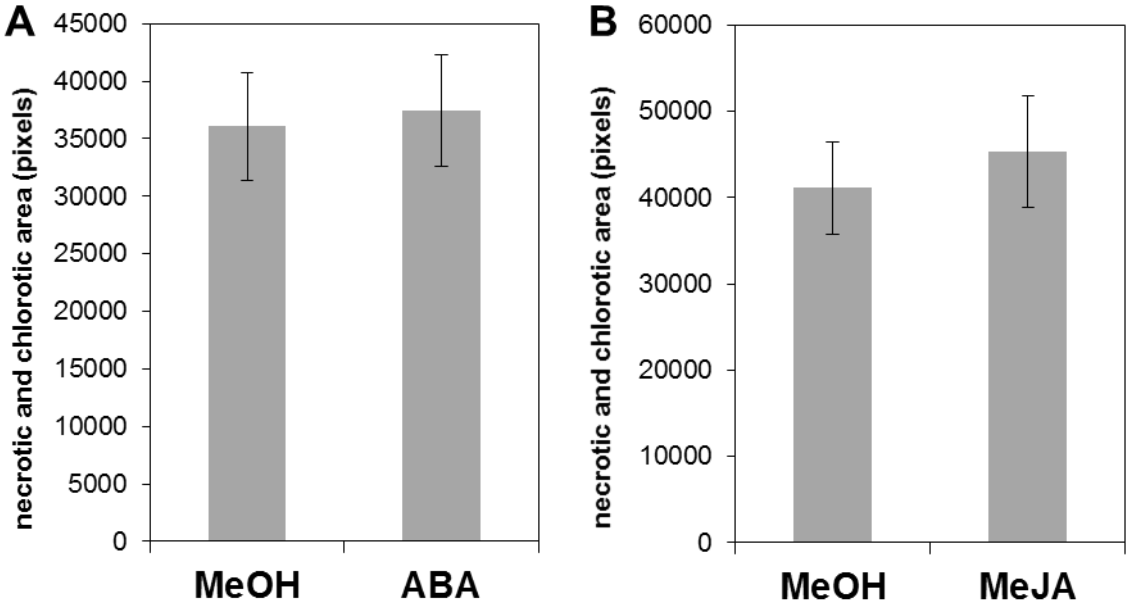

Supplemental Figure 3. Size of necrotic and chlorotic area caused by *P. teres* on the leaves of barley (GP) treated with ABA or MeJA. Barley was syringe-infiltrated in the first true leaf with 0.025% MeOH as control or 100 µM ABA **(A)** or MeJA **(B)** in 10 mM $MgCl_2$ as indicated below the bars. Five days later, plants were infected in the second true leaves by applying droplets of a solution containing *P. teres* spores to the leaf surface. Necrotic lesions were photographed at 4 days after infection and measured using the ImageJ macro PIDIQ. Bars show 5 **(A)** or 4 **(B)** merged experiments plus/minus standard error.

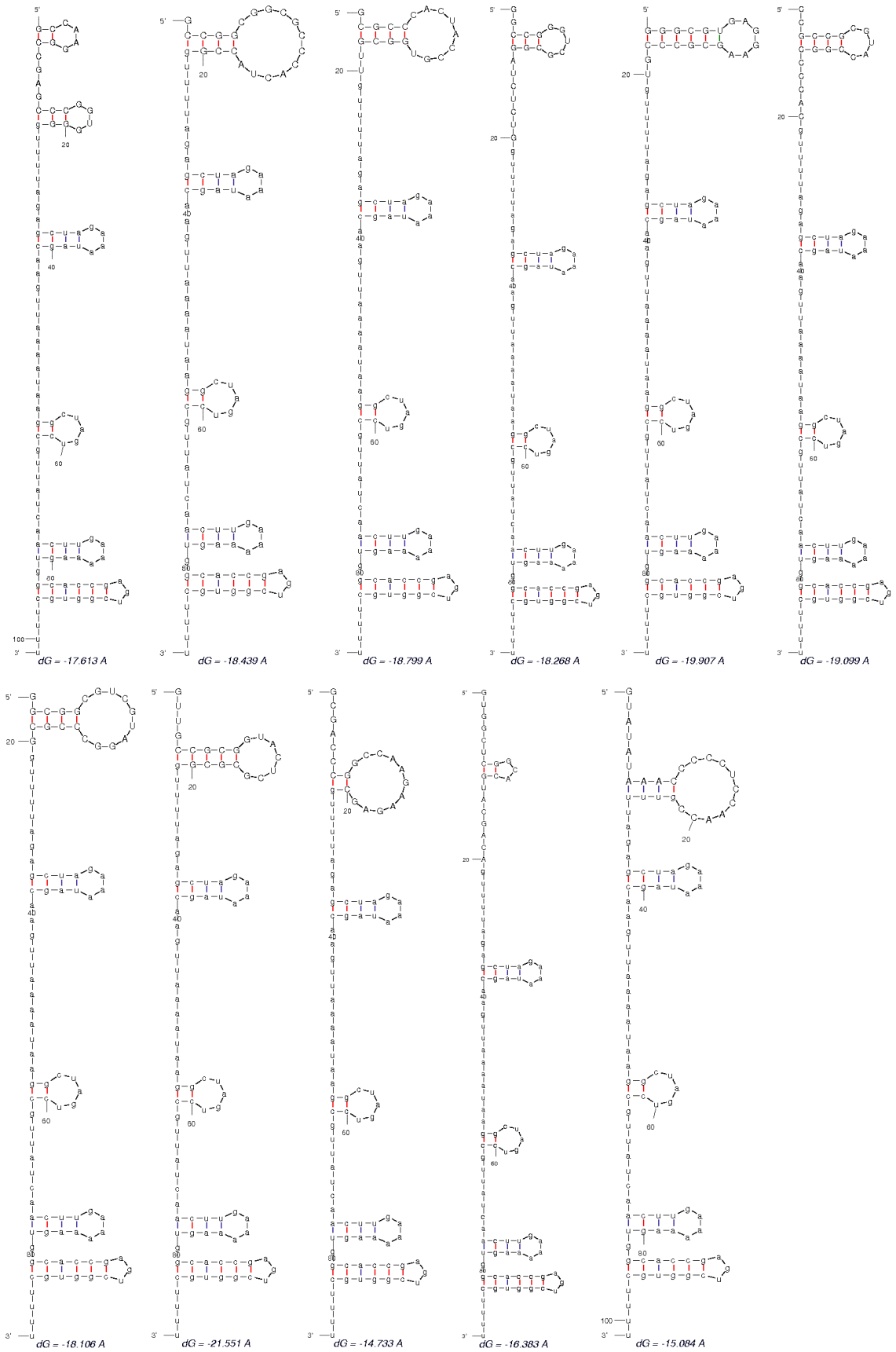

Supplemental Figure 4. gRNA structures with minimum free energy as computed by the mfold webserver (Zuker 2003)**.** Upper panels show gRNA1-gRNA6, lower panels show gRNA7-gRNA10 and control gRNA, from left to right, respectively.

8.2 Supplemental tables

Supplemental Table 1. Number of base pairs in the guide region of gRNAs.

gRNA	base pairs in the guide region
gRNA1	2+3
gRNA2	4
gRNA3	4
gRNA4	3
gRNA5	6
gRNA6	4
gRNA7	4
gRNA8	5
gRNA9	2
gRNA10	2
control	4

Supplemental Table 2. Oligonucleotides used for cloning of genes for sequencing.

name	sequence 5' → 3'	description	T_m (°C)
ML 5	CACCGACTGCGCCGAGTTTTATTC	forward primer for gateway cloning of HvERF4 (MLOC 73358)	63
ML 6	CAACTACTCTCCGGCGAAAA	reverse primer for gateway cloning of *HvERF4*	63
ML 7	CACCAGTCAAACCGCATGCTGAC	forward primer for gateway cloning of *HvERF-like* (MLOC 24530)	62
ML 8	TTTACAGGGCTCCTCGGTCT	reverse primer for gateway cloning of *HvERF-like*	62
ML 13	CACCAGTCAAACCGCTCCCGACTG	forward primer for gateway cloning of *HvERF4*	63
ML 14	ACCCACCCAAACGCACTTAC	reverse primer for gateway cloning of *HvERF4*	63
ML 15	CACCGCGAAGAAGACACATCCCATAATTC	forward primer for gateway cloning of *HvERF4*	63
ML 16	ACATCCATCTCTCTGGCTCTCT	reverse primer for gateway cloning of *HvERF4*	63
ML 33	CACCCGAACACTCGGCGCCAC	forward primer for gateway cloning of *ERF44411* (MLOC 44411)	66
ML 26	CTTGCTTTACTTCCGAGCCG	reverse primer for gateway cloning of *ERF44411*	66

name	sequence 5' → 3'	description	T_m (°C)
ML 27	CACCGCCTCGAACCGGAAGGAAG	forward primer for gateway cloning of *HvWRKY38/1*	68
ML 28	CGGAGTAATCGACACCGCAA	reverse primer for gateway cloning of *HvWRKY38/1*	68
ML 29	CACCTCGCTTCACTCACCATCTCAC	forward primer for gateway cloning of *HvWRKY22* (MLOC_45055)	66
ML 30	ACACATGCACTGACCCAAGA	reverse primer for gateway cloning of *HvWRKY22*	66

Supplemental Table 3. Oligonucleotides used to introduce gRNA sequences into shuttle vectors.

name	sequence 5' → 3'	description
gRNA1	gttgCCAAGGCCGAGCCCGGTGGG	HvERF-like gRNA1f
gRNA2	aaacCCCACCGGGCTCGGCCTTGG	HvERF-like gRNA1r
gRNA3	gttGCCGGCGGCGCCCACTACCG	HvERF-like gRNA2f
gRNA4	aaacCGGTAGTGGGCGCCGCCGG	HvERF-like gRNA2r
gRNA5	gttGCGCCCACTACCGTGGCGTT	HvERF-like gRNA3f
gRNA6	aaacAACGCCACGGTAGTGGGCG	HvERF-like gRNA3r
gRNA7	gttGGCCGGGTCGCGGATCTCTG	HvERF-like gRNA4f
gRNA8	aaacCAGAGATCCGCGACCCGGC	HvERF-like gRNA4r
gRNA9	gttGGGCGTGAGGAAGCGCCCGT	HvERF4 gRNA5f
gRNA10	aaacACGGGCGCTTCCTCACGCC	HvERF4 gRNA5r
gRNA11	gttgCCGCCGCGTACCGGCCCCAC	HvERF4 gRNA6f
gRNA12	aaacGTGGGGCCGGTACGCGGCGG	HvERF4 gRNA6r
gRNA13	gttGGCGGCGTCGTAGGCCCGCG	HvERF4 gRNA7f
gRNA14	aaacCGCGGGCCTACGACGCCGC	HvERF4 gRNA7r
gRNA15	gttGTTGCCGCGGTACTCGCGCG	HvERF4 gRNA8f
gRNA16	aaacCGCGCGAGTACCGCGGCAA	HvERF4 gRNA8r
gRNA17	gttGCGACCCGGCCAAGAAGAGC	MLOC_24530 & 73358 gRNA9f
gRNA18	aaacGCTCTTCTTGGCCGGGTCG	MLOC_24530 & 73358 gRNA9r
gRNA19	gttGTGGCTCGGCACGTACGACA	MLOC_24530 & 73358 gRNA10f
gRNA20	aaacTGTCGTACGTGCCGAGCCA	MLOC_24530 & 73358 gRNA10r

name	sequence 5’ → 3’	description
gRNA25f	gttggcgacgggggccgcgttct	MLOC_44411 gRNA25f
gRNA25r	aaacAGAACGCGGCCCCCGTCGC	MLOC_44411 gRNA25r
gRNA26f	gttggcatggagcccaggttccg	MLOC_44411 gRNA26f
gRNA26r	aaacCGGAACCTGGGCTCCATGC	MLOC_44411 gRNA26r
gRNA27f	gttgccgtggggcaggtacgcgg	MLOC_44411 gRNA27f
gRNA27r	aaacCCGCGTACCTGCCCCACGG	MLOC_44411 gRNA27r
gRNA28f	gttgaggaaggcgcgcgtctggct	MLOC_44411 gRNA28f
gRNA28r	aaacAGCCAGACGCGCGCCTTCCT	MLOC_44411 gRNA28r
gRNA29f	gttGGGATTTGCGGTGCGTGCAA	MLOC_45055 gRNA29f
gRNA29r	aaacTTGCACGCACCGCAAATCC	MLOC_45055 gRNA29r
gRNA30f	gttgAGATCACGTCGAAGAGCGTC	MLOC_45055 gRNA30f
gRNA30r	aaacGACGCTCTTCGACGTGATCT	MLOC_45055 gRNA30r
gRNA31f	gttGCACACGTGCGTTCATAAGA	MLOC_45055 gRNA31f
gRNA31r	aaacTCTTATGAACGCACGTGTG	MLOC_45055 gRNA31r
gRNA32f	gttGCAGGAGCCTACTCGCGCCC	MLOC_45055 gRNA32f
gRNA32r	aaacGGGCGCGAGTAGGCTCCTG	MLOC_45055 gRNA32r
gRNA33f	gttgCTGAGCCTCGACCTGCACGT	MLOC_60890 gRNA33f
gRNA33r	aaacACGTGCAGGTCGAGGCTCAG	MLOC_60890 gRNA33r
gRNA34f	gttgTGGTGGTGCGGGTGCCCCAT	MLOC_60890 gRNA34f
gRNA34r	aaacATGGGGCACCCGCACCACCA	MLOC_60890 gRNA34r
gRNA35f	gttgTCATCGGCGGCGCCTGGTAT	MLOC_60890 gRNA35f
gRNA35r	aaacATACCAGGCGCCGCCGATGA	MLOC_60890 gRNA35r
gRNA36f	gttGTTCTCCTCCACGAGGATCT	MLOC_60890 gRNA36f
gRNA36r	aaacAGATCCTCGTGGAGGAGAA	MLOC_60890 gRNA36r

Supplemental Table 4. Oligonucleotides used to introduce gRNA target sequences into reporter vectors.

name	sequence 5’ → 3’	description
target gRNA1	attgCCAAGGCCGAGCCCGGTGGG	target for gRNA1
target gRNA2	ccctCCCACCGGGCTCGGCCTTGG	
target gRNA3	attGGCCGGCGGCGCCCACTACCG	target for gRNA2
target gRNA4	ccctCGGTAGTGGGCGCCGCCGGC	
target gRNA5	attgGCGCCCACTACCGTGGCGTT	target for gRNA3
target gRNA6	ccctAACGCCACGGTAGTGGGCGC	

name	sequence 5’ → 3’	description
target gRNA7	gttGGGCCGGGTCGCGGATCTCTG	target for gRNA4
target gRNA8	ccctCAGAGATCCGCGACCCGGCC	
target gRNA9	attgGGGCGTGAGGAAGCGCCCGT	target for gRNA5
target gRNA10	ccctACGGGCGCTTCCTCACGCCC	
target gRNA11	attgCCGCCGCGTACCGGCCCCAC	target for gRNA6
target gRNA12	ccctGTGGGGCCGGTACGCGGCGG	
target gRNA13	attgGGCGGCGTCGTAGGCCCGCG	target for gRNA7
target gRNA14	ccctCGCGGGCCTACGACGCCGCC	
target gRNA15	attgGTTGCCGCGGTACTCGCGCG	target for gRNA8
target gRNA16	ccctCGCGCGAGTACCGCGGCAAC	
target gRNA17	attgGCGACCCGGCCAAGAAGAGC	target for gRNA9
target gRNA18	ccctGCTCTTCTTGGCCGGGTCGC	
target gRNA19	attgGTGGCTCGGCACGTACGACA	target for gRNA10
target gRNA20	ccctTGTCGTACGTGCCGAGCCAC	
gRNA527.1f	attgTATATAAACCCCCTCCAACC	target for control gRNA
gRNA527.1r	ccctGGTTGGAGGGGGTTTATATA	

8.3 Sequences

Protospacer/target sequences are identical to guide sequences of gRNA (except for T, which becomes U) and are underlined with solid lines. PAMs on the sense or antisense strand are displayed on a grey background. The localisation of mutations generated in this work is indicated by white letters on black background, with the inserted nucleotide being localised between the two marked letters, but not written down.

***ERF-like* (MLOC_24530, now HORVU3Hr1G078150)**

ATGGCGCCTAGAGCGGCGGAGAAGGCGCCTGTCTCCCCGCCCACCGGGCTCGGCCTTGGCGT
TGGCGGCGGCGTCGGGGTCGTAGCCGGCGGCGCCCACTACCGTGGCGTTCGGAAGCGCCCCT
GGGGACGTTTCGCCGCAGAGATCCGCGACCCGGCCAAGAAGAGCAGGGTGTGGCTCGGCACG
TACGACACGGCGGAGGAGGCCGCGCGCGCCTACGACACCGCCGCGCGCGAGTTCCGCGGCGC
CAAGGCCAAAACGAACTTCCCGTTCCCTTCGTCGTCGTCGCCGTCTCCTCTCGCCGCCGGCG
GCGGCAGCCCGAGCAGCAACAGCACCTTGGACTCGAGCGGTGGTGGGAGCGGCGGCTGCGCC
CAGGCGCCTATGCAGGCCATCCCGCTGCCGCCCGCCCTCGACCTGGACCTCTTCCACCGCGC
GGCGGCCGTGACCGCCGGCGGCATGCGCTTTCCATTCAACGGTTACCCGGTGGCGCCGCGCC
AGCCCCTGCACCCGTACTTCTTCTACGAACAGGCCGCGGCCGCCGCGGCGGCTTCGTCAGGT
TACCGCACGCTGAAGATGGCGCAGCCGGTCACCGTGGCGGCCGTTGCCCAGAGCGACTCCGA
CTCCTCGTCGGTCGTTGATCTGTCCCCGTCGCCCCCAGCGGTGACAGCGCATAAGGCGGTCG
CGTTTGATCTGGATCTGAACCGGCCGCCGCCTTCGGAGGACTAG

***ERF4* (MLOC_73358, now HORVU1Hr1G067110)**

ATGGCGCCCAGGACGTCCGACAAGACGGCGACGCCGCCCGCTGCCGCGGTCGCCGCGACCGG
CCTGGCGCTCGGCGTCGGCGGCGGCGCCAACGGTGGAGGCGTCGGCCCGCACTACAGGGGCG
TGAGGAAGCGCCCGTGGGGCCGGTACGCGGCGGAGATCCGCGACCCGGCCAAGAAGAGCCGG
GTGTGGCTCGGCACGTACGACACGGCCGAGGAGGCCGCGCGGGCCTACGACGCCGCCGCGCG
CGAGTACCGCGGCAACAAGGCCAAGACCAACTTCCCCTTCGCCTCCGCGCCGCCCGCCGCAG
CCCTCACCGGCGACGGCAGCCGGAGCAGCAACAGCAGCACCGTGGACTCCTTCGGCGGCGAC
GTGCAGGCACCCATGCAGGCCATGCCGCTCCCTCCCTCCGTCGAGCTCGACCTGTTCCACCG
CGCGGCCAGCACCGCCGGGGCCGGCATGCGGTTCCCTTTCAGCGGCTACCCCGTTTCGCACC
CGTACTACTTCTTCGGACAGGCCGCGGCGGCCGCCGCCGCCGGCTGCCACATGTACAACCTG
GCCCCGAAGGTCACCGTGGCGTCCGTGTCCCCGAGCGACTCCGACTCCTCGTCGATCGTGGA

TCTGGCGCCGTCGCCGCCCGCAAGGAAGCCCGTCCCTTTTGATCTTGACCTGAACTGCCCGC
CGCCGGCCGAGCACTGA

ERF44411 **(MLOC_44411, now probably HORVU2Hr1G099890)**

ATGGCTCCCAAGAACGCGGCCCCCGTCGCCGTCGCAGCCGCAGCCGCAGCGGGCGGCGGCAT
GGAGCCCAGGTTCCGCGGCGTGCGGAAGCGGCCGTGGGGCAGGTACGCGGCGGAGATCCGCG
ACCCGGCCAGGAAGGCGCGCGTCTGGCTCGGCACCTTCGACACCGCCGAGGCCGCCGCGCGC
GCCTACGACGCCGCCGCGCTCCACTACCGCGGGCCCAAGGCCAAGACCAACTTCCCCGTCGG
CACCGTCGCCGCCTACGCGCACGTCCCGCTCCCGCTCCCGCTCCCGCCGCCCAAGAAGCTGG
CCGTCAGCCCCAGCAGCAGCACCGTCGAATCCTCGTCCCGGGACACTCCGGCTGCTTCCCCC
GCGGCCCCGCCGGCGCTCGACCTGAGCCTGGCGATGCCGGCCATGGTGGCGGCGCAGCCGTT
CCTGTTCCTGGACCCCAGGGTCGCGGTGACCGTGGCCGTCGCGGCGCCGGCGCCGGCGCCCT
GCCGATCAGCGGCGATCAGCGGCATGAAGAACAAGGTGGCGTCCCGCGAGGAAGAGCAGAGC
GACACCGGGTCGTCGTCATCCGTGGTGGACGCCTCGCCGGCCGTGGGCGTGGGGTTCGACCT
GAACCTGCCGCCGCCGGTGGAGATGGCATAG

WRKY22 **(MLOC_45055, now HORVU5Hr1G034830)**

GTGCAACATTGCAGGGGGTACTACCGTTGCACGCACCGCAAATCCCAGGGATGCGCGGCGAC
GAAGCAGGTGCAGCGCGCCGACGAGGACCCGACGCTCTTCGACGTGATCTACCACGGCGAGC
ACACGTGCGTTCATAAGACGGTGGCGGCGTTAGCGGCGGGACACGCGGAGGAGAACCCGGGC
GCGAGTAGGCTCCTGCAGAACCTGAGCACGAGCCTGACGGTGAACACCGAGGGGCTTACGGC
GACGGCGGGTCACCAGGGCTGCAGCACCACCACGTCCTTCTGCTTCTCCTCGCAGGCGGCGC
GCGTGCTGGCGCCGCAAGAGCACTACCCGTTCTCCATGCCGTCAACGCCGGAGAACTGCTTT
GGGCAAGGCGCGTCGCTGTCAACGTCCCTCGAACCCTCGCCGGTGACCTCGGACTCGAACCG
CTTCTCCATGACCCCGTTCCAGGCGGAGTGGAGGGCGCGGTCTGAGTTGGACGAGGTGGTGT
CCGCGCTCGTGGCCGCGGGGGCGCCCGCCATGGAGGAGACCCCCTTCTCGCTGGACGGGTTT
GAGTTTGACGTTTCTGGCTTCTTTGCATGA

WRKY38/1 **(MLOC_60890, now HORVU6Hr1G028790)**

ATGGATCCATGGATGGGCAGCCAGCCATCCCTGAGCCTCGACCTGCACGTCGGCCTACCGCC
GATGGGGCACCCGCACCACCACCAGAGCCAATACCAGGCGCCGCCGATGATCGCGCTGGCCA
AGCCCAAGATCCTCGTGGAGGAGAACTTCATGCCACTCAAGAAGGACCCTGAG..Intron.

GTTGCGGTTCTTGAGTCGGAGCTACAGCGGGTGAGCGAGGAGAACCGGCGGCTGGGCGAGAT
GCTCAGGGAGGTGGCCTCCAAGTACGAGGCCCTGCAGGGCCAGTTCACCGACATGGTCACGG
CCGGCGGCAACAACAACCACTACCACAACCAGCCGTCCTCCGCGTCGGAGGGCGGGTCGGTG

TCGCCGTCGAGGAAGCGCAAGAGCGAGGAGAGCCTCGGCACGCCGCCACCGTCGCATACTCA
GCAGCAGCACTATGCCGCCGGCCTCGCGTACGCGGTGGCGCCGGACCAGGCGGAGTGCACGT
CCGGCGAGCCGTGCAAGCGCATCCGGGAGGAGTGCAAGCCCGTCATCTCCAAGCGCTACGTC
CACGCCGACCCCTCCGACCTCAGCCTGGTGGTGAAGGACGGGTACCAATGGCGCAAGTACGG
GCAGAAGGTGACCAAGGACAACCCATGCCCCAGAGCCTACTTCCGGTGCTCCTTCGCCCCCG
GCTGCCCCGTCAAGAAGAAGGTGCAGAGGAGCGCCGAGGACAAGACCATACTCGTGGCGACG
TACGAGGGCGAGCACAACCACACCCAGCCCCCGCCGTCGCAGCCGCAGCAGCAGAACGACGG
CTCCGGCGCCGGCAAGAACGCCGGGAACGGGAAGCCGCCCCAGGCGCCGGCCACGCCTCACC
ACCCGCAGCAGCAGCACAAGCAGGAAGCGGCAGCGGTCGTCGTCAGCGGCGAATCGGCCGCG
GCGGCGTCCGAGCTGATCCGGCGCAACCTGGCGGAGCAGATGGCCATGACGCTGACGAGGGA
CCCCAGCTTCAAGGCGGCGCTGGTCACCGCGCTCTCCGGCCGGATCCTCGAGCTCTCGCCGA
CCAGGGACATCAATTAA

9 Acknowledgements

I would like to thank the many people who made this PhD thesis possible.

First and foremost, I want to express my deepest gratitude to Prof. Dr. Jörg Durner for giving me the opportunity of working in his institute. His immense knowledge and his interest in my work were of enormous help for the progress of this project.

I am also very grateful to Prof. Dr. Ramon Torres, who was a member of my thesis committee and the chair of my defence. I have greatly benefited from his insightful comments and encouragement, but also from the hard questions he asked in our meetings.

Also, I would like to extend my sincere thanks to Prof. Dr. Ralph Hückelhoven for being willing to be the second examiner in my defence and for the support during the many joint experiments that we were allowed to perform at his chair.

I am truly indebted and grateful to Dr. Corina Vlot-Schuster. She provided me with a great topic to work on. I am very thankful for her constant advice and guidance regarding the progress of my experiments. She gave me the opportunity to make my own research decisions and encouraged me when I was insecure. Also, her understanding, support, patience, belief in my work, and honest criticism throughout the duration of this project was unparalleled.

Special thanks to Prof. Karl-Heinz Kogel and Dr. Jafargholi Imani for the numerous transformations of barley with my CRISPR/Cas vectors. Also, I would particularly like to thank Dr. Johannes Stuttmann for the CRISPR/Cas and reporter vectors he constructed and for continuously improving them.

In addition, I owe sincere and earnest thankfulness to Marion Wenig and Claudia Knappe for their help and support with my experiments. Marion, I really appreciate you for all the hours of discussion about experiment results and optimisation as well as for the many stainings you performed. Claudia, thank you so much for bringing all my work on the transgenics to tangible results and for the many qPCRs you did.

Furthermore, I want to thank my former bachelor students Veronika Wolf and Franz Seitz for their work and the experiments they did to support me. I surely learnt a lot while I was supervising you and I hope it was the same the other way around. Special

thanks also to Florian Hug, who helped me with a myriad of DNA isolations and PCRs. Without you, genotyping would have been a lot more difficult.

I have been fortunate to work with nice and helpful colleagues. I would like to thank Dr. Inonge Gross, Dr. Finni Wittek, Dr. Felicitas Mengel, Dr. Sanjukta Dey-Irmler, Dr. Elisabeth Pabst, Jenny Sales, Konny Bauer, Lucia Gößl, Elke Mattes, and Eva Rudolf for the agreeable working atmosphere, their helpful ideas, and constant assistance. Moreover, thank you for keeping me company and making me laugh during our joint breakfast and lunch breaks.

Außerdem möchte ich mich bei meiner Familie und meinen Freunden bedanken. Vielen Dank an meine Eltern, an meine Cousine und vor allem an meine Omas für ihre Liebe, ihr Interesse, ihre Geduld und Unterstützung. Ganz besonders möchte ich mich bei meiner Oma Hilde bedanken, die mir in allen Situationen immer eine tatkräftige Hilfe und Stütze war. Des Weiteren kann ich meinen Freundinnen Carla Karmann, Franziska Walz, Katharina Franke und Sophie Königsberger gar nicht genügend danken; euer offenes Ohr, eure Einschätzungen und eure emotionale Unterstützung haben mir wahnsinnig oft geholfen.

Zu guter Letzt geht ein ganz besonders herzliches Dankeschön an meinen Mann Stefan und unsere beiden Kinder Alex und Helena. Danke, dass ihr mich unterstützt habt und so viel Verständnis für mich hattet, auch wenn es mal wieder etwas später wurde. Und danke dafür, dass ihr immer an mich geglaubt habt, selbst wenn ich es nicht konnte. Ohne euch hätte ich das alles niemals geschafft. Danke für alles. Ich liebe euch.

10 Curriculum Vitae

Name	Miriam Lenk	**Geburtsdatum**	03.04.1988
Adresse	Steinseestr. 15, 81671 München	**Geburtsort**	München
E-Mail	lenk.miriam@gmail.com		

11/2015-10/2018	**Promotion**
	HelmholtzZentrum München (TU München)
	Institut für Biochemische Pflanzenpathologie (Prof. Jörg Durner)
	Arbeitsgruppe Dr. A. Corina Vlot-Schuster
	Promotionstitel: From model to crop plants: induced resistance in barley
10/2010-09/2012	**Masterstudium**, Abschluss: M. Sc.
	TU München
	Masterarbeit am HelmholtzZentrum München, Institut für Biochemische Pflanzenpathologie (Prof. Jörg Durner)
	Arbeitsgruppe Dr. A. Corina Vlot-Schuster
	Titel: Validation of promoter-*GFP* constructs for tracking of systemic acquired resistance signalling in plants
10/2007-09/2010	**Bachelorstudium**, Abschluss: B. Sc.
	TU München
	Bachelorarbeit am Lehrstuhl für Genetik (Prof. Alfons Gierl)
	Arbeitsgruppe Dr. Monika Frey
	Titel: Klonierung, Expression und Reinigung von BX9 in *Escherichia coli*
09/1998-05/2007	Maria-Ward-Gymnasium München Nymphenburg, Abschluss: Abitur

Publications

Publications	Lenk, M., Wenig, M., Mengel, F., Häußler, F., and Vlot, A. C. 2018. *Arabidopsis thaliana* Immunity-Related Compounds Modulate Disease Susceptibility in Barley. Agronomy. 8:142
Conference contributions (posters)	SEB Florence 2018 (Florence, Italy) International Conference of SFB924 2017 (Freising, Germany)
Publications in preparation	Lenk, M., Wenig, M., Bauer, K., Hug, F., Knappe, C., Lange, B., Häußler, F., Mengel, F., Dey, S., Vlot, A. C. 2018. Pipecolic acid is associated with innate immune responses in barley.

11 Eidesstattliche Erklärung

Ich erkläre an Eides statt, dass ich die bei der promotionsführenden Einrichtung Wissenschaftszentrum Weihenstephan für Ernährung, Landnutzung und Umwelt der TUM zur Promotionsprüfung vorgelegte Arbeit mit dem Titel:

From model to crop plants: induced resistance in barley

am HelmholtzZentrum München für Gesundheit und Umwelt, Institut für biochemische Pflanzenpathologie unter der Anleitung und Betreuung durch Prof. Dr. Jörg Durner ohne sonstige Hilfe erstellt und bei der Abfassung nur die gemäß § 6 Ab. 6 und 7 Satz 2 angebotenen Hilfsmittel benutzt habe.

Ich habe keine Organisation eingeschaltet, die gegen Entgelt Betreuerinnen und Betreuer für die Anfertigung von Dissertationen sucht, oder die mir obliegenden Pflichten hinsichtlich der Prüfungsleistungen für mich ganz oder teilweise erledigt.

Ich habe die Dissertation in dieser oder ähnlicher Form in keinem anderen Prüfungsverfahren als Prüfungsleistung vorgelegt.

Ich habe den angestrebten Doktorgrad noch nicht erworben und bin nicht in einem früheren Promotionsverfahren für den angestrebten Doktorgrad endgültig gescheitert.

Die öffentlich zugängliche Promotionsordnung der TUM ist mir bekannt, insbesondere habe ich die Bedeutung von § 28 (Nichtigkeit der Promotion) und § 29 (Entzug des Doktorgrades) zur Kenntnis genommen. Ich bin mir der Konsequenzen einer falschen Eidesstattlichen Erklärung bewusst.

Mit der Aufnahme meiner personenbezogenen Daten in die Alumni-Datei bei der TUM bin ich einverstanden.

Ort, Datum, Unterschrift